THE INSTITUTION OF ENGINEERS, MALAYSIA
Bangunan Ingenieu, Lot 60 & 62 Jalan 52/4, P.O.Box 223, (Jalan Sultan) 46720 Petaling Jaya, Selangor.
Tel: 03-7968 8001/4002 Fax: 03-7957 7678 E-mail: sec@iem.org.my Homepage: http://www.iem.org.my

SPECIAL EDITION
on Energy and Environment

IEM JOURNAL

THE JOURNAL OF THE INSTITUTION OF ENGINEERS, MALAYSIA

KDN PP5476/10/2010 (026477)
ISSN 0126-513X
Vol. 71, No 3
September 2010



Vol. 71, No.3, September 2010
KDN PP5476/10/2010 (026477) ISSN 0126-513X

CONTENTS

THE INSTITUTION OF ENGINEERS, MALAYSIA
Bangunan Ingenieur, Lots 60 & 62, Jalan 52/4, P.O.Box 223 (Jalan Sultan),
46720 Petaling Jaya, Selangor Darul Ehsan.
Tel: 03-7968 4001/4002 Fax: 03-7957 7678
E-mail: sec@iem.org.my Homepage: http://www.iem.org.my

Printed by: WISE ORGANISATION (M) SDN. BHD. (888671-H)
No. 5, Jalan Industri PBP 11, Taman Industri Pusat Bandar Puchong,
47100 Puchong, Selangor Darul Ehsan.
Tel: 603-5891 7363 Fax: 603-5891 7232
E-mail: weprint.wise@gmail.com

PRINT QUANTITY: *4,500 Copies*

We are pleased to announce that the articles in the IEM Journals have been indexed by other organisation *i.e. Linda Hall Library of Science, Engineering and Technology, Kansas City.*

PREFACE FOR THE SPECIAL EDITION ON ENERGY AND ENVIRONMENT

Following the successful publication of the previous Special Edition on Chemical Engineering in the IEM Journal (Vol. 70, No. 4, December 2009) on schedule, the Chemical Engineering Technical Division decided to champion another Special Edition in the IEM Journal for 2010, with the theme of "Energy and Environment". This is to respond to the needs for sustainable development for the country. A call for paper for the Special Edition was announced in January 2010, with the deadline for manuscript submission set on 1 March 2010. A total of 9 papers were received and finally 7 papers were selected for publication after a thorough evaluation process.

SUMMARY OF PAPERS

The first paper is a review contributed by M. A. A. Musa, C.-Y. Yin and R. M. Savory of Universiti Teknologi MARA. The review summarises recent works on the synthesis, characterisation and application of Covalent Organic Frameworks for hydrogen storage, as well as to hypothesise its use in other areas, *e.g*. gas storage, separation processes, and catalytic reactions. The second paper is the output of an international collaboration work among researchers from Universiti Putra Malaysia (W. A. Wan Ab Karim Ghani, M. S. F. Abdullah, K. A. Matori), Universiti Teknologi MARA (A. B. Alias) and the University of Melbourne, Australia (G. da Silva). The collaborators investigated the correlation of physical and thermochemical properties of four Malaysian biomasses (rice husk, palm kernel shell, coconut shell and wood sawdust) during a pyrolysis process, in order to exploit the potential application as commercial products in the industry.

Third, fourth and the fifth papers focus on various optimisation studies. The third paper contributed by R. R. Tan of De La Salle University-Manila, Philippines, presents a bi-level mathematical optimisation model for carbon constrained energy planning problem. In the fourth paper, an experimental optimisation study was reported on the analysis of the factors of a two-step enzymatic hydrolysis of sweet sorghum by commercially available enzymes. The paper is generated from a collaboration work between International Islamic University Malaysia (N. Nadir, M. Mel, M. I. A. Karim), and Universiti Malaysia Pahang (R. M. Yunus). The fifth paper reports the potential of sulphated zirconia as a heterogeneous acid catalyst for the esterification of free fatty acid to biodiesel. The paper is contributed by S. E. E. Misi, W. N. N. Wan-Omar and N. A. S. Amin from Universiti Teknologi Malaysia.

The last two papers in this special issue focus on safety and health aspects, which are understandably linked with environmental issues. The sixth paper is contributed by M. Z. Abidin and M. S. Takriff of Universiti Kebangsaan Malaysia. The paper presents a methodology to integrate consequence analysis with process simulation, which enables process design decision to be made by taking into account the potential consequence of process accidents at preliminary design stage.

The last paper in this issues is a Brief Paper (*concise description of new technical concepts or applications within the scope of IEM Journal* – see Information for Authors) that involves international collaboration between Universiti Teknologi Malaysia (M. H. Hassim) and Aalto University (formerly known as Helsinki University of Technology), Finland (M. Hurme). The paper introduces a new concept of inherent occupational health. It is hoped that this introduction as well as the establishment of its definition will have a significant impact on the appreciation and understanding of this subject matter especially in the chemical process industry.

ACKNOWLEDGMENTS

We would like to express our gratitude to the IEM Standing Committee on Information and Publications and Chemical Engineering Technical Division for their support in making this Special Edition a reality. Assistance given by the publication Secretariat Puan Nor Aziah Budin and Puan Nurul Aida Mustafa deserves a word of praise. We would also like to express our warmest appreciation to the following reviewers in providing fast and accurate review for the submitted papers:

- Professor Dr Raymond Tan (*De La Salle University-Manila, Philippines*)
- Dr Mimi Haryani Hassim (*Aalto University, Finland; Universiti Teknologi Malaysia*)
- Dr Chong Mei Fong (*University of Nottingham Malaysia Campus*)
- Dr Sachin Jangam (*National University of Singapore, Singapore*)
- Dr Fabiano André Narciso Fernandes (*Universidade Federal do Ceara, Brazil*)
- Dr Jui-Yuan Lee (*National Taiwan University, Taiwan*)

Guest Editors by Invitation

Ir. Associate Professor Dr Dominic Foo Chwan Yee
Ir. Associate Professor Dr Abdul Aziz bin Abdul Raman
Ir. Associate Professor Dr Law Chung Lim

Chemical Engineering Technical Division

A REVIEW OF NANOPOROUS MATERIALS DERIVED FROM COVALENT ORGANIC FRAMEWORKS

(Date received: 13.5.2009/ Date accepted: 25.6.2010)

Muhammad Afiq Aizuddin Musa[1], Chun-Yang Yin[2] and Robert Mikhail Savory[3]
[1,2,3] Faculty of Chemical Engineering, Universiti Teknologi MARA,
40450 UiTM Shah Alam, Selangor
E-mail: [2]yinyang@salam.uitm.my

ABSTRACT

The implementation of nanoporous materials is becoming increasingly more prevalent due to their unique characteristics, which make them highly applicable in a multitude of different functionalities. Covalent Organic Frameworks (COFs) are one of the new types of nanoporous material constructed from covalently bonded non-metals. COFs exhibit several advantages over conventional nanoporous materials such as low density, high thermal stability and the framework can be tailored for specific applications. This paper reviews recent works on synthesis, characterisation and applications of this new class of nanoporous materials. It is obvious from various studies that 3-dimensional COFs can, at least, compete with established nanoporous materials such zeolite and metal organic frameworks (MOFs) in terms of potential for H_2 storage, if not improve upon them. While previous studies focused on applying COFs for hydrogen storage, it is postulated that COFs can be further developed for various chemical engineering applications such as gas storage, separation processes, and catalytic reactions.

Keywords: *Adsorption; Covalent Organic Frameworks; Gas Storage; Nanoporous Materials*

1.0 INTRODUCTION

One of the ultimate goals of chemists, material scientists and chemical engineers in terms of sustainable technologies is to develop an efficient hydrogen storage material in order to initiate the global hydrogen economy. A commonly used standard to develop such a material is the United States Department of Energy target of a nanoporous material capable of storing up to 6 wt% of hydrogen at ambient temperature and pressure. This challenge drives scientists and engineers to synthesize novel lightweight nanoporous materials to replace conventional porous materials such as activated carbon, zeolite and silicate frameworks for such application.

Yaghi *et al*. [1] in 1995 first published work regarding modular metal organic frameworks (MOFs) and provided the stepping stone towards the development of organic frameworks for various applications, including hydrogen storage. MOFs are composed of metal or metal oxide vertices connected by organic linker molecules containing functional groups, which coordinate with the metal corners and thus complete the MOF unit. These materials can be composed of numerous metal, metal oxide and organic linker molecule combinations, thus enabling the formulation of many application specific MOFs. Precise coordination geometries between the organic linker molecules and metal vertices result in highly-ordered, periodic porous structures [2]. Such porous materials are characterised by pore dimension, low density, high thermal stability, high surface area and crystalline [3;4]. MOFs are well-established nanoporous materials and used in adsorption, separation, catalysis, extraction and gas storage technologies. However, they still have a significant drawback in terms of presence of '*heavy*' metal atoms within their frameworks which add weight in the structure without enhancing hydrogen storage capacity.

An obvious improvement in the gravimetric capacity of these nanoporous materials can occur by substituting the metal cluster with another lighter building block or by a novel family of materials that will exhibit the large surface area and the aromaticity of the organic linkers that MOFs have, but without the drawback of the presence of heavy metals [5]. In this sense, covalent organic frameworks (COFs) provide an alternative to improve on this characteristic since their molecular frameworks are made up of light elements (carbon, boron, hydrogen and oxygen) that reduce the relative weight of the structure. The term "*covalent organic framework*" refers to an extended covalent organic network having clusters connected by linking groups [6]. COFs were discovered by Côté and co-workers in 2005 whilst searching for a new porous, crystalline material composed of building blocks linked together by strong bonds. Networks which are assembled via strong covalent bonds exhibitenhanced stability over many coordinatively linked materials [7].

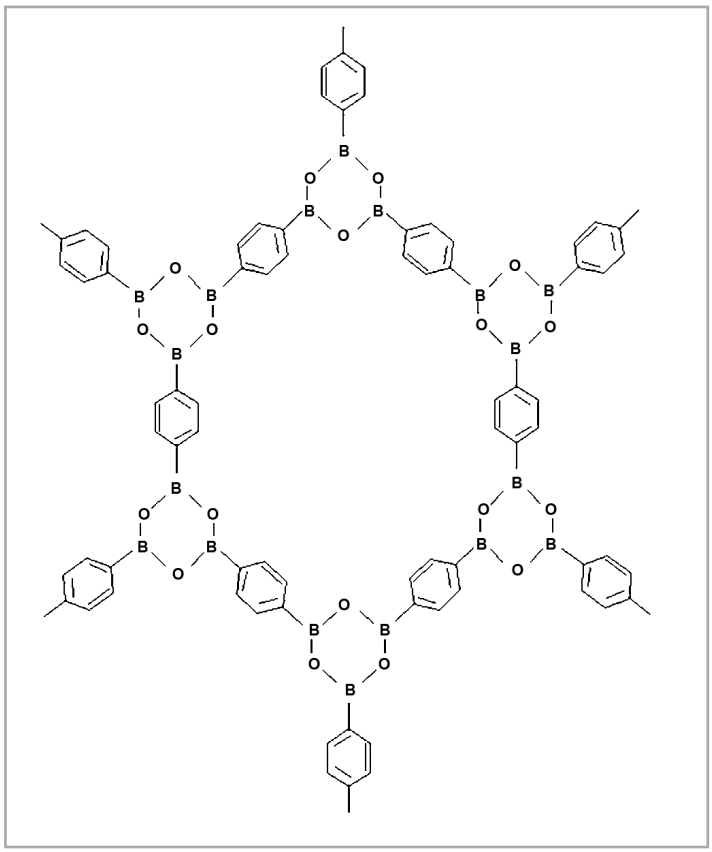

Figure 1: COF-1 structure [8]

The first synthesized COF, named COF-1 (($C_3H_2BO)_6$ and $(C_9H_{12})_1$) (*Figure 1*), is obtained from the molecular dehydration of 1,4-benzenediboronic acid (BDBA) [8]. The reversible formation of COFs, specifically COF-1, allows for the reordering of the framework yielding a material of significantly greater structural organisation than that found in rigid polymers. Such formation enables specific manipulation and tailoring of the framework hence enabling the development of reaction/process specific COFs. The porous frameworks have high thermal and chemical stability with surface areas, which surpass those of the well-established porous zeolite and silicate frameworks.

The development of COFs, while still in its early stages, has exhibited great potential for application in the field of hydrogen storage. The aim of this review is to critically assess and summarise the recent works concerning synthesis, characterisation and application of COFs for hydrogen storage, as well as to hypothesise on other areas for future development and application within the realm of chemical engineering processes.

2.0 SYNTHESIS OF COFs

Intriguingly, COFs can exist as one, two and three dimensional structures. Two dimensional structures resemble layered graphite composed of graphene sheets [9], whereas three dimensional COFs are composed of triangular and tetrahedral nodes; COF-102, 103, 105 and 108 [10]. COF-102 and 103 have similar characteristics except that COF-103 uses silicon atoms at the tetrahredral nodes rather than carbon. COF-NT, a one dimensional COF, also known as the armchair or zig-zag, is constructed by rolling a COF layer in a particular direction in a manner similar to that of carbon nanotubes [9]. It is widely known that Omar M. Yaghi's group are the pioneers behind the synthesis of COFs via reticular chemistry (linking molecular building blocks into extended structures by strong covalent bonds [11]. Table 1 presents existing COFs synthesised by the Yaghi group to date. The synthesis temperatures to produce these COF systems are relatively low (< 150 ºC) and this may present another plus point in terms of safety considerations.

Besides the Yaghi group, other researchers [12-15] have also synthesized COF variants. Kuhn *et al*.[12] synthesized a new class of high performance polymer frameworks with regular and irregular porosity formed from simple, cheap, and abundant aromatic nitriles via dynamic trimerisation in ionothermal conditions (molten zinc chloride at high temperature). This new class of frameworks is designated as covalent triazine-based framework (CTF-1) which resembles the boron oxide-based (COF-1) and has a surface area of up to 2475 $m^2\ g^{-1}$ and a total pore volume of 2.44 cm^3g^{-1}.

Tilford *et al*. [14] tailored the pore dimensions and COF environment through the condensation of dialkyl-substituted bis-diols with triboronic acids. In general terms, they incorporated hydrophobic and sterically bulky groups (alkyl groups, *e.g.* methyl, ethyl and propyl) in the pores while maintaining the same basic COF structure. They found that modification of the pore interior with increasingly larger alkyl groups caused a decline in nitrogen uptake, but an increase in the molar amount of hydrogen adsorbed by the network.

Another COF variant is the Surface Covalent Organic Framework (SCOF), which has been developed and synthesized by Zwaneveld *et al*. [15]. SCOFs are functionally and structural controllable due to their complimentary bicomponent composition; HHTP (2,3,6,7,10,11-hexahydroxytriphenylene) and BDBA (benzenediboronic acid). The networks produced are connected by boronate covalent bonds generated by the molecular dehydration of BDBA with three boronic acid molecules reacting to form a six-membered B_3O_3 rings, SCOF-1, and the condensation reaction of BDBA and HHTP forming dioxaborate heterocycles, SCOF-2. It is of note that the quality of the network is highly dependent upon the removal of impurities and water during synthesis.

3.0 CHARACTERISTICS OF COFs

3.1 Density and Thermal Stability

One of the major obstacles to the extensive use of hydrogen as a fuel is the lack of lightweight storage materials with high thermal stability capable of storing large volumes of hydrogen gas. COFs have been reported to be able to withstand temperatures as high as 600°C [8]. Metal hydrides have been considered as practical means for high pressure liquid hydrogen storage using physisorption according to the works of Frost and Snurr [2], however this approach has inherent problems including hydrogen embrittlement and handling issues. COFs have greater pore size control and most importantly lower densities than MOFs, *e.g.* COF-108 has a density of 0.17 g cm^{-3} compared to MOF-5 and

MOF-177 with respective densities of 0.59 and 0.42 g cm^{-3}. Another characteristic of COFs is their high thermal resistivity, which derives from their strong covalently bonded framework and makes their application in high-temperature processes viable.

3.2 Surface Area and Pore Characteristics

Surface area, or specific surface area, is one of the major factors that influences the characteristics, or behavior, of many materials and can be used as an indicator to determine the efficiency of the material with respect to hydrogen adsorption. Thus, it can be said that, a porous material with a large surface area and good adsorption characteristics govern the volume of adsorbate by maximising the adsorption capability [16]. COFs are porous materials with particularly large surface areas; the specific surface areas of COF-5, COF-102 and COF-103 are 1590, 3472 and 4210 $m^2 g^{-1}$ respectively, which are larger than zeolite Y (904 $m^2 g^{-1}$) [10;17] and double that of MCM-41 (Mobile Crystalline Material 41) [18] . The latest synthesized COFs; COF-202 was found to have a BET surface area and Dubinin-Radushkevich pore volume of 2690 $m^2 g^{-1}$ and 1.09 $cm^3 g^{-1}$, respectively [11]. Table 2 compares the textural characteristics of existing COFs to conventional porous materials. The intended application of COF systems for gas capture or storage is clearly reflected by their small pore sizes which are predominantly microporous (< 2 nm or < 20 Angstrom) with the exception of COF-5, COF-10 and TP-COF.

Adsorbent specific area can be calculated from the adsorption data of nitrogen vapour at 77 K using a linear form of Brunauer-Emmett-Teller (BET) surface area equation for non-porous, macroporous and mesoporous COFs. Isothermal correlation of the Langmuir surface area equation for microporous materials is used to infer the pore characteristics, *e.g.* COF-5 contains mesopores (0.998 $cm^3 g^{-1}$) and has a surface area of 1590 $m^2 g^{-1}$ [19]. In addition to surface area, pore volume is also considered as one of the main factors in achieving good adsorption with varying pressure. The level of solid-fluid interaction will dictate the quantity and efficiency in capturing gas molecules.

Pore distribution and size are vital components of a porous material, because the function and adsorption strength of the different sized pores changes with process conditions. Increasing adsorbate molecule size results in decreasing adsorption capacity due to the exclusion of access to the smaller pores [20]. Hence, the pore size must be tailored to suit the size of the adsorbate molecules. El-Kaderi *et al*. [10] reported the synthesis of COF-108: a crystalline mesoporous material with two different primary pore sizes of 15.2 Å and 29.6 Å, and a carbon Van der Waals radius of 1.7 Å. It is preferential for reaction-based porous materials to have either meso- or micropores, because the larger meso pores act to channel and transport the adsorbate molecules to the micropores, which are filled; once the micropores are full, then the mesopores are progressively filled.

Further to this, three dimensional simulation work by Garberoglio [17] on COF-102, -103, -105 and -108 show that the

Table 1: Recent works conducted by Yaghi group on synthesis of COFs

Researchers	Designation	Synthesis process	Synthesis condition
Côté *et al.*, 2005	COF-1	Dehydration of 1,4 benzenediboronic acid (BDBA)	120°C for 72 hours
Côté *et al.*, 2005	COF-5	Dehydration of phenylboronic acid and HHTP*	100°C for 72 hours
Côté *et al.*, 2007	COF-6	Co-condensation of HHTP * and 1,3,5-benzenetriboronic acid (BTBA)	85°C for 48 to 120 hours
Côté *et al.*, 2007	COF-8	Co-condensation of HHTP * and 1,3,5-benzenetris (4-phenylboronic acid) (BTPA)	85°C for 48 to 120 hours
Côté *et al.*, 2007	COF-10	Co-condensation of HHTP * and 4,4'-biphenyldiboronic acid (BPDA)	85°C for 72 hours
El-Kaderi *et al.*, 2007	COF-102 and COF-103	Self-condensation of tetra(4-dihydroxyborylphenyl) methane (TBPM) or silane analog (TBPS) and HHTP *	85°C for 96 hours
El-Kaderi *et al.*, 2007	COF-105 and COF-108	Co-condensation of TBPM or TBPS with HHTP *	85°C for 96 hours
Hunt *et al.*, 2008	COF-202	Condensation of tert-butylsilane triol with monotopic boronic acid to form a high symmetry borosilicate cage.	120°C for 72 hours

* HHTP = 2, 3, 6, 7, 10, 11-hexahydroxytriphenylene

uptake of adsorbate molecules, namely hydrogen gas, at 77 *K* and low pressures is better for COF-102 and -103 due to better solid-fluid interactions. Hence, the more compact the microscopic structure the better the solid-fluid interactions and the greater the adsorption capability. At low pressures, large pore sizes in the macroscopic range (> 50 nm) are detrimental to the adsorption capability, because the solid-fluid interactions are insufficiently strong to ensure adherence of the adsorbate molecules to the porous surface. According to Garberoglio *et al.*[21] and Latroche *et al*. [22] this is a common problem inherent in MOFs. However, at high pressure, the inverse trend is found with respect to COF-102, -103, -105 and -108 in which COFs with larger pore size have higher uptakes than the smaller ones (COF-102 and -103). This is due to the increased pressure driving the adsorbate molecules deeper into the macropores and sufficiently close to the surface to facilitate sufficiently strong solid-fluid interactions to cause adsorption.

Although cryogenic results evidently indicate that COFs have superior uptakes, it is under ambient conditions that the uptake is of greater importance; due to the high costs associated with cryogenics and the consequent cost saving benefits of ambient condition storage. Unfortunately, to date, no high uptake porous materials exist [17]. A primary advantage that COFs have over MOFs and zeolites is that COFs have no latent edges (minutely-sized edges not visible to the naked eyes) within their three dimensional arrangement, thus optimising access to the faces and edges of the molecular framework units., which means larger surface areas and statistically increases the number of available adsorption sites at the aromatic ring centres [17].

Table 2: Comparison between textural characteristics of COF systems and conventional nanoporous systems

Designation	Surface area (m2g-1)	Pore size (Å)	Reference(s)
COF-1	711	15.0	8
COF-5	1590	27.0	19,8
COF-6	980*	8.6	19,33
COF-8	1400*	16.4	19,33
COF-10	2080*	31.7	19,33
COF-18 Å	1260	18	4,7
COF-102	3472	8.9	10
COF-103	4210	9.6	10
COF-202	2690#	11.0	11
TP-COF	868	31.4	40
26 Å MCM-41	680	26.0	8
32 Å MCM-41	1140	32	18
Carbon Black Pearls, BP700	170	212.0	38
Carbon Black Pearls, BP2000	520	456.0	38
Zeolite Y	904	7.4	10,39
MOF-177	4500	11.8	4,37
MOF-5 @ IRMOF-1	2900	15.2	17,37
CTF-1	791	12.0	12
MIL-53 (Al)	1020	6.4	37
MIL-101	4100	-	10

**Langmuir surface area; generally higher than BET surface area*
 # measured with argon

3.3 Enhancing Adsorption Capacity

The enhancement of adsorption capability at ambient conditions is a focal point of COFs research, because it is essentially the limiting step in its wider implementation. Methods such as increased pore density, increased adsorption energy, the use of atomic hydrogen, increased carbon bridging and spillover technology (interphase diffusion of adsorbed active species) induce greater gas uptake. However, all of these methods have their limitations and they are discussed in the following.

Increasing the pore density appears to be comparatively simple since the COF structures can be manipulated to generate a high density of smaller pores, which inherently causes an increase in surface area and hence provides greater storage capability. Even so, this requires systematic synthesis and a large degree of control over the reaction mechanism and the synthesis of specific reagents, all of which, ultimately, increase synthesis and processing costs. Adjusting the adsorption energy through enhanced activation of the COFs surface improves the solid-fluid interaction and increases the likelihood of adsorbate molecule capture. Bhatia and Myersn [23] conducted work with integration of simulation components, suggested that increasing the value to 15 kJ mol^{-1} is necessary to improve adsorption. In another separate development, experimental findings reported by Dinca *et al*.[24;25] showed that adsorption isotherms measured at 77 and 87 K indicate high H_2 adsorption enthalpies in the range 7.0–9.5 kJ/mol, depending on the degree of loading.

In order to facilitate greater adsorption, it will require much greater interaction energy throughout the COFs structure to generate any significant improvement in the adsorbate uptake. Another means to increase the adsorption energy is through carbonisation of the carbon bridges [26]. Although high temperatures in excess of 250°C are required for this process, COFs are thermally stable to well above this temperature and this provides a viable method to activate the adsorption surface. Experimental work conducted by Li and Yang [26] has shown that the molecular hydrogen take-up of COF-1 increases by 2.6 times and the bridge structure remains unsaturated, thereby maintaining the original adsorption sites and structure. This approach can also be used to generate a greater degree of bridging thus enabling secondary spillover and providing an increased number of adsorption sites which combined with the use of atomic hydrogen provides an increase in overall hydrogen adsorption.

Another approach to overcome the problem of low uptake and the difficulties associated with increasing adsorption energy is to increase the number of available adsorption sites and using all existing sites to their full potential. [16] Morris and Wheatley [16] suggest the use of atomic rather than molecular hydrogen, which would improve the use of the available pore space since the smaller atoms can penetrate deeper into the pores. Choi *et al*.[27] studied hydrogen storage mechanisms on pure and metal ion-decorated COFs via first principles calculations and discovered that the H_2 binding characteristics of pure COFs are very similar to those of MOFs. The research suggest that using Li^+ and Mg^{2+} ions yield more advantageous activated structures, but at the price of higher COFs weights which can be construed as a significant drawback. In a theoretical study, Kim *et al*. [28] inserted pillar molecules (pyridine) between the organic layers of COF-1 to improve the physisorption ability for hydrogen molecules in which they observed puckering in the cluster model of the COF, which were caused by binding of pyridine molecules.

4.0 APPLICATIONS OF COFs

4.1 Hydrogen Storage

One intended application of COFs is for H_2 storage. Judging by recent research, it can be generally agreed that 3-D COFs are most advantageous compared to conventional storage materials. Han *et al*. [29] used grand canonical Monte Carlo (GCMC) simulations to hypothesise that the best COFs for hydrogen storage are COF-105 and COF-108, each of which lead to maximum excess H_2 uptakes of 10 wt % at 77 *K* (the highest value reported for associative H_2 storage of any material).The very low uptake temperature at 77 *K* is the stumbling block for commercialisation of COFs. In light of this, it has been suggested that in order to obtain high H2 uptake at 300 *K*, doping of COFs with electropositive elements such as Li, Na, *K* should be carried out in order to increase H_2 binding energy.[30]

In a theoretical study, Klontzas *et al*.[31] reported that the gravimetric uptake for COF-108 reached the value of 21 wt % at 77 *K* and 100 bar conditions and the very promising value of 4.5 wt % in room temperature and 100 bar conditions. They also indicated the gravimetric uptake of COFs is in some cases 2 times larger than that of the best known MOFs while the volumetric results remain comparable. Kuhn *et al*. [12] experimentally found that covalent triazine-based framework could adsorb up to 1.55wt% H_2 at 1.00 bar and 77 *K* while Tilford *et al*. [14] reported that their customised COFs could store up to 1.5 wt% H2 at 77*K* and 760mm Hg. A general consensus from all these combined theoretical and experimental studies shows that 3-D COFs can, at least, compete with established MOFs in terms of potential for H_2 storage, if not improve upon them. Two-dimensional COFs, however, are relatively ineffective and less likely to be used for H2 storage in the future according to Garberoglio and Vallauri [32], who conducted computer simulation and found that the quantity of H_2 adsorbed in these materials was generally half that adsorbed by other organic frameworks under the same conditions, either on both gravimetric and volumetric bases.

4.2 Carbon Dioxide and Methane Storage

Recent studies have indicated that COFs have high potential for the storing of other gases such as CO_2 and CH_4. Barbarao and Jiang [33] reported that COF-102 exhibited CO_2 high capacity at considerably low pressures. They further reported that COF-102 could reach CO_2 saturation (> 13 mmol/ cm^3) at a pressure of approximately 1000 kPa, which is less than half of the saturation pressures observed for MOFs for similar volumetric saturation. This indicates that COFs can be further developed to be incorporated into more effective and safer CO_2 sequestration systems.

Methane is a major component of natural gas and is a very promising fuel source. However, it is found normally in the gas phase, which makes it difficult to store. Currently, methane is stored in pressurised containers to maintain it in its liquid phase at ambient temperatures. This phase change and added safety comes at a high price; the installation of multiple safety procedures to guard against the possibility of leakage and consequent possible explosion is vital. COFs offer an alternative means to storage of

methane gas. The COFs enable storage of the gas in large quantities due to their extensive porous structures. Garberoglio [17] reported that COF-102 had the potential to meet or even exceed the DOE target of 180 cm^3 (STP)/cm^3 at 35 bar for methane adsorption. It was also found that methane adsorption in various COFs revealed the presence of a large volume with strong interaction energy in COF-102. Both studies by Barbarao and Jiang [33] as well as Garberoglio [17] observed that the packing of atoms in COF-102 was rather compact and, hence, has a significant overlap of spaces with attractive interaction with carbon dioxide molecules.

COFs have also been considered for the storage of other hydrocarbons, but it is possible that COFs could be used for general gas storage, including medical purposes (*e.g.* nitric oxide and oxygen), and as a way to store environmentally hazardous gases (*e.g.* carbon monoxide, ammonia, and sulphur dioxide) on a long term basis to help preserve our world and health.[16] Essentially the application of COFs on a large industrial scale is not unimaginable, but it will require further research and tailoring of existing COF technology.

4.3 Catalytic Support/Carrier

The ideal catalyst carrier is a porous, inert substrate with a large surface area, added benefits include chemical and heat resistance. Based on this criterion, COF would make an ideal catalyst carrier and its ability to be tailored would ensure that optimised catalyst loading is possible, irrespective of the catalyst size or shape, ensuring catalysis is performed effectively. The lightweight character of COFs would also enable a wider application as a catalyst carrier. Lino *et al.* [34] reported that 2-dimensional COF extended sheet systems could be rolled up to form stable nanotubes which could be applied as molecular filters/carriers, gas storage and building blocks for 3-dimensional structures.

4.4 Separation Processes and Other Applications

Separation is the process of dividing a mixture into two or more components, which is significant in the industrial sector. On an industrial level, separation constitutes enrichment, concentration, purification, refining and isolation [35] and may involve adsorption, decantation, filtration and drying. Ideally, one would wish to have a cheap, simple, easy to maintain and highly effective separation process, but in reality one finds that a compromise must be reached. COFs offer a tailorable, highly resistant, lightweight porous substrate, which can be activated to optimise separation of multi-component mixtures, which would make them an ideal candidate for use in the oil and gas industry.

Other modern technologies, including membranes and saline separation processes as well as biorection could benefit from the development of tailored COFs. Membrane and saline technologies require pore sizes to be of specific sizes so as to prevent ions passing through them; COFs could be tailored to selectively prevent ionic passage. COFs could be used in bioreactors, which require the immobilisation of microorganisms and enzymes on the surface of porous inert substrates. Coupled with the need for large surface areas is the requirement of a bimodal pore size distribution, whereby the smaller and larger pores act as immobilisation sites and transport channels for the carrier fluid, respectively [36]. However, it should be noted that saline separation and bioreaction processes involve presence of water, which can reverse the synthesis of COF frameworks and subsequently breaks them into stating materials. As such, extensive experimental studies to determine the state of COF frameworks in liquid flows should be conducted to shed light on this issue.

5.0 CONCLUSION

COFs, while mainly used for hydrogen storage, have great potential in other fields including catalysis and separation due to their highly desirable textural characteristics and varied framework structures. The physicochemical properties of COFs mean that their application is viable in many modern industrial processes, although it has yet to be proven that COFs are comprehensively superior to zeolites and MOFs in the long term. Preliminary technical studies have shown the huge potential of COFs in storing H_2, CO_2 and CH_4, which indicate their importance within the field of energy and environmental sustainable technologies. While there have been a multitude of studies on the effectiveness of COFs, studies on other aspects such as economics as well as environmental implications of using them in existing process systems are lacking. This is crucial since 3-D COFs are relatively more complicated and more expensive to produce. Further strides need to be taken to develop this highly promising group of compounds and enable process specific tailoring to be achieved without compromising cost-effectiveness and environmental sustainability, which many previously considered gas storage materials have failed in the past.

6.0 ACKNOWLEDGEMENT

The authors gratefully acknowledge the Ministry of Science, Technology and Innovation, Malaysia for providing the necessary funding for this project (ScienceFund 03-01-01-SF0213). ■

REFERENCES

[1] Yaghi OM, Li G and Li H (1995). "Selective Binding and Removal of Guests in a Microporous Metal-Organic Framework." Nature. 378:703-706.

[2] Frost H and Snurr RQ (2007). "Design Requirement for Metal-Organics Frameworks as Hydrogen Storage Material." J Phys Chem C. 111:18794-18803.

[3] Li Y, Yang FH and Yang RT (2007). "Kinetics and Mechanistic Model for Hydrogen Spillover on Bridged Metal-Organic Frameworks." J Phys Chem C. 111: 3405–3411.

[4] Mastalerz M (2008). "The Next Generation of Shape-Persistent Zeolite Analogues: Covalent Organic Frameworks." Angew Chem Int Ed. 47:445-447.

[5] Klontzas E, Tylianakis E and Froudakis GE (2008). "Hydrogen Storage in 3D Covalent Organic Frameworks. A Multiscale Theoretical Investigation." J Phys Chem C. 112:9095-9098

[6] Budd PM, (2007). "Chemistry: Putting Order into Polymer Networks." Science. 316:210-211.

[7] Niu W, O'Sullivan C, Rambo BM, Smith MD and Lavigne JJ (2005). "Self-Repairing Polymers: Poly(dioxaborolane) s Containing Trigonal Planar Boron." Chem Commun. 34:4342–4344.

[8] Cote AP, Benin AI, Ockwig NW, O'Keeffe M, Matzger AJ and Yaghi OM (2005). "Porous, Crystalline, Covalent Organic Frameworks." Science. 310:1166-1170.

[9] Babarao R and Jiang J (2008). "Molecular Screening of Metal-Organic Frameworks for CO_2 Storage." Langmuir. 24:6270-6278.

[10] El-Kaderi HM, Hunt JR, Mendoza-Cortés JL, Cote AP, Taylor RE, O'Keeffe M and Yaghi OM (2007). "Designed Synthesis of 3D Covalent Organic frameworks." Science. 316:268-272.

[11] Hunt JR, Doonan CJ, LeVangie JD, Cote AP and Yaghi OM (2008). "Reticular Synthesis of Covalent Organic Borosilicate Frameworks." J Am Chem Soc. 130:11872–11873.

[12] Kuhn P, Antonietti M and Thomas A (2008). "Porous Covalent Triazine-Based Frameworks prepared by Ionothermal Synthesis." Angew Chem Int Ed 47:3450 –3453.

[13] Tilford RW, Gemmil R, zurLoye HC and Lavigne JJ (2006). "Facile Synthesis of a Highly Crystalline, Covalently linked Porous Boronate Network." Chem Mater 18:5296–5301.

[14] Tilford RW, Mugavero SJ, Pellechia PJ and Lavigne JJ (2008). "Tailoring Microporosity in Covalent Organic Frameworks." Adv Mater 20:2741–2746.

[15] Zwaneveld NAA, Pawlak R, Abel M, Catalin D, Gigmes D, Bertin D and Porte L (2008). "Organized Formulation of 2D Extended Covalent Organic Frameworks at Surface." J Am Chem Soc 130:6678-6679.

[16] Morris RE and Wheatley PS (2008). "Gas Storage in Nanoporous Materials." Angew Chem Int Ed 47:2-20.

[17] Garberoglio G (2007). "Computer Simulation of the Adsorption of Light Gases in Covalent Organic Frameworks." Langmuir 23:12154-12158.

[18] Kruk M, Jaroniec M and Sayari A (1997). "Adsorption Study of Surface and Structural Properties of MCM-41 Materials of different Pore Sizes." J Phys Chem B 101:583-589.

[19] Cote AP, El-Kaderi HM, Furukawa H, Hunt JR and Yaghi OM (2007). "Reticular Synthesis of Microporous and Mesoporous 2D Covalent Organic Frameworks." J Am Chem Soc 129:12914-12915.

[20] Patrick JW (Ed) (1995). "Porosity in Carbons-Characterization and Applications." Arnold.

[21] Garberoglio G, Skoulidas AI, and Johnson JK (2005). "Adsorption of Gases in Metal Organic Materials: Comparison of Simulations and Experiments." J Phys Chem B 109:13094-13103.

[22] Latroche M, Surble S, Serre C, Mellot-Draznieks C, Llewellyn P, Lee JH, Chang JS, Jhung S and Frey G (2006). "Hydrogen Storage in the Giant-Pore Metal-Organic Frameworks MIL-100 and MIL-101." Angew Chem Int Ed 45:8227-8231.

[23] Bhatia SK and Myers AL (2006). "Optimal Conditions for Adsorptive Storage." Langmuir 22:1688-1700.

[24] Dinca M and Long JR (2005). "Strong H_2 Binding and Selective Gas Adsorption within the Microporous Coordination Solid Mg_3 $(O_2C\text{-}C_{10}H_6\text{-}CO_2)_3$." J Am Chem Soc 127:9376– 9377.

[25] Dinca M, Dailly A, Liu Y, Brown CM, Neumann DA and Long JR (2006). "Hydrogen Storage in a Microporous Metal-Organic Framework with Exposed Mn^{2+} Coordination Sites." J Am Chem Soc 128:16876–16883.

[26] Li YW and Yang RT (2008). "Hydrogen Storage in Metal-Organic Frameworks and Covalent-Organic Frameworks by Spillover." AIChE J 54:269-279.

[27] Choi YJ, Lee JW, Choi JH and Kang JK (2008). "Ideal Metal-Decorated Three Dimensions Covalent Organics Frameworks for Reversible Hydrogen Storages." Appl Phys Lett 92:173102-1–173102-3.

[28] Kim D, Dong DH, Choi SH, Kim J and Choi K (2008). "Theoretical Studies on Pillared Covalent Organic Frameworks for a Hydrogen Storage Material." J Korean Phys Soc 52:1255-1258.

[29] Han SS, Furukawa H, Yaghi OM and Goddard WA (2008). "Covalent Organic Frameworks as Exceptional Hydrogen Storage Materials." J Am Chem Soc 130:11580-11581.

[30] Han SS and Goddard WA (2007). "Lithium-Doped Metal-Organic Frameworks for Reversible H_2 Storage at Ambient Temperature." J Am Chem Soc 129:8422-8423.

[31] Klontzas E, Tylianakis E and Froudakis GE (2008). "Hydrogen Storage in 3D Covalent Organic Frameworks. A Multiscale Theoretical Investigation." J Phys Chem C 112:9095-9098.

[32] Garberoglio G and Vallauri R (2008). "Adsorption and Diffusion of Hydrogen and Methane in 2D Covalent Organic Frameworks."Microp Mesop Mat doi:10.1016/j.micromeso.2008.05.023.

[33] Babarao R and Jiang J (2008). "Exceptionally High CO_2 Storage in Covalent-Organic Frameworks: Atomistic Simulation Study." Energy Environ Sci. 1:139-143.

[34] Lino MA, Lino AA and Mazzoni MSC (2007). "Porous Nanotubes and Fullerenes Based on Covalent Organic Frameworks." Chem Phys Lett 449:171-174.

[35] Seader JD and Henly EJ,(1998). "Separation Process Principles." John Wiley & Sons, Inc.

[36] Ishizaki K, Komarneni S and Nanko M (1998). "Porous Materials- Process Technology and Applications." Kluwer Academics Publishers.

[37] Rowsell JLC and Yaghi OM (2005). "Strategies for Hydrogen Storage in Metal-Organic Frameworks." Angew Chem Int Ed 44:4670–4679 .

[38] Madsena C and Jacobsen CJH (1999). "Nanosized Zeolite Crystals—Convenient Control of Crystal Dize Distribution by Confined Space Synthesis." Chem Commun 673–674.

[39] Cui Y, Kita H and Okamoto KL (2003). "Preparation and Gas Separation Properties of Zeolite T Membrane." Chem Commun 2154–2155.

[40] Wan S, Guo J, Kim J, Ihee H, and Jiang D (2008). "A Belt-Shaped, Blue Luminescent, and Semiconducting Covalent Organic Framework." Angew Chem 120:8958 – 8962.

PHYSICAL AND THERMOCHEMICAL CHARACTERISATION OF MALAYSIAN BIOMASS ASHES

(Date received: 24.3.2010/ Date accepted: 19.6.2010)

W. A. Wan Ab Karim Ghani[1,4], M.S.F. Abdullah[1], K. A. Matori[2], A. B. Alias[3] and Gabriel da Silva[4]

[1] Department of Chemical and Environmental Engineering, Faculty of Engineering, Universiti Putra Malaysia, 43400 UPM Serdang, Selangor

[2] Department of Physics, Faculty of Science, Universiti Putra Malaysia, 43400 UPM Serdang, Selangor

[3] Faculty of Chemical Engineering, Universiti Teknologi MARA Malaysia, 40450 Shah Alam, Selangor

[4] Department of Chemical and Biomolecular Engineering, The University of Melbourne, Victoria 3010, Australia

ABSTRACT

The agriculture sector in Malaysia has been growing rapidly over the years and this leads to large amount of agricultural waste. However, sustainable development and increasing fuel demand necessity had identified biomass ashes can be exploited into many commercial industrial products (i.e. energy, carbon storage, ceramics, construction materials, etc). In this paper, pyrolysis of biomass from four sources (rice husk, palm kernel shell, coconut shell and wood sawdust) has been performed to investigate its correlation with their physical and thermochemical properties in order to exploit their potential application as commercial products in the industry. Generally, biomass ashes have average bulk density between 0.61 and 1.21 gcm^{-3} characterised with high porosity (up to 80%) but low thermal conductivity (below 1 W m^{-1} K^{-1}). Thermogravimetric analysis on the raw biomass revealed that the heating profile of the biomass governed by three major decomposition of hemicellulose, cellulose, and lignin at respective temperatures of 325°C, 375°C, and 400 to 500°C. Inductively coupled plasma (ICP) detected insignificant amounts of toxic metals in the biomass ashes samples. Silica has found to be major compounds in most biomass ashes samples especially rice husk ashes which explain its highest water absorption properties. Other compounds found include calcium, magnesium and potassium. The large variation observed in biomass ashes properties need to be considered when applying these materials to the environmental systems or designing a commercial product, where outcomes may be correlated with these features.

Keywords: *Biomass Ashes; Characterisation; Lignin; Porosity; Thermal*

1.0 INTRODUCTION

In Malaysia, more than 2 million tones agricultural wastes are produced annually and potentially an attractive feedstock for energy production as it contributes little or no net carbon dioxide to the atmosphere. Agricultural production in Malaysia continued to record positive growth from 2000 to 2005 and expected to expand more in 2010 consistent to the government policies [1]. There are significant amount of wastes and residues also called as agricultural wastes produced from the post-processing of these products. Major agricultural products are palm oil, sawlogs, paddy and tropical fruits. Table 1 report the production, residues generated and potential energy for selected biomass. In Malaysia, rice husk and paddy straw are among major agricultural wastes that can be applied as biomass- based power generation. Rice husk referred to an outer cover of rice and in form of hull. The husk account for 22% of the weight of paddy and 78% of the weight is received as rice, broken rice and bran throughout the milling process [2]. While for oil-palm sectors, oil-palm solid wastes (including shell, fibre and its EFB) are cheap and abandoned materials produced during palm oil milling process. For every ton of oil-palm fruit bunch being fed to the palm-oil refining process, about 0.07 tons of palm shell, 0.146 tons of palm fiber and 0.2 tons of EFB are produced as the solid wastes [3]. For bagasse, 3×10^5T per year was reported in 1999 while rubber wood residues generate 11.32×10^6m^3 in 2000, respectively. Bagasse is the matted cellulose fibre residue from sugar cane that has been processed in a sugar mill. Despite the decreasing acreage, coconut still plays an important role in the

Table 1: Oil palm, paddy and wood production in Malaysia in 2008[3]

Type of Industry	Production (10^6× Tone)	Residue	Residue product Ratio (%)	Residue Generated (10^3*Tone)	Potential Energy, (E) PJ*
Oil Palm (62707×10^6 Tone)	62707	EFB	20.44	11698	57
		Fiber	14.63	8373	108
		Shell	6.58	3766	55
		Total solid		23837	15308
		Other (POME)		38870	
Paddy (214×10^6 Tone)	2141	Rice Husk	22	471	7.6
		Paddy Straw	40	856	8.8
Wood	2937679	Sawn timber	0.5-0.6	1629718	5.2
	523336	Plywood and veneer	0.18-0.65	121000	0.374
	147813	Moulding	0.2-1	75600	0.232

** sample calculation is shown in appendix*

socio-economic position of the Malaysian rural population that involves 80,000 households. About 63% of coconut production is for domestic consumption and 37% is for export and industrial processing. The domestic demand for coconut products takes in the form of fresh coconut, tender coconut, coconut oil and processed cream powders. In terms of exports, the country has seen an increase in the export of products of coconut such as desiccated coconut, coconut milk powder and activated carbon. In 2007, exports of coconut and coconut- based products were valued at RM 485,771,416 an increase from the 466.2 million in 2006 [4]. This large amount of residues need to be disposed at landfill and required substantial area to be mounted. By converting these materials into commercial products, this not only will solve landfill problem but also create wealth to the country.

Thermal conversion of solid agricultural waste seems to have a feasible application and has been developed attractively for industrial applications [5]. Recently, biomass ashes have attracted a lot of research with a focus on the application of biomass ashes (biochar) to soils not only contribute to carbon storages but at the same time act as fertilisers [6]. Despite the range of feedstock and techniques available to produce biomass ashes, very little work has been reported on properties of biomass ashes. Thus, detail investigation to evaluate their thermal behavior and structural characteristics is important before they were applied. The aim of the present paper was to characterise the physico-thermochemical properties Malaysian biomass ashes produced via pyrolyses in a bench-scale furnace system. Physical properties such as bulk density, apparent porosity, water absoprtion and thermal conductivity were determined using standard procedures. A scanning electron microscopy (SEM) were used to observe biomass ashes surfaces and their porosity. For thermal characterisation, themogravimetric analyser (TGA) were used to measure the thermal degradation of the raw biomass. For chemical characterisation, the ultimate analyser and inductive coupled plasma (ICP) were used to characterise chemical compositions.

2.0 EXPERIMENTAL

2.1 Raw Material and Ash Preparation

Rice husk, palm kernel shell, coconut shell and sawdust from local (Selangor, Malaysia) mills are chosen for the study. The biomass samples were dried in crucibles in an oven at 110°C for 24 hours to remove moisture. The samples were then ground and sieved to 2 to 3 mm particle sizes. The biomass ashes were obtained by burning (pyrolysis) the raw biomass materials at 800°C for 2 hours in a closed furnace.

2.2 Biomass Ashes Characterisation

Several techniques were used to assess the physical and chemical properties of the ashes. Physical properties such as bulk density, apparent porosity, water absoprtion and thermal conductivity were determined using standard procedures. For example, the apparent porosity was determined according to ASTM C 134/95, apparent density according to ASTM C 773/88. A scanning electron microscope (SEM) was used to observe the

char surfaces in order to verify the presence of porosity. For SEM studies, the sample were mounted in gold tabs and examined with a HITACHI S 3400 N by different accelerations voltages, depended on the roughness and conductivity of the specimen surface. A thermogravimetric analyser (Metler ToledoSDRA15e) was used to measure and record the mass change with temperature for biomass samples. Tests were conducted at heating rate of 10°C min^{-1} over the temperatures 100 to 950°C. For all the pyrolysis runs, 30 mg of sample was used and nitrogen flow was around $30cm^3min^{-1}$. The chemical characterisation was performed in order to determine ash content and heavy metal content for each biomass ashes samples. Leaching of heavy metal ions was estimated by the toxicity characteristics leaching procedure (TCLP) method of the US Environmental protection Agency (EPA) by using inductively coupled plasma (ICP).

3.0 RESULTS AND DISCUSSION

3.1 Fuel Properties

Biomass ashes, being derived from a variety of biological feedstock that has thermally degraded exhibit a correspondingly large range in composition and chemistry. Table 2 presents the proximate and ultimate analyses of studied raw biomass samples. In the proximate analyses, biomass in general was characterised by high moisture content and high ash content. The moisture and ash content of the fuel is essential for the choice of the appropriate combustion and gas cleaning technologies. The lower moisture content fuel is preferable in power generation as this parameter will influenced the amount of heat required for the pyrolysis or combustion technologies. Furthermore, the lower ash content also would benefits power or energy production as fly ash formation, ash deposit formation as well as logistics concerning ash storage and ash utilisation/disposal depend on the ash content of the fuel [7].

Fuels with low ash content are therefore preferable. Agricultural waste usually contains relatively high amount of ash (coconut shell in this case) as compared to coal. However, this problem can be solved by using grate or fluidised bed boilers which are suitable for ash-rich fuels. Furthermore, the composition, density, size and amount of the fly ash emissions formed are influenced by the amount of ash-forming elements in the fuel as well as by the combustion technology and process control applied. A more detailed insight into ash content is given in section 3.4.

The elemental compositions of Carbon(C), hydrogen (H) and oxygen (O) are the main componens found in the ultimate analyses (Table 2). C and H are oxidised during combustion by exothermic reaction (formation of CO_2 and H_2O). The content of C and H contributes positively to the calorific value, the content of O negatively. The C contents of coal and palm kernel shell are higher than those of coconut and rice husk, which explain the slightly higher calorific value. During thermal decomposition the fuel N is almost entirely converted to gaseous N_2 and nitric oxides (NOx (NO, NO_2). Like nitrogen, the sulfur (S) contained in the solid fuels forms mainly pollutant gaseous sulfur dioxides (SO_2) and alkali as well as earth-alkali sulphates.

Furthermore, the calorific value of the biomass material was lower as double compared to coal. This mean the amount required biomass to produce the equivalent energy as coal is doubled. This phenomenon may contribute logistic problem such as storage when the biomass is utilised.

Table 2: Main characteristics of Malaysian Raw Biomass samples

	Rice Husk	Palm kernel shell	Coconut shell	Sawdust	Coal
Proximate analysis (wt% db)					
Volatile matter	60.68	72.47	30.62	51.39	29.2
Fixed carbon	15.02	18.56	26.41	14.29	54.0
Ash	24.30	8.97	42.98	22.67	14.8
Ultimate analysis (wt% db)					
Carbon	34.9	51.63	45.24	53.4	70.0
Hydrogen	5.50	5.52	5.04	6.7	8.5
Nitrogen	0.10	1.89	1.46	3.1	2.21
Sulfur	0.00	0.05	0.06	0	0.8
Oxygen(by different)	59.5	40.91	48.2	36.8	18.5
Calorific values (MJ/kg)	13.5	22.97	16.07	18.3	29.4

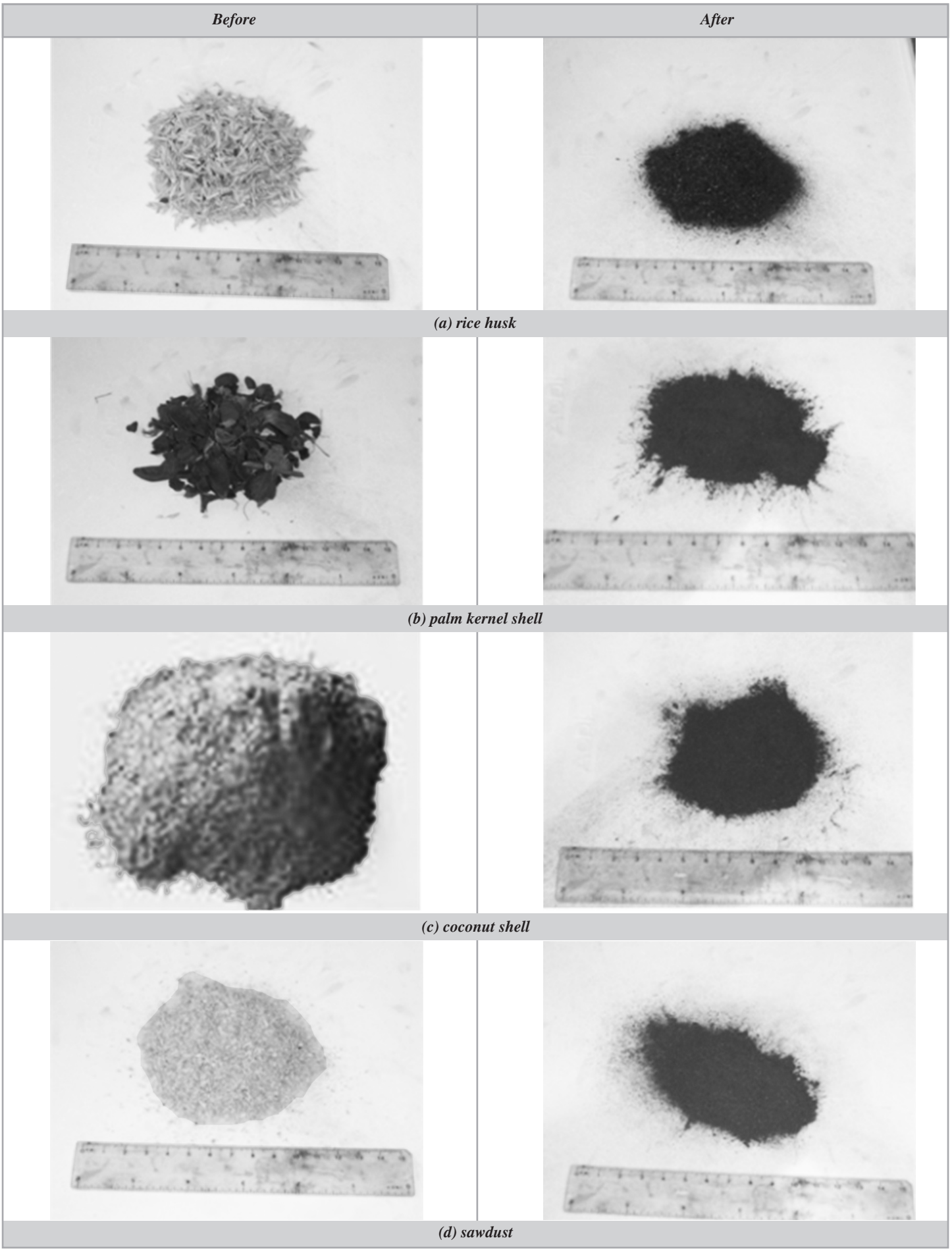

Figure 1: Pictures of biomass samples before and after the thermal treatment

3.2 Physical and Surface Analyses

This section focuses on the physical and macrostructure of biomass ashes. Figure 1 shows the biomass samples before and after thermal treatment while Table 3 lists the physical properties of biomass ashes. As summarised in this table, rice husk ashes showed the lowest bulk density and thermal conductivity but the highest water absorption as compared to other biomass ashes. On the contrary, palm kernel shell had a high thermal conductivity compared to other but very low percentage of porosity. The amount of the entrapped air will increases with increases porosity of the refractory. Hence, the thermal conductivity decreases.

Microscopic observation shows particle shape and structure variation in all raw ashes after heating. Figure 2 illustrates the scanning electron microscope (SEM) that described a fundamental macrostructure of the produced biomass ashes (biochar) for different biomass samples. The presence of aligned honeycomb-like groups of pores most likely the carbonaceous skeleton from the capillary structure of the botanical origin confirmed this structure [8]. As anticipated from the regular size and arrangement of plant cells in most biomass from which biochars are derived, the macro-pore size distribution is composed discrete groups of pores sizes rather than a continuum [13].

Table 3: Physical properties of biomass ashes

	Rice husk	Palm kernel shell	Coconut shell	Wood
Bulk density (gcm-3)	0.61	0.78	1.21	0.98
Apparent porosity (%)	79.7	25.9	28.9	33.7
Water absorption (%)	37.41	19.75	19.99	20.3
Thermal conductivity (W K-1 m-1)	0.15	0.97	0.85	0.80

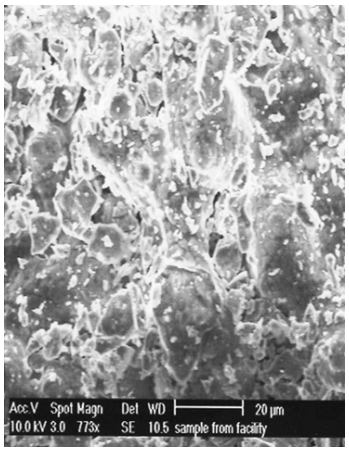

(a) Rice husk ash

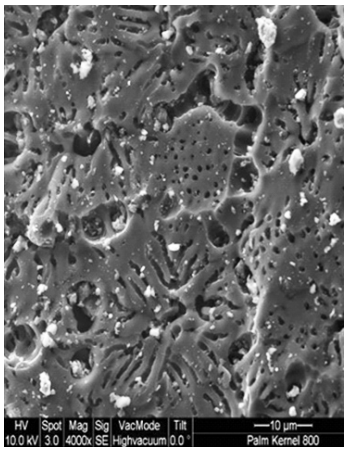

(b) palm kernel ash

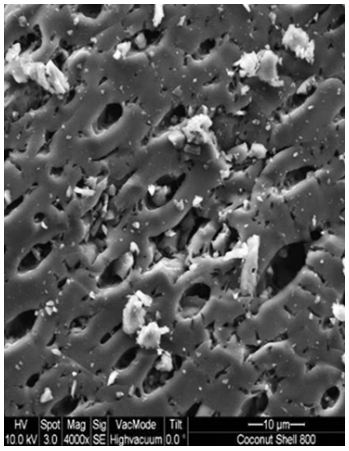

(c) coconut shell ash

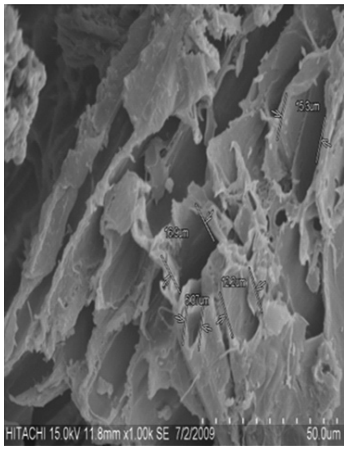

(d) sawdust

Figure 3: Scanning Electron Microscope (SEM)

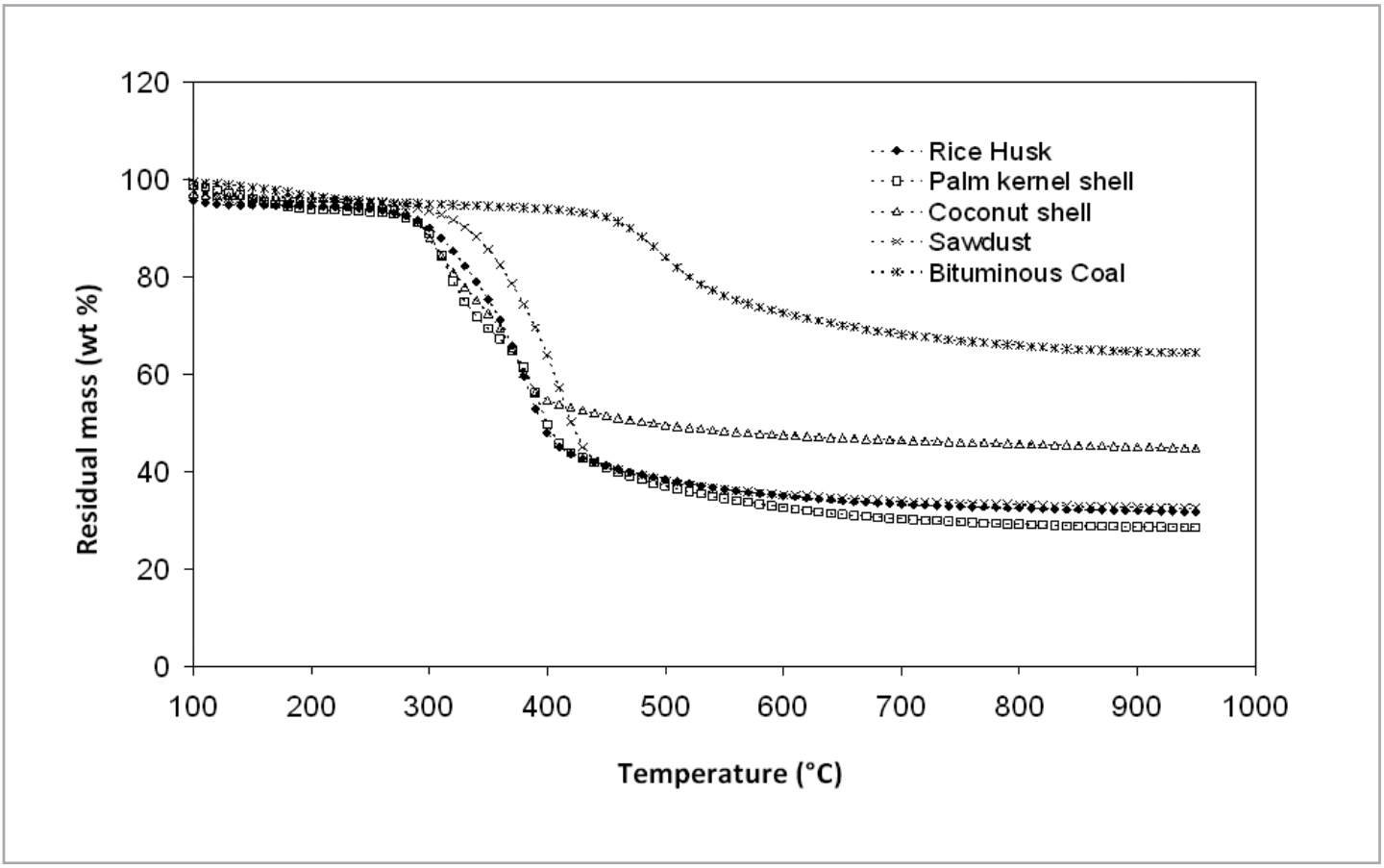

Figure 4: Thermogravimetric analysis (TG) of the pyrolysis of biomass sampples at constant heating rate (10°C min^{-1}) with N_2 sweep gas at 120 mL min^{-1}

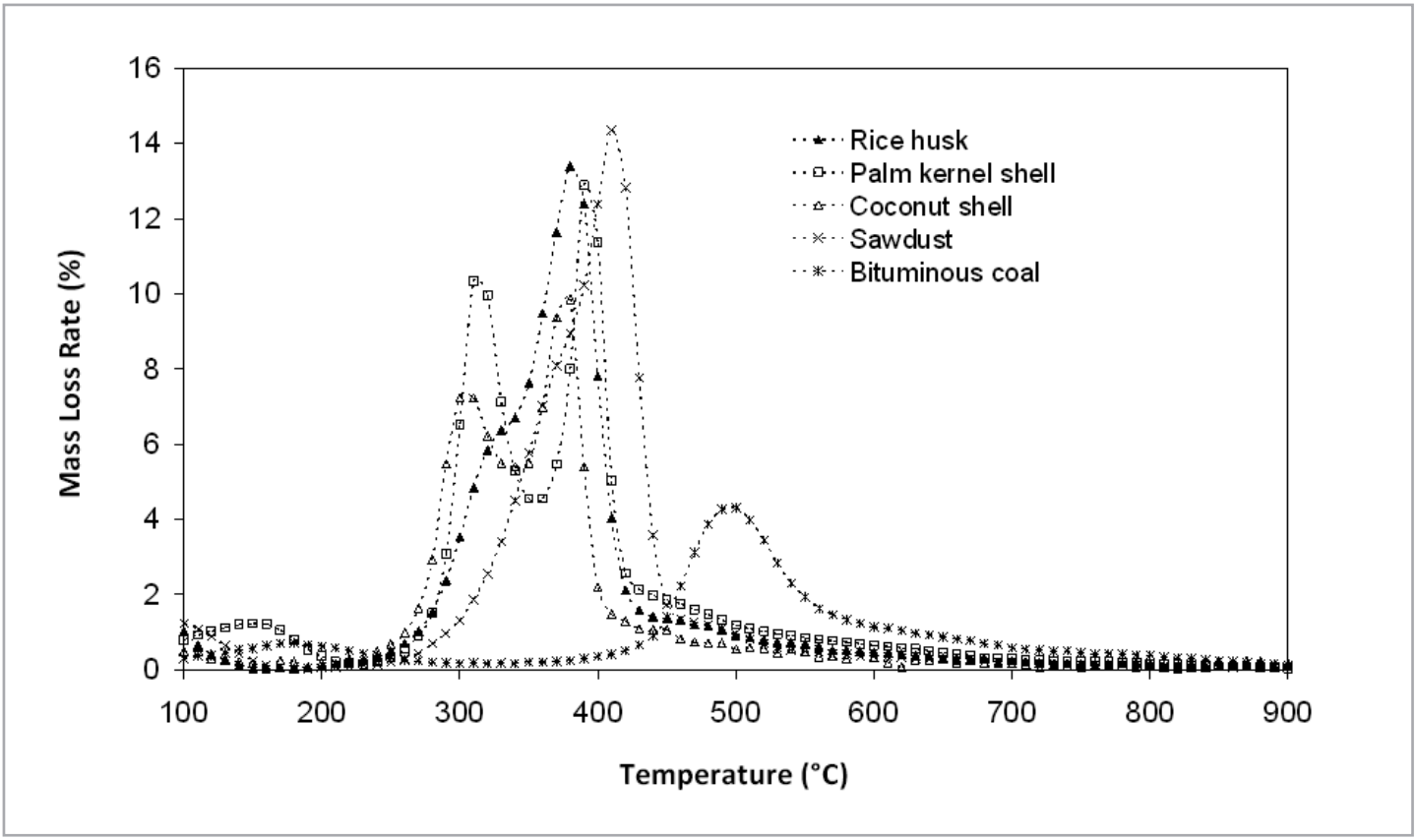

Figure 5: Differential thermogravimetric analysis (DTG) of the pyrolysis of biomass samples at constant heating rate (10°C min^{-1}) with N_2 sweep gas at 120 mL min^{-1}

3.3 Thermal Analyses

The thermogravmetric (TG) and derivative of thermogravimetric (DTG) curves for of coal and studied raw biomass undergoing pyrolysis in a nitrogen atmosphere at a heating rate of 10°C min^{-1} is shown in Figures 4 and 5, respectively. The thermal decomposition starts at lower temperature approximately 200°C for agricultural waste compared to 350°C for coal. Furthermore, agricultural waste samples showed two overlapping peaks and a flat tailing section. Its have been debated by other researchers that the lower temperature peak represents the decomposition of hemicellulose in the material and the higher temperature peak represents the decomposition of cellulose [8-11]. The flat tailing section of the DTG curves at higher temperature represents lignin, which is known to decompose slowly over a very broad temperature range [11]. The TGA shows about 17 wt% losses of physically bound water at 100°C. This could be due to volatilisation of unburned carbon and other organic matter present due to incomplete combustion as well as SiO_2 present in agricultural waste ash samples. On the contrary, in case of rice husk ash the weight loss is insignificant. This can be attributed to the fact that rice husk comprises primarily of silica with negligible amounts of volatile oxides. On the other hand, for the TGA curves of bituminous coal, the decomposition starts at about 350 °C, which is significantly higher than the one corresponding to the biomass samples. The maximum pyrolysis rate occurs at 500 °C, at a level of 3 x 10^{-2} min^{-1} which is 5 to 7 times lower than that of the biomass materials, thus indicates that bituminous coal is less reactive. This phenomenon is reflective in the DTG curves which represent by peak height and peak temperature. Hence, the higher potential for energy production would be suggested for pyrolysis and gasification [12].

3.4 Chemical Characterisations

Table 4 shows the selected major elements formed in the ash components of the biomass ashes (biochar). From the results it is observed that SiO_2 is predominant in most of the ashes except for wood samples. Other compounds of phosphorus, magnesium, aluminium, calcium, iron and potassium are also present. These elements are of relevance for ash melting, deposition, formation, emissions as well as corrosion. A high content of potassium (K) and silica (Si) in all of the agricultural wastes are observed. This usually will decrease the ash melting point which may cause sintering or slag formation in the combustion chamber. In addition, melts occurring in fly ash particles may cause hard deposit formation on cooled furnace walls or heat exchanger tubes [6]. However a low content of aluminium and iron are observed in coconut shell sample. It tends to suggest that the origin of the ash is mostly inherent, rather than adventitious material from sand, clays and soil [13].

Table 4: Ash composition of Biomass Ashes (biochar)

	Percentage (%)			
Compound	***Rice husk***	***Palm kernel shell***	***Coconut shell***	***Sawdust***
SiO_2	89.57	31.73	42.45	8.78
Al_2O_3	1.32	3.46	3.31	13.89
Fe_2O_3	1.43	1.78	2.57	2.35
P_2O_5	1.04	2.57	2.33	19.32
CaO	0.77	20.27	1.21	2.72
TiO_2	1.01	12.39	1.33	35.72
MgO	0.76	1.01	21.36	0.35
Na_2O	1.15	1.38	1.97	1.04
K_2O	1.65	1.51	2.01	1.93
Cl	1.3	0.08	0.98	0.07
MnO	-	1.27	1.91	-
C	-	12.55	19.67	13.83

Table 5: Results of TCLP tests for selected biomass ashes

Heavy metals	Rice husk ash (ppm)	Palm kernel shell (ppm)	Coconut shell (ppm)	Limit (ppm) [15]
Cd	0.084	0.099	0.082	1.0
Cr	0.702	0.069	0.049	1.75
Cu	0.962	0.108	0.281	100
Pb	0.149	0.215	0.016	0.25
Ni	0.083	0.058	0.035	100

Generally, much of the mineral content in the biomass is carried over into the biomass ashes (biochar) where it is concentrated due to loss of C, H and O during pyrolysis. The amount and distribution of mineral ash in the biochar is influenced by its feedstock and process conditions. However, Table 5 reveals that all the toxic metals of selected biochar samples by TCLP tests were found to be below than regulation limit. Bridgewater suggested that the partial pressure of O_2, steam and carbon dioxide (CO_2) controls the amount of mineral ash in the biochar [14].

3.5 Potential Application of Biomass Ash

Based on the above properties, it appears that the presence of porosity and high water absorption, low thermal conductivity and immobilised toxic metals of the most biomass char (biochar) will make them suitable to be recycled for ceramic products such as insulators, filters, structural ceramics, adsorbent materials, etc. These applications have not been explored for biomass ashes. For instance, ceramic membranes can be used for clarification, separation and decontamination in several industries such as food processing, petrochemical and wastewater treatment [2]. In perspective with typical soil application, these structures vital soil functions such as aeration and hydrology [14], soil water holding capacity and adsorption capacity [16-18]. Furthermore, food-processing industries in Malaysia (dairies, beverage) where rice husk is commonly used in the boilers, can be use ceramic membranes for separation (*e.g.* removal of whey protein from whey) and clarification (fruit juice clarification).The presence of unburnt carbon in biomass ash could enhance its adsorbent properties. There is also the possibility to separate and activate the unburnt carbon as has been done for coal fly ash. The advantages of using unburnt carbon includes high yields of activated carbon since the carbon has already undergone devolatalisation and simplified process since only activation is required. Recently, biomass ashes (biochar) also claimed can be use to mitigate a greenhouse gases especially carbon dioxide (CO_2) from atmosphere or from power plant.

4.0 CONCLUSION

Physico-chemical properties of the biomass ashes are found to be varies and greatly influenced by the origin of their raw materials. Physically, biomass is characterised with high moisture and ash content but lower calorific value as compared to coal. These properties indirectly contributed to high water absorption and low thermal conductivity to the materials. Morphologically, SEM images reveal the presence of irregular shape and porous structure in all biomass ashes. Furthermore, thermal analysis shows most of the weight loss is in the range of 320-600°C which mainly governed by decomposition of cellulose, hemicelluloses and lignin in the raw biomass samples. These findings not only will gave some temperature profile of the raw materials but also will provide useful appropriate operating temperatures to deal with biomass samples depends on the target products. Furthermore, biomass-derived ashes exhibits a correspondingly large range in composition and chemistry over the studied pyrolysis temperature. Generally, SiO_2 is predominant in most of the biomass ashes except for wood samples. A high content of potassium (K) and silica (Si) in all of the agricultural wastes are observed. Apart from high ash content, insignificant amount of metals were found in the biochar samples except for Ca, Fe and Zn, albeit in very low concentration (less than 100 ppm). In conclusion, the properties of biomass ashes (biochar) products may affect many of the functional roles that they may play in environmental management applications. The large variations of their physical, thermal, and chemical characteristics observed in the biomass-ashes (biochar) will be more effective than others in certain applications. Hence, it is important that these characterisations are undertaken before they were experimentally applied to environmental systems and variations outcomes maybe correlated with these features.

ACKNOWLEDGEMENT

The authors express their gratitude to the Ministry of Science, Technology and Innovation (MOSTI) of Malaysia and Academy Science of Malaysia and for the financial supports. ■

APPENDIX

a) Calculation of potential energy

Potential Energy (*E*) = Mass of biomass (*tonne*) × Calorific Value of biomass (*kJ/kg*)

Example : energy potential from palm fibre residues (*refer Table 1 for values*)

E = 11698×10^3 Tonne × 4.87* (***kJ/kg***)
= 11698×10^3 Tonne × 4.87×10^9 (***J/Tonne***)
= 56.9×10^{12} ***J***
= ***57 PJ***

** from experimental data / literature data*

REFERENCES

[1] Ninth Malaysia Plan 2006-2010, Economic Planning Unit, Prime Minister's Department, Malaysia. Website: http://www.epu.jpm.my.

[2] Umamaheswaran K. and V.S. Batra (2008). "Physico-chemical Characterization of Indian Biomass Ashes." Fuel. **ISSN** 0016-2361, 87 (6): pp628-638.

[3] Oil World magazine. Website:http://www.oilworld.biz/

[4] Sivapragasam. Coconut in Malaysia-current Developments and Plantation for Re- vitalization. International Plantation Industry Conferency. Malaysia, (IPICEX 2008).

[5] Purevsuren B. Avid, Tesche B. and Davajaav (2003). "A Biochar from Casein and Its properties." Journal of Materials Science. **ISSN** 0022-2461, 38(11): pp2347-2351.

[6] Glaser B., Lehmann J., and Zech W (2002). "Ameliorating Physical and Chemical Properties of Highly Weathered Soils in the Tropics with Charcoal: A review." Biological and Fertiliser of Soils. **ISSN** 0178-2762, 35(4): pp219-230.

[7] Orberberger, I., Brunner, T and Barnthaler, G. 2007. Chemical Properties of solid biofuels-significace and impact. Journal of Biomass and Bioenergy. **ISSN** 0961-9534, 30(11): pp973-982.

[8] Cozzani, V., Nicolella, C., Petarca, L. Rovatti, M. and Tognotti, L. (1995), "A fundamental study on conventional pyrolysis of a Refused-Derived Fuel". Industrial and Engineering Chemistry Research. **ISSN** 0888-5885, 3-4(6):pp2006-2020

[9] Werther, J., M. Saenger, *et al.* (2000), "Combustion of agricultural residues". Pogress in Energy and Combustion Science. **ISSN** 0360-1285, 26(1):pp1-27.

[10] Williams, P. T., and Besler, S (1991). The Pyrolysis of Rice Husks, the Influence of Temperature and Heating Rate on the Product Composition. In: Grassi, G.,Collinna, A., Zibetta, H., editors. Biomass for energy, industry and environment, 6th E.C. Conference, London; Elsevier Applied Science.

[11] Vamvuka, D., Kakarasb, E., Kastanakia, E. and Grammelis, P (2003). "Pyrolysis Characteristics and Kinetics of Biomass Residuals Mixtures with Lignite." Fuel. **ISSN** 0016-2361, 82 (15-17): pp1949–1960.

[12] Mangut,V., Sabio,E., Ganan, J., Gonzalez, J. F., Ramiro, A., Gonzalez, C. M. Roman, S., and A. Al-Kassir. 2006. "Thermogravimetric study of the pyrolysis of biomass residues from tomato processing industry". Journal of Fuel Processing Technology. **ISSN** 0016-2361, 87: pp109-115.

[13] Bridgeman, T.G., Darvell, L. I., Jones, J. M., Williams, P. T., Fahmi, R., Bridgwater, A.V., Barraclough,T., Shield, I., Yates, N., Thain, S.C and Donnison, I.S (2007). "Influence of Particle Size on the Analytical and Chemical Properties of Two Energy Crops. Fuel. **ISSN** 0016-2361, 86 (1-2): pp60–72.

[14] Bridgwater, A. V (2003). "Renewable Fuels and Chemicals by Thermal Processing of Biomass." Chemical Engineering Journal. **ISSN:** 1385-8947, 91:pp87-102.

[15] US EPA, 1982. Test Methods for evaluating Solid Waste, Physical Chemical Methods, SW-846, Method 1310A/1311. US Environmental Protection Agency, Washington DC.

[16] Day, D., Evans, R.J., Lee, J.W., and Reicosky, D (2005). "Economical CO2, SOx, and NOx Capture from Fossil-fuel Utilization with Combined Renewable Hydrogen Production and Large-scale Carbon Sequestration." Energy. **ISSN:** 0360-5442, 30 (14): pp2558-79.

[17] Ogawa, M., Okimori, Y., and Takahashi, F (2006). "Carbon Sequestration by Carbonization of Biomass and Forestation: Three case studies. Mitigation and Adaptation Strategies for Global Change. **ISSN**: 1573-1596, 11: pp429-44.

[18] Yu, X.-Y., Ying, G.-G., and Kookana, R.S (2006). "Sorption and Desorption Behaviors of Duron in Soils Amended with Charcoal." Journal of Agriculture and Food Chemistry. **ISSN** 0021-8561, 54: pp8545–8450.

PROFILES

DR WAN AZLINA WAN AB KARIM GHANI

Dr Wan Azlina has a B Eng in Chemical Engineering from Universiti Teknologi Malaysia and a PhD in the area of Biomass combustion technology from University of Sheffield under supervision of Dr. Keith Cliffe. Later, she applies her knowledge as a lecturer cum active researcher towards biomass conversion technologies, particularly thermal treatment such as combustion, gasification and pyrolysis technologies. She further enhanced her interest in biomass pyrolysis product (biochar) for carbon capture study to mitigate global climate change in her fellowship research in University of Melbourne, Australia. Currently, she is a senior lecturer in Department of Chemical and Environmental Engineering, University Putra Malaysia. She had published several articles in high citation index journals, refereed journals and also manuscripts in conference proceedings.

MOHD. SYAFIK FIRDAUS ABDULLAH

Mohd Syafik has a B. Eng in Chemical Engineering from Universiti Putra Malaysia and continuing his Master degree entitled "Vitrification of Biomass ashes". He managed to publish several articles in conference proceedings during his study period.

DR KHAMIRUL AMIN MATORI

Dr Khamirul Amin Matori joined the Department of Physics, Universiti Putra Malaysia in 2000 as a Lecturer followed by eventual promotion to Senior Lecturer in 2008. He attained his PhD from the University of Sheffield under supervision of Professor W.E. Lee and Dr M.I. Ojovan in 2007 in the area of glass and glass ceramics. He has wide ranging research interests in glass and ceramic science, with particular emphases on the processing, microstructures and properties as well as waste immobilisation. Current research topics include development of nanostructured mullite-base ceramic composites from waste, design of phase change material composites for high-temperature ceramics. Other work includes fabrication of willemite-based glass and glass ceramics, preparation of oxide/carbide coatings and novel armour materials and waste-treatment.

AZIL BAHARI ALIAS

Mr Azil bahari Alias has a B. Eng in Chemical Engineering from Universiti Teknologi Malaysia, Master of Science from University Technology MARA (UiTM) and pursuing his PhD in Energy and Environment in University of Melbourne, Australia. He currently a lecturer in Faculty of Chemical Engineering, University Technology MARA Malaysia. His research interest includes biomass combustion characterization, co-combustion of biomass with coal, coal cleaning/treatment and municipal solid waste management. From his excellencies in research, he has won several awards national and international exhibitions namely Invention, Innovation and Technology Exhibition (ITEX 2008) and British Invention Show (BIS 2008). Apart from that, he had published several articles in high citation index journals, refereed journals and also manuscripts in conference proceedings.

DR GABRIEL DA SILVA

Dr Gabriel da Silva studied PhD and B. Eng. in Chemical Engineering in University of Newcastle, Australia. During his bachelor study, he held a position as an Engineering Research Assistant at BHP Billiton, Biohydrometallurgy Research Group (2000 – 2002), Postdoctoral Research Fellow, New Jersey Institute of Technology, Chemistry and environmental Science (2005 – 2007) and later as a Lecturer in The University of Melbourne, Chemical and Biomolecular Engineering, (2007 – present). Dr da Silva's research interests are broadly in the area of energy and the environment, using computational chemistry techniques and reaction rate theory to model complex reaction networks relevant to combustion and atmospheric chemistry, as well as environmentally important organic reaction mechanisms. The current research focus is directed toward understanding and modeling reaction processes related to the use of biofuels (ethanol, biodiesel, and biomass), allowing us to optimize their combustion and thereby support the uptake of these green, renewable energy-sources. Studies are also underway to model the formation and atmospheric reactions of pollutants like soot, persistent free radicals, and ozone depleting substances. A further area of interest is bioleaching, where naturally occurring bacteria are used to leach base and precious metals from sulphide minerals.

DETERMINING APPROXIMATE STACKELBERG STRATEGIES IN CARBON CONSTRAINED ENERGY PLANNING USING A HYBRID FUZZY OPTIMISATION AND ADAPTIVE MULTI-PARTICLE SIMULATED ANNEALING TECHNIQUE

(Date received: 29.3.2010/ Date accepted: 31.5.2010)

Raymond R. Tan
Chemical Engineering Department
De La Salle University, 2401 Taft Avenue, 1004 Manila, Philippines
E-mail: raymond.tan@dlsu.edu.ph

ABSTRACT

In recent years, there has been growing international concern about climate change as a result of greenhouse gas emissions from human activity. Various process integration techniques have thus been developed to assist in determining the optimal allocation of energy sources to sectoral or regional demands under carbon footprint constraints; for example, the source-sink representation of this problem has been solved using graphical and algebraic pinch analysis techniques as well as linear programming. This work presents an extension of the original problem by incorporating a game-theoretic, two-level decision framework, which is a more accurate representation of real-life energy planning applications. The upper level decision-maker (i.e., the government) seeks to minimise total costs to society by selecting appropriate emission limits for each sector as well as subsidy levels for clean energy sources; on the other hand, the lower level decision-maker (i.e., industry) seeks to minimize total energy-related costs subject to the emission limits set by the government. This problem is a static Stackelberg game which may be formulated as a fuzzy bi-level optimisation model. A numerical example from literature is used to illustrate the modeling approach. The case study is then solved using an adaptive multi-particle simulated annealing algorithm to yield an approximate Stackelberg solution.

Keywords: *Bi-level Programming; Carbon Constraints; Energy Planning; Source-sink Model; Stackelberg Game*

1.0 INTRODUCTION

In recent years, growing international concern about climate change has led to increased research emphasis on mitigation of emissions of greenhouse gas (GHG) emissions. Since a large portion of global GHG emissions are in the form of CO_2 from energy use, various approaches to achieve this goal include fuel substitution, efficiency enhancement and carbon capture. Process systems engineering (PSE) techniques have also been developed to optimise the utilisation of different fuels in energy systems with carbon emission constraints. For example, Tan and Foo (2007) developed a graphical pinch analysis approach for allocating fossil fuels to different energy sinks or demands, so as to minimise the requirement for clean or low-carbon energy sources such as renewable or nuclear power. The technique is based on approximating such energy sources as having virtually zero carbon emissions, which is justified by their low carbon footprint in comparison to conventional fossil fuels. The graphical method was also shown to be equivalent to a linear programming (LP) problem. A subsequent paper (Foo *et al.*, 2008) showed how the same problem may be solved numerically through cascade analysis.

The basic carbon pinch approach was then extended to segregated targeting problems (Lee *et al.*, 2009; Bandyopadhyay *et al*., 2010), as well as problems involving demand growth (Atkins et al., 2010), carbon capture and storage or CCS (Tan *et al.*, 2009a) and carbon footprint visualisation for industrial plants (Tjan *et al.*, 2010). Furthermore, the methodology was also shown to be applicable to land use (Foo *et al.*, 2008), water footprint (Tan *et al.*, 2009b) and emergy (Bandyopadhyay *et al.*, 2010) constraints in energy planning. More recently, there has been a shift in emphasis towards mathematical programming, which is able to handle complex energy planning considerations that are not possible using purely pinch-based approaches. For example, Pękala et al. (2010) extended the basic LP model from Tan and Foo (2007) to cases involving biofuel production with trade considerations, and to deployment of CCS retrofits in the power sector (Tan *et al.*, 2009a).

The main limitation of these insight-based and mathematical programming-based optimisation approaches is the implicit assumption that a single decision-maker exists for the energy system. In reality, energy planning involves the complex interaction of multiple players or stakeholders. Thus, such problems are best dealt with using game theory, which accounts for the self-interested behavior of independent agents. In its simplified form, the interaction may be reduced to one that occurs between an upper level regulatory decision-maker (*i.e.*, government) on one hand, and a lower level decision-maker (*i.e.*, private industry) on the other. In general it may be assumed that the government plays the role of trying to influence industry to behave in an environmentally responsible manner (through regulations or economic incentives), while industry seeks to maximise profit. This sort of leader-follower interaction may be represented as a Stackelberg game (Stackelberg, 1951; Simaan and Cruz, 1973) where the leader's problem is to determine appropriate incentive strategies that induce the follower to react in a manner that favors the leader's interests (Salman and Cruz, 1981). This situation requires that the leader anticipates the follower's reactions. A static Stackelberg game can be formulated as a bi-level mathematical programming problem (Bard, 1998) which essentially consists of one optimisation model (representing the follower's desires) nested within an outer model (representing the leader's objective).

This paper presents a bi-level optimisation model for the carbon constrained energy planning problem originally posed by Tan and Foo (2007). The approach assumes that the leader decides on the emission limits and subsidy levels for clean energy, while the follower seeks only to maximise profit (or minimise cost). The model is described in the next section. A hybrid approach is then shown for determining an approximate Stackelberg strategy, which involves relaxation of constraints in a fuzzy optimisation model, followed by determination of a highly satisfactory (*i.e.*, "satisficing") solution using an adaptive multi-particle simulated annealing (AMPSA) algorithm. A case study based on literature is then used to illustrate the methodology. Finally, conclusions are drawn and prospects for future research are identified.

2.0 PROBLEM STATEMENT

The idealised bi-level carbon constrained energy planning problem may be stated as follows. The problem consists of two decision makers, the first representing government and the second representing industry. Assume that there are m energy sources, for which the available quantity and carbon intensities are known. In addition, there is one additional resource denoted as clean or zero-carbon energy, whose carbon intensity is so low when compared to the other fuels as to be negligible; there is no specified limit for this energy source. There are also n sinks, each with a fixed energy demand and carbon emission limit imposed by the upper level decision maker. The problem is for the upper level decision maker to minimise external costs (borne by society as a result of emissions) by setting appropriate levels of subsidy for clean energy and emission limits, subject to the lower level decision maker's objective to minimise direct energy costs, and subject to system-wide energy balances. A further simplifying assumption is that all energy sources are fully interchangeable.

3.0 BI-LEVEL PROGRAMMING MODEL

Parameters	
B	External cost per unit of carbon dioxide emissions
C_z	Unsubsidized cost per unit of clean energy
C_i	Cost per unit of energy source i
D_j	Energy demand of sink j
$F_{max,j}$	Maximum allowable carbon emission intensity limit per unit energy for sink j
H_i	Carbon footprint per unit of energy source i
R	Maximum fraction of clean energy cost to be subsidized
S_i	Maximum availability of energy source i
Leader's Variables	
A	Subsidy per unit of clean energy
F_j	Carbon emission intensity limit per unit energy for sink j
G_1	Total cost burden to society
Follower's Variables	
E_{ij}	Amount of energy from source i allocated to sink j
G_2	Total energy cost
Z_j	Amount of clean energy allocated to sink j

The leader's objective (Equation 1) is to minimise the cost burden to society:

$$\min G_1 \tag{1}$$

subject to:

$$G_1 = A\sum_j Z_j + B\sum_j F_j D_j \tag{2a}$$

$$F_j \le F_{max\,j} \qquad \forall j \tag{2b}$$

The first term in Equation 2 is the cost of subsidising clean energy in the system, while the second term is the external cost of environmental impacts arising from carbon emissions. The follower's objective (Equation 3) is to minimise total energy costs:

$$\min G_2 \tag{3}$$

subject to:

$$G_2 = (C_z - A)\sum_j Z_j + \sum_i C_i \sum_j E_{ij} \tag{4}$$

The first term in Equation 4 is the cost of the subsidised clean energy, while the second term is the cost of fossil energy. A limit may be set for the fractional subsidy (R) of clean energy cost, as in Equation 5:

$$A \le RC_z \tag{5}$$

The energy balance for each demand is:

$$Z_j + \sum_i E_{ij} = D_j \qquad \forall j \tag{6}$$

The first and second terms on the left hand side of Equation 6 indicate the amount of clean and fossil fuel allocated to a given sink, respectively. The carbon emission balance for each demand is:

$$\sum_i H_i E_{ij} \le F_j D_j \qquad \forall j \tag{7}$$

Equation 7 assumes that clean energy generates negligible carbon emissions, and that whatever emissions are generated by fossil fuel use should fall within the limits imposed by the leader. The energy balance for each source is:

$$\sum_j E_{ij} \le S_i \qquad \forall i \tag{8}$$

Equation 8 simply states that the amount of each energy source allocated to the sinks cannot exceed the available supply. In addition to these equations, all variables are non-negative. The corresponding non-negativity constraints are no longer listed here so as to save space. It can be seen that bilinear terms are present in Equations 2 and 4, and thus the model is a non-linear programming (NLP) formulation.

4.0 FUZZY BI-LEVEL PROGRAMMING MODEL

Fuzzy Model Parameters	
A'	Subsidy level per unit of clean energy based on follower's optimum
A^*	Subsidy level per unit of clean energy based on leader's optimum
F'_j	Carbon emission intensity limit per unit energy for sink j based on follower's optimum
F^*_j	Carbon emission intensity limit per unit energy for sink j based on leader's optimum
G'_1	Total cost burden to society based on follower's optimum
G^*_1	Total cost burden to society based on leader's optimum
G'_2	Total energy cost based on follower's optimum
G^*_2	Total energy cost based on leader's optimum
Fuzzy Model Variables	
λ	Fuzzy Degree of Satisfaction

The fuzzy approach to solving the general bi-level mathematical programming model was first proposed by Lai (1996) and Shih *et al.* (2001), and has since been developed further, for example by Lee (2001) and Sinha (2003). The general approach is applicable to both linear and non-linear problems.

The main steps are as follows:

- The model is solved as a single-level optimisation problem using the leader's objective function (Equation 1), and disregarding the follower's objective function (Equation 3). All the constraints (Equations 2a, 2b, 4 – 8) are also used in this step. This step determines the values of the objective functions G^*_1, G^*_2, and the leader's variables A^* and F^*_j. This is the solution if the leader is in a position to decide on the values of all the variables in the system. Inspection of the model clearly shows that finding the solution is trivial, and that the leader's preferred solution is $G^*_1 = A^* = F^*_j = 0$. Thus, the model reduces to an LP which can easily be solved to find a global optimum.
- The model is again solved as in the previous step, this time using the follower's objective function (Equation 3) and disregarding the leader's (Equation 1). As in the previous step, all the constraints (Equations 2a, 2b, 4 – 8) are considered. In this step, the values of G'_1, G'_2, and the leader's variables A' and F'_j are determined, which correspond to the solution if the follower was in control of all the variables in the system. It can also be seen easily that the follower will obviously prefer maximum subsidy and emission limits, which entails saturating the constraints given by Equations 2b and 5. Once these are set to the limiting values, the model again reduces to an LP for which the global optimum can be found readily.
- If the solutions in Steps 1 and 2 coincide, then they correspond to the exact Stackelberg strategy for the system. However, such cases will be rare. Thus, in general, it will be necessary to reconcile the conflict of interest between leader and follower. The procedure entails having the leader set fuzzy bounds for his objective and control variables; likewise, the follower also sets fuzzy bounds for his own objective function. Generally, these fuzzy bounds are subjectively defined (Lai, 1996; Lee, 2001; Shih ***et al.***, 2001; Sinha, 2003), but the solutions to Steps 1 and 2 can be used as basis for identifying reasonable values. The leader then relinquishes control to the follower, on the condition that his fuzzy bounds are used as constraints, in addition to all other constraints listed in the previous section. For simplicity, the fuzzy bounds are assumed to be defined by linear membership functions (Lai, 1996; Lee, 2001; Shih ***et al.***, 2001; Sinha, 2003) as follows:

$$G_1 - G'_1 \ge \lambda\,(G^*_1 - G'_1) \tag{9}$$

$$A - A' \ge \lambda\,(A^* - A') \tag{10}$$

$$F_j - F'_j \ge \lambda\,(F^*_j - F'_j) \qquad \forall j \tag{11}$$

$$G_2 - G^*_2 \ge \lambda\,(G'_2 - G^*_2) \qquad \forall j \tag{12}$$

- The variable λ which ranges from 0 to 1 is introduced as an index of fuzzy degree of satisfaction of the constraints. A solution is partially satisfactory in the fuzzy sense when $0 < \lambda < 1$. Note that when $\lambda \to 1$, G_1, A and F_j approach the optimal values from Step 1 while G_2 approaches the optimum from

Step 2. Hence, it is in effect possible to seek a compromise that may be considered as an approximate Stackelberg strategy (Tan *et al*., 2010) by maximising the value of λ:

$$\boldsymbol{max}\ \lambda \tag{13}$$

Thus, the original bi-level problem has been translated into an equivalent single-level fuzzy optimisation problem. The non-linear programming (NLP) model may then be solved using an appropriate optimisation algorithm. The next section describes the stochastic algorithm used in this work.

5.0 ADAPTIVE MULTI-PARTICLE SIMULATED ANNEALING (AMPSA)

AMPSA Nomenclature	
α	Random walk coefficient
β	Particle interaction coefficient
$\Delta_{k,t+1}$	Change in fitness value of the kth solution between successive iterations
$f(\boldsymbol{x}_{k,t+1})$	Fitness value of the kth candidate solution in iteration $t + 1$
$f(\boldsymbol{x}_{k,t})$	Fitness value of the kth solution in iteration t
$\boldsymbol{P}_{k,t+1}$	Probability of updating the kth solution
$\boldsymbol{r}_{k,t+1}$	Vector of random numbers in the interval [–0.5, 0.5]
$\boldsymbol{R}_{k,t+1}$	Matrix with diagonals comprised of random numbers in the interval [0, 1] and with all non-diagonal elements at 0
ρ	Adaptive cooling coefficient
s_t	Standard deviation of all fitness values in iteration t
T_t	Temperature in iteration t
$\boldsymbol{x}_{k,t+1}$	Vector of decision variables corresponding to the kth candidate solution in iteration $t + 1$
$\boldsymbol{x}_{1,t}$	Vector of decision variables corresponding to best solution in iteration t
$\boldsymbol{x}_{k,t}$	Vector of decision variables corresponding to kth solution in iteration t

This section describes the simulated annealing (SA) based stochastic algorithm used to solve the fuzzy NLP derived from the original bi-level model. SA was originally developed by Kirkpatrick *et al.* (1983) based on a mathematical analog of metallurgical annealing. In the latter, the crystalline lattice of a heated metallic substance is allowed to reach the lowest possible energy levels by means of slow cooling. The enhanced algorithm is described below.

The adaptive multi-particle simulated annealing (AMPSA) technique was developed by Tan (2008) for general optimisation problems encountered in process systems engineering applications. The algorithm combines features of SA and particle swarm optimisation (PSO); the latter optimisation method was developed by Kennedy and Eberhart (1995). Unlike conventional SA, it involves parallel search using multiple particles that interact among themselves in order to accelerate the search for near-optimal solutions. In every iteration, a candidate solution is determined through a random perturbation of each of the multiple particles or solutions currently present in the algorithm:

$$\boldsymbol{x}_{k,t+1} = \boldsymbol{x}_{k,t} + \alpha \boldsymbol{r}_{k,t+1} + \beta \boldsymbol{R}_{k,t+1}(\boldsymbol{x}_{1,k} + \boldsymbol{x}_{k,t}) \qquad \forall k,t \tag{14}$$

Equation 14 shows that the random perturbations consist of a random walk component (given by the second term on the right side of the equation) plus an interaction component (given by the last term) which biases the search of each particle towards the direction of the best solution currently available (*i.e.*, $k = 1$). Note that the final term disappears for the "lead particle" corresponding to the best solution. The next step is to determine whether the candidate solution determined by Equation 14 is to be accepted or not. The probability of acceptance is given by the Metropolis criterion:

$$\boldsymbol{P}_{k,t+1} = \boldsymbol{min}\left[1, e^{-\left(\frac{\Delta_{k,t+1}}{T_k}\right)}\right] \qquad \forall k,t \tag{15}$$

where:

$$\Delta_{k,t+1} = f(\boldsymbol{x}_{k,t+1}) - f(\boldsymbol{x}_{k,t}) \qquad \forall k,t \tag{16}$$

Equations 15 and 16 assume that the problem is one of function minimisation. If the new solution is better than the current one, then a "greedy" heuristic is employed and the new solution automatically replaces the old one. It thus becomes the starting point for the next iteration. If, however, the new candidate solution is worse than the previous one, it is not rejected outright. Instead, it is accepted with a probability defined by the exponential distribution in Equation 15. It can be easily seen that the probability of accepting such solutions declines as the extent of fitness deterioration increases. The probability distribution is modulated by the temperature parameter, which in AMPSA is a linear function of the standard deviation (or degree of diversity) of the currently available multiple solutions:

$$\boldsymbol{T}_t = \rho \boldsymbol{s}_t \qquad \forall t \tag{17}$$

In general, the diversity of the different solutions being computed in parallel declines as the algorithm progresses; as a result, the value of the temperature parameter falls as well. This achieves the cooling effect that is normally accomplished by geometric progression in conventional SA. In this case, the temperature is said to be adaptive since it responds to the quality of the solutions found by the algorithm to date.

It should be emphasized that, in practice, AMPSA, as with most stochastic algorithms, does not exhibit true convergence in the strict mathematical sense. Solutions found by such techniques are said to be "satisficing," *i.e.*, not strictly optimal, but highly satisfactory (or near-optimal) from the application standpoint. Furthermore, a stochastic algorithm will not necessarily give exactly the same solution each time when it is used to solve the same

optimization problem repeatedly. In this work, the algorithm was implemented in a program coded in Visual Basic for Applications (VBA) (Tan, 2008).

6.0 CASE STUDY

This illustrative case study is based on the example from Tan and Foo (2007), which involves the static allocation of clean or zero-carbon energy, along with coal, oil and natural gas, across three regions. Each region has a specified energy demand and a carbon emissions limit to be set by the leader. The data for the sources and sinks are shown in Table 1. The maximum allowable emissions limits in the final column correspond to carbon intensity limits of 20, 50 and 100 *kt/EJ* for Regions I, II, and III, respectively. However, the leader's objective is to minimise total costs to society, which consists of the cost to subsidise clean energy plus the external costs associated with carbon emissions.

Table 1: Energy sources and sinks (Tan and Foo, 2007) [16]

Source	Quantity (EJ)	Carbon footprint (kt/EJ)	Sink	Requirement (EJ)	Emissions limit (kt)
Coal	600	105	Region I	1000	20,000
Oil	800	75	Region II	400	20,000
Natural gas	200	55	Region III	600	60,000
Zero-carbon	No limit	0	Total	2000	100,000

Table 2: Solution to case study

Variable	Leader's model	Follower's model	Fuzzy limits	Fuzzy model solved by AMPSA
λ	n/a	n/a	n/a	0.11 ± 0.02
G_1(10^3 cost units)	0	390	0 – 390	315 ± 10
G_2 (10^3 cost units)	3,200	2,353	2,353 – 2,700	2,662 ± 8
A (cost units/*EJ*)	0	320	0 – 200	180 ± 4
F_1 (*kt/EJ*)	0	20	0 – 12	9.0 ± 1.5
F_2 (*kt/EJ*)	0	50	0 – 40	29.2 ± 5.7
F_3 (*kt/EJ*)	0	100	0 – 50	39.9 ± 5.8
Z_1 (*EJ*)	1,000	773	n/a	902 ± 15
Z_2 (*EJ*)	400	133	n/a	274 ± 32
Z_3 (*EJ*)	600	0	n/a	344 ± 44
E_{11} (*EJ*)	0	100	n/a	70 ± 24
E_{12} (*EJ*)	0	0	n/a	81 ± 34
E_{13} (*EJ*)	0	500	n/a	159 ± 57
E_{21} (*EJ*)	0	127	n/a	22 ± 21
E_{22} (*EJ*)	0	267	n/a	41 ± 44
E_{23} (*EJ*)	0	100	n/a	97 ± 77
E_{31} (*EJ*)	0	0	0	0
E_{32} (*EJ*)	0	0	0	0
E_{33} (*EJ*)	0	0	0	0

Table 3: Example of a satisficing energy allocation network (values given in EJ)

	Zero-carbon	Coal	Oil	Natural gas
Region I	933	24	43	0
Region II	275	110	16	0
Region III	327	219	54	0
Excess	n/a	248	687	200

Here it is assumed that the maximum acceptable value for the subsidy ($\boldsymbol{A}$) is 320 cost units per *EJ*, equivalent to 20% of the cost of clean energy, while the coefficient for environmental costs is B = 1 unit per kiloton (***kt***) of CO_2. The follower seeks to minimize the cost of supplying energy to the different sinks, assuming that the costs of clean energy, coal, oil and natural gas are 1,600, 1,000, 1,200 and 1,250 units per *EJ*, respectively. In this case study, fictitious cost units are used but the relative magnitudes of the coefficients are based on realistic assumptions. A similar approach to costing is used by Pękala *et al.* (2010).

Solving the model using the leader's objective function while disregarding the follower's objective (Step 1) gives the result in the second column of Table 2. Note that this step assumes that the leader is able to dictate all decisions within the system. Since this step reduces the model to *LP*, the solution can be easily found using any optimization software; in this case, Lingo 11.0 was used. The optimal level of subsidy ($\boldsymbol{A}$) as well as the emission limits ($\boldsymbol{F_1}$, $\boldsymbol{F_2}$ and $\boldsymbol{F_3}$) are all zero, which leads to the external costs borne by society ($\boldsymbol{G_1}$) to be zero as well. These limits force the follower to use only zero-carbon energy sources to meet the demands of the three regions, such that fossil energy use ($\boldsymbol{E_{ij}}$ for all $\boldsymbol{i}$ and $\boldsymbol{j}$) becomes zero throughout the system. The corresponding cost for the follower ($\boldsymbol{G_2}$) becomes $3{,}200 \times 10^3$ units.

On the other hand, Step 2 involves solving the model using the follower's objective function, while disregarding the leader's, which then gives the result in the third column of Table 2. Here it is assumed that the follower dictates the decisions; the model again reduces to a simple *LP* which is solved here with Lingo 11.0. Thus, subsidy level for clean energy ($\boldsymbol{A}$) as well as regional emission limits $\boldsymbol{F_1}$, $\boldsymbol{F_2}$ and $\boldsymbol{F_3}$) reach their maximum levels, which leads to an external cost ($\boldsymbol{G_1}$) of 390×10^3 units, while the total of energy costs ($\boldsymbol{G_2}$) is at the minimal level of $2{,}353 \times 10^3$ units. Note that the energy sources used are 906 *EJ* (773 + 133 + 0 *EJ*) of clean energy, 600 *EJ* (100 + 0 + 500 *EJ*) of coal and 494 *EJ* (127 + 267 + 100 *EJ*) of oil. Interestingly, there is no usage of natural gas at all in either the leader's or the follower's solution. Thus, the use of this fuel may be excluded from the fuzzy model as well.

The next step is to determine the fuzzy bounds for the leader's control variables and objective function, relative to his previously determined optimum. The fuzzy range for the follower's objective function is also determined. It should be noted that, in general, these limits may be determined subjectively (Lai, 1996; Shih *et al.*, 2001, Lee, 2001 and Sinha, 2003); however, the solutions to Steps 1 and 2 provide some indication of reasonable numerical values to be used so that a partially acceptable solution can be found. These ranges are given in the fourth column of Table 2 and are then integrated into a single, unified fuzzy NLP model, as described previously. The model is then solved for a near-optimal or satisficing solution using an AMPSA program coded in VBA (Tan 2008). This program has twenty particles and terminates after 1,000 iterations, which gives a total of 20,000 function evaluations ($20 \times 1{,}000$) per run. As with most stochastic algorithms, AMPSA does not exhibit convergence towards an optimum in the strict mathematical sense, but in general will yield satisficing solutions if properly tuned. The final column of Table 2 shows the range of values (average ± standard deviation) found for ten repeated runs using AMPSA. It can be seen that the results for λ as well as the leader's and follower's objectives ($\boldsymbol{G_1}$ and $\boldsymbol{G_2}$) are fairly consistent. On the other hand, there is considerable variation in the final values of the decision variables, with the exception of the level of subsidy ($\boldsymbol{A}$). This result indicates that the problem exhibits degeneracy – *i.e.*, there may be multiple solutions that exhibit the same optimal or near-optimal objective function values.

Table 3 shows an example of an allocation network for which $\lambda = 0.10$, $\boldsymbol{A} = 180$ cost units/*EJ*, $\boldsymbol{F_1} = 5.8$ *kt/EJ*, $\boldsymbol{F_2} = 31.7$ *kt/EJ* and $\boldsymbol{F_3} = 45.1$ *kt/EJ*. This solution is randomly selected from the ten runs implemented for the case study; it must be emphasized that it is only one of many possible schemes that achieves an approximate Stackelberg strategy. In this case, the resulting objective function values are $\boldsymbol{G_1} = 322 \times 10^3$ cost units for the leader and $\boldsymbol{G_2} = 2{,}666 \times 10^3$ cost units for the follower; it may be seen that both of these values fall within the statistical range of variation given in Table 2. Note that, in this solution, the three region use a combined 1,535 *EJ* (933 + 275 + 327 *EJ*) of clean energy, as compared to only 906 *EJ* without the leader's intervention in the form of carbon emission limits and subsidies. Thus, by using an approximate Stackelberg strategy, the leader is able to induce environment-friendly behavior even when the decision of the follower is motivated purely by cost considerations.

7.0 CONCLUSION

A hybrid approach to the determination of approximate Stackelberg solutions in bi-level carbon-constrained energy planning problems has been developed. This technique assumes that the upper level decision-maker, or leader, controls the emission limits to be imposed on the lower-level decision-maker, or follower, as well as subsidy levels for clean energy sources. The leader (*i.e.*, government) seeks to minimise total costs to society as a result of environmental impacts as well as the direct expense of the clean energy subsidy. On the other hand, the follower (*i.e.*, industry) is assumed to control the actual allocation of energy sources to different demands in order to minimise energy costs while meeting the emission limits imposed by the leader. The solution procedure involves relaxing the conflicting solutions of

the leader and follower to yield a fuzzy non-linear program (NLP); a satisficing or near-optimal solution can then be found using an adaptive, multi-particle simulated annealing algorithm (AMPSA). As demonstrated by a numerical case study, the model makes it is possible for the leader to identify appropriate emission limits and subsidy levels to induce the follower to allocate energy sources in an environmentally responsible manner, even when the latter's principal goal is to minimize costs. Further research can still be done to extend the model to more realistic cases by relaxing some of the simplifying assumptions used in this paper.

ACKNOWLEDGEMENT

The author wishes to acknowledge the financial support of De La Salle University through the University Research Coordination Office. Special thanks are also due to Prof. Jose B. Cruz, Jr. for helpful inputs on the concept of Stackelberg games. ■

REFERENCES

[1] Atkins, M. J., Morrison, A. S. and Walmsley, M. R. W. 2010. Carbon Emissions Pinch Analysis (CEPA) for emissions reduction in the New Zealand electricity sector. Applied Energy 87: 982 – 987.

[2] Bandyopadhyay, S., Sahu, G., Foo, D. C. Y. and Tan, R. R. 2010. Segregated targeting for multiple resource networks using decomposition algorithm. AIChE Journal 56: 1235 – 1248.

[3] Bard, J. F. 1998. Practical bilevel optimization. Algorithms and applications. Kluwer Academic Publishers, Dordrecht.

[4] Foo, D. C. Y., Tan, R. R., and Ng, D. K. S. 2008. Carbon and Footprint-Constrained Energy Sector Planning Using Cascade Analysis Technique, Energy, 33, 1480-1488.

[5] Kennedy, J. and Eberhart, R., 1995, Particle swarm optimization, Proceedings of the IEEE International Conference on Neural Networks, Perth, Australia 1942–1948.

[6] Kirkpatrick, S., Gelatt, C.D. and Vecchi, M.P. 1983. Optimization by simulated annealing. Science 220: 671 – 680.

[7] Lai, Y. J. 1996. Hierarchical optimization: a satisfactory solution. Fuzzy Sets and Systems 77: 321 – 335.

[8] Lee, E. S. 2001. Fuzzy multiple level programming. Applied Mathematics and Computation 120: 79 – 90.

[9] Lee, S. C., Ng, D. K. S., Foo, D. C. Y. and Tan, R. R. 2009. Extended pinch targeting techniques for carbon-constrained energy sector planning. Applied Energy 86: 60 – 67.

[10] Pękala, L. M., Tan, R. R., Foo, D. C. Y. and Jeżowski, J. J. 2010. Optimal energy planning models with carbon footprint constraints. Applied Energy 87: 1903 – 1910.

[11] Salman, M.A. and Cruz, J. B., Jr. 1981. An incentive model of duopoly with government intervention. Automatica 17: 821-829.

[12] Shih, H. S., Lai, Y. J. and Lee, E. S. 1996. Fuzzy approach for multi-level programming problems. Computers and Operations Research 23: 73 – 91.

[13] Simaan, M. and Cruz, J. B., Jr. 1973. On the Stackelberg strategies in non-zero sum games. Journal of Optimization Theory and Applications 11: 533 – 555.

[14] Sinha, S. 2003. Fuzzy mathematical programming applied to multi-level programming problems. Computers and Operations Research 30: 1259 – 1268.

[15] Stackelberg, H.V. 1952. The theory of the market economy. Oxford University Press, London.

[16] Tan, R. R., and Foo. D. C. Y. 2007. Pinch Analysis Approach to Carbon-Constrained Energy Sector Planning, Energy, 32, 1422-1429.

[17] Tan, R. R. An Adaptive Swarm-Based Simulated Annealing Algorithm for Process Optimization. Presented at the 11th Conference on Process Integration, Modeling and Optimisation for Energy Saving and Pollution Reduction (PRES 2008), Prague, August 24 – 28, 2008.

[18] Tan, R. R., Ng, D. K. S. and Foo, D. C. Y. 2009a. Pinch analysis approach to carbon-constrained planning for power generation. Journal of Cleaner Production 17: 940 – 944.

[19] Tan, R. R., Foo, D. C. Y., Aviso, K. B. and Ng, D. K. S. 2009b. The Use of Graphical Pinch Analysis for Visualizing Water Footprint Constraints in Biofuel Production, Applied Energy, 86, 605 – 609.

[20] Tan, R. R., Aviso, K. B., Cruz, J. B., Jr. and Culaba, A. B. 2010. A Note on an Extended Fuzzy Bi-Level Optimization Approach for Water Exchange in Eco-Industrial Parks with Hub Topology. Process Safety and Environmental Protection (in review).

[21] Tjan, W., Tan, R. R. and Foo, D. C. Y. 2010. A graphical representation for carbon footprint reduction in chemical processes. Journal of Cleaner Production 18: 848 – 856.

PROFILE

RAYMOND R. TAN

Raymond R. Tan is a Full Professor of Chemical Engineering and University Fellow at De La Salle University, Manila, Philippines. His main research interests are process systems engineering, life cycle assessment and pinch analysis. Prof. Tan received his BS and MS in chemical engineering and PhD in mechanical engineering from De La Salle University, and is the author of more than fifty published and forthcoming articles in ISI-indexed journals in the fields of chemical, environmental and energy engineering. He is a member of the editorial board of the journal *Clean Technologies and Environmental Policy* and co-editor of the forthcoming book *Recent Advances in Sustainable Process Design and Optimization*. He is also the recipient of multiple awards from the Philippine National Academy of Science and Technology (NAST) and the National Research Council of the Philippines (NRCP).

OPTIMISATION OF HYDROLYSIS CONDITIONS FOR ETHANOL PRODUCTION FROM SORGHUM STARCH

(Date received: 28.2.2010/ Date accepted: 18.8.2010)

Najiah Nadir[1], Maizirwan Mel[2], Mohamed Ismail Abdul Karim[3] and Rosli Mohd Yunus[4]
[1, 2, 3] Bioprocess and Molecular Engineering Research Group,
Department of Biotechnology Engineering, Faculty of Engineering
International Islamic University Malaysia,
P. O. Box 10, 50728 Kuala Lumpur
[4] Department of Chemical Engineering,
Faculty of Chemical and Natural Resources Engineering
Universiti Malaysia Pahang, MEC City,
26300 Gambang, Kuantan, Pahang
E-mail: [1]najdir@yahoo.com

ABSTRACT

The conversion of starch to sugar can be achieved by hydrolysis process. The two-step enzymatic hydrolysis of sweet sorghum was performed by commercially available α-amylase and glucoamylase. An optimisation study was carried out to optimise the factors of the hydrolysis process, namely, amount of substrate, liquefaction and saccharification temperature, liquefaction and saccharification time, and amount of α-amylase and glucoamylase enzymes. The screening of significant hydrolysis factors were done by using the two-level factorial design (TLFD) under the factorial design (FD). The results indicated that the liquefaction and saccharification temperature, and amount of glucoamylase enzyme were found to be the major factors for further optimisation. The major factors for hydrolysis were optimised by the central composite design (CCD) under the response surface method (RSM). The analysis of variance (ANOVA) result showed that glucoamylase enzyme ($p < 0.0021$) and saccharification temperature ($p < 0.0181$) were significant factors for hydrolysis of sorghum starch. Also, the statistical analysis showed that the optimum dextrose equivalent (69.07% (g/g)) were obtained at 90°C of liquefaction temperature, 47°C of saccharification temperature, and 0.24% (v/w) of glucoamylase enzyme.

Keywords: *α-amylase, Glucoamylase, Liquefaction, Optimisation, Saccharification, Sorghum Starch*

1.0 INTRODUCTION

The world's leading manufacturers and industries are seeking to substitute petrochemical-based feedstock with agricultural-based materials as petroleum supplies continue to decline [1]. Great attention has been given to the ethanol production using various substrates which can be classified into three main types of materials, which are sugars (from sugarcane, sugar beet, sweet sorghum, molasses, and fruits), starches (from sweet sorghum grain, cassava, corn, potato, and root crops), and cellulose materials (from agricultural residue, wood, and paper mills) [2], because of the increase in demand for ethanol which is considered as an alternative energy source [3]. Furthermore, the commercial success of amylases is associated to utilisation of starchy biomass as an industrial raw material. Agricultural substrates like corn, wheat, sorghum and other cereal grains contain around 60-75% (w/w) starch on a dry basis, hydrolysable to glucose and thus offer a good resource in fermentation processes [4].

Sweet sorghum (*Sorghum biocolor* (L.) Moench) is one of the most favourable crops for industrial applications [1]. Sorghum is a C_4 plant characterised by a high biomass- and sugar-yielding crop [5]. It contains approximately equal quantities of soluble (glucose and sucrose) and insoluble carbohydrates (cellulose and hemicellulose) [6]. Sweet sorghum has the ability of remaining dormant during the driest periods and is often judged to be one of the most drought resistant agricultural plants [7; 8]. Thus, it can be planted primarily in semiarid and dried parts of the world, especially in areas too dry for maize [1]. Also, it has been considered as an important energy plant for the production of fuel bioethanol [9].

Sweet sorghum grain is a starch-rich grain [1]. Starch consists of two types of polysaccharides, the linear molecule, amylose and a highly branched molecule, amylopectin [10]. Amylose is a linear molecule of (1→4) linked α-D-glucopyranosyl units (α-D-(1→4)-glucan), but it is well established that some molecules are slightly branched by (1→6)-α-linkages. Meanwhile,

amylopectin is a highly branched component of starch formed through chains of α-D-glucopyranosyl residues linked together mainly by (1→4) linkages but with 5-6% of (1→6) bonds at the branch points. It is a branched polysaccharide composed of hundreds of short (1→4)-α-glucan chains, which are interlinked by (1→6)-α-linkages [11; 12]. In most common types of cereal endosperm starches, the relative weight percentages of amylose range between 18-33% and amylopectin range between 72-82% [11].

Starchy grains and effluent generated from starch processing units are the cheap feedstocks and could be used as potential raw materials for ethanol fermentation [13]. The sweet sorghum starch hydrolysis may be regarded as a first and important step in sorghum processing for bioethanol production [12]. Enzymatic hydrolysis is essential for the production of glucose syrups from starch because of the specificity of enzymes allows the sugar syrups production with well-defined physical and chemical properties and the milder enzymatic hydrolysis results in few side reactions and less "browning" [2]. Conventional process for production of bioethanol from starch basically involved a three-stage process; liquefaction of starch by α-amylase, saccharification of liquefied starch by glucoamylase and followed by fermentation of sugar to ethanol using *Saccharomyces cerevisiae* [12].

The aim of this study was to investigate the liquefaction and saccharification processes of sweet sorghum by commercially available α-amylase and glucoamylase. In order to achieve the optimum conditions, the present study was carried out in two stages: firstly, the two-level factorial design was applied to select the most significant conditions of starch hydrolysis such as the substrate and enzyme concentrations, and the temperature and time required for the enzymatic action, which affect glucose production. Secondly, the central composite design (CCD) was employed to obtain the optimum level of the significant factors by developing a model followed by other statistical tests such as analysis of variance (ANOVA), coefficient of determination, 2D contour and 3D surface plots for the glucose production of from sweet sorghum starch.

2.0 MATERIALS AND METHODS

2.1 Substrates

Sweet sorghum grains were obtained from Indonesian Bioenergy Foundation and blended into small size of approximately 20 μm to enhance the hydrolysis process.

2.2 Enzymes

Both α-amylase from *Bacillus subtilis* and glucoamylase from *Aspergillus niger* were obtained from enzyme industry in Jakarta, Indonesia. The activities of the two enzymes were identified to be 25,000 U/mL and 130,000 U/mL, respectively.

2.3 Hydrolysis

The shake flask was filled with 100 ml of distilled water and heated to 80°C. Then, 25 g of sweet sorghum was added to the flask (to make 25% (w/v) of substrate). After that, 0.2% (v/w) of α-amylase (from the amount of sorghum) was added and the mixture was cooked at 80 °C and mixed at 250 rpm for 1 h. After 1 h, the mixture was cooled down to 60 °C and 0.1% (v/w) of glucoamylase was added and the mixture was left for 4 h with 250 rpm agitation.

2.4 Enzymes

Samples for dextrose equivalent (DE) determinations were centrifuged at 5000 rpm for 30 min to remove the substrates. The supernatant was filtered through a 0.45 μm membrane and analysed by high performance liquid chromatography (HPLC) equipped with a refractive index detector. The column used for separation was a SUPELCOGEL C-610H column. 10 μl of sample was injected into HPLC and separation was performed at 30 °C with 0.1% H_3PO_4 as the mobile phase at a flow rate of 0.5 mL/min. Glucose was used as a standard. DE was calculated as follows:

$$DE = \frac{g\ reducing\ sugar\ expressed\ as\ glucose}{g\ dry\ solid\ weight} \times 100 \quad (1)$$

2.5 Experimental design

2.5.1 Two-level factorial design

The two-level factorial design was used to identify which factors of hydrolysis process have significant effects on the response, DE. The factors selected for the experiment were the amount of substrate (A, % (w/v)), liquefaction temperature (B, °C), liquefaction time (C, h), amount of α-amylase [D, % (v/w)], saccharification temperature (E, °C), saccharification time (F, h), and amount of glucoamylase [G, % (v/w)]. The factors were examined at two different levels (low and high) coded (1 and 2, respectively) as shown in Table 1. This design gave an output of eight experimental runs (combinations) with seven independent variables. All the experiments were performed in triplicate and the average of DE was used as the response (dependant variable). The two-level factorial design is based on the first order model which is as follows:

$$Y = b_0 + \sum b_i x_i \quad (2)$$

where Y is the response (DE value), b_0 is the model intercept and b_i is the linear coefficient, and x_i is the level of the independent variable. This model does not describe the interaction among the factors and it is used to evaluate and select the important factors that influence the response.

Table 1: Independent variables in the two-level factorial experimental design

Variables	Symbol	Coded levels	
		1	2
Amount of substrate, % (w/v)	A	25	35
Liquefaction temperature, °C	B	80	90
Liquefaction time, h	C	1	2
Amount of α-amylase, % (v/w)	D	0.1	0.2
Saccharification temperature, °C	E	50	60
Saccharification time, h	F	2	4
Amount of glucoamylase, % (v/w)	G	0.1	0.2

2.5.2 Central composite design

The central composite design was used to demonstrate the nature of the response surface in the experimental region and clarify the optimal conditions of the most significant independent variables. Three major variables namely liquefaction temperature (X_1, °C), saccharification temperature (X_2, °C), and amount of glucoamylase [X_3, % (v/w)] were included in this model. The factors were examined at five different levels (relatively low, low, basal, high, relatively high) coded (-2, -1, 0, +1, + 2) as shown in Table 2. Other variables were fixed from the result of the two-level factorial design. According to the CCD for three variables, 20 experimental runs (6 runs at centre point) were executed and the results were fitted to the following second order polynomial model:

$$Z = \beta_0 + \beta_1 X_1 + \beta_2 X_2 + \beta_3 X_3 + \beta_{11} X_1^2 + \beta_{22} X_2^2 + \beta_{33} X_3^2 + \beta_{12} X_1 X_2 + \beta_{13} X_1 X_3 + \beta_{23} X_2 X_3 \quad (3)$$

where Z is the dependent variable (dextrose equivalent); X_1, X_2 and X_3 are the independent variable (liquefaction temperature, saccharification temperature and amount of glucoamylase); β_0 is the regression coefficient at centre point; β_1, β_2 and β_3 are the linear coefficients; β_{11}, β_{22} and β_{33} are the quadratic coefficients; and β_{12}, β_{13} and β_{23} are the second order interaction coefficients.

Table 2: Independent variables in the central composite experimental design

Variables	Symbol	Coded levels				
		-2	-1	0	+1	+2
Liquefaction temperature, °C	X_1	75	80	85	90	95
Saccharification temperature, °C	X_2	40	45	50	55	60
Amount of glucoamylase, % (v/w)	X_3	0.10	0.15	0.20	0.25	0.30

The developed regression model was calculated by analysing the values of regression coefficients, analysis of variance (ANOVA), *p*- and *F*-values. The quality of fit of the model equation was confirmed by the coefficient of determination, R^2. The statistical software package Design-Expert®6.0.8 (Stat Ease Inc., Minneapolis, USA) was used to identify the experimental design as well as to establish a regression model to predict the optimum combinations considering the effects of linear, quadratic and interaction on dextrose equivalent value.

3.0 RESULTS AND DISCUSSION

3.1 Screening of significant hydrolysis parameters for glucose production using two-level factorial design

Seven hydrolysis parameters were screened by the two-level factorial design, which showed eight experimental runs for glucose production (Table 3). The main effect of each parameter on dextrose equivalent was estimated as the difference between the average of the measurements made at the low (1) and high level (2) of the factors. The main effects of each hydrolysis parameter are shown in Figure 1.

Table 3: The two-level factorial design for the screening of hydrolysis parameters

Run	*Factors*							*Response*
	A [% (w/v)]	*B (°C)*	*C (h)*	*D [% (v/w)]*	*E (°C)*	*F (h)*	*G [% (v/w)]*	*Y [% (w/w)]*
1	25	80	1	0.2	60	4	0.1	27.70
2	35	80	1	0.1	50	4	0.2	51.97
3	25	90	1	0.1	60	2	0.2	54.28
4	35	90	1	0.2	50	2	0.1	51.26
5	25	80	2	0.2	50	2	0.2	61.62
6	35	80	2	0.1	60	2	0.1	20.67
7	25	90	2	0.1	50	4	0.1	52.04
8	35	90	2	0.2	60	4	0.2	41.73

The screening results were analysed using the analysis of variance (ANOVA) as appropriate to the experimental design used as shown in Table 4. The computed *F*-value (46.87) indicates that the model was highly significant at high confidence level. The probability *p*-value was also relatively low (*p*-value > *F* = 0.0210) which indicates the significance of the model. The Fisher variance ratio, the *F*-value is a statistically valid measure of how well the factors describe the variation in the mean of data. The greater the *F*-value indicates that the factors explain adequately the variation in the data about its mean, and the estimated factor effects are real. Also, the *F*-value is inversely proportional to *p*-value > *F*. Higher *F*-value will result to lower *p*-value > *F*.

Table 4: Analysis of variance (ANOVA) for screening

Source	Sum of Squares	*F*-value	*p*-value > *F*
Model	1389.47	46.87	0.0210
A	112.59	18.99	0.0488
B	174.31	29.40	0.0324
E	657.19	110.83	0.0089
F	25.88	4.36	0.1719
G	419.51	70.75	0.0138

For the independent variables, the *p*-value for saccharification temperature is the lowest (0.0089), followed by amount of glucoamylase (0.0138), liquefaction temperature (0.0324), amount of substrate (0.0488), and lastly saccharification time (0.1719). The *p*-values were used to check the significance of each coefficient. The lower the *p*-value indicates the more significant correlation of coefficients (*p*-value < 0.05 indicate the model terms are significant; *p*-value < 0.01 indicate the model terms are highly significant).

When the factor is highly significant, the small change in the factor (either increase or decrease) will give big impact on the response. Positive effect means increasing the factor will result to an increase in the response while negative effect means reducing the factor will result to an increase in the response. Linear and quadratic effects of parameters were significant, meaning that they can act as limiting factor and little variation in their value would change either the growth rate or the product formation rate or both to a considerable extent [14].

From the plot in Figure 1, three factors, which are liquefaction temperature, the amount of α-amylase and glucoamylase gave positive effect to the response. On the other hand, the amount of substrate, liquefaction time, saccharification temperature and time, gave negative effect to the response. The results showed that the highest value represents the most significant factor, by considering the absolute value only (neglect the positive and negative sign). The saccharification temperature gave highest impact on dextrose equivalent, followed by amount of glucoamylase, liquefaction temperature, amount of substrate, saccharification time, liquefaction time, and lastly amount of α-amylase enzyme. Positive linear coefficient means positive effect and vice versa. Therefore, the most important factors that affect the hydrolysis process of sweet sorghum are the liquefaction and saccharification temperature, and glucoamylase enzyme.

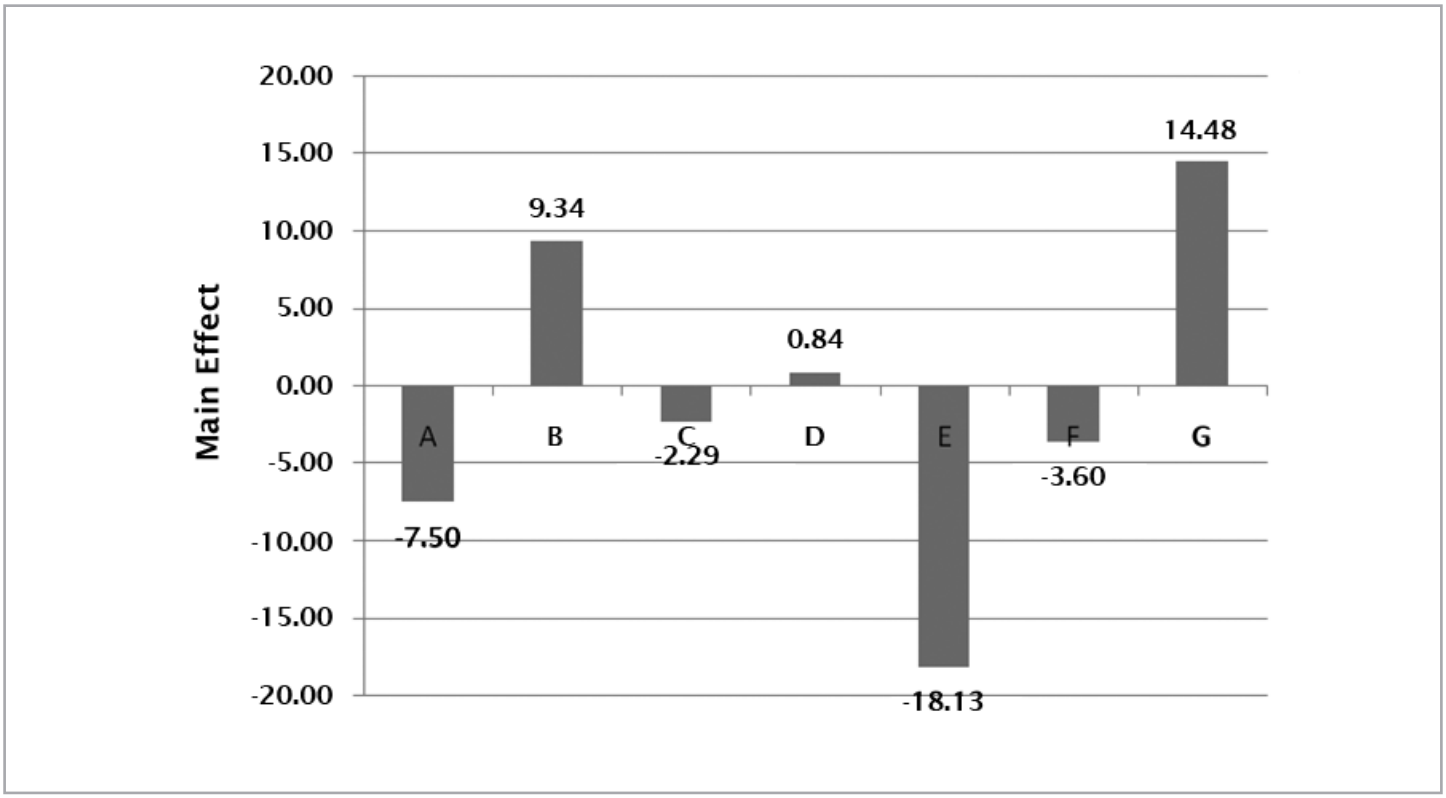

Figure 1: Main effects of the hydrolysis parameters on dextrose equivalent

In this study, the substrate concentration has negative effect on hydrolysis process, which means lower amount of substrate gives higher amount of dextrose equivalent. According to Mojović et al. [12], the substrate concentration had a pronounced effect on the starch hydrolysis and the ethanol fermentation. Regarding the yields, lower amount of substrate is more appropriate as substrate inhibition could be avoided. Furthermore, Aggarwal *et al*. [15] mentioned that 25% (w/v) of sorghum slurry was more appropriate for liquefaction process. This is because, at 35% (w/v), the mixing and homogenization were less efficient as the viscosity of the slurry is very high. Thus, the maximum concentration of sorghum slurry that suitable for liquefaction was observed to be 25% (w/v). This is because at lower substrate concentration, mixing and homogenisation of the reaction mixture was possible [16].

The liquefaction time has slightly negative effect on the amount of DE. As the liquefaction time increases, the amount of DE decreases. This is because the longer exposure of the enzyme to high temperatures, which are needed for gelatinisation of the starch granules and for achieving a good susceptibility to enzyme action, could lead to slight enzyme deactivation [12]. According to Shewale and Pandit [16], liquefaction of sorghum slurry 25% (w/v) was completed in only 1 hour.

For α-amylase enzyme, it provides very low positive effect on the DE. In one study, Shewale and Pandit [16] found that liquefaction of 25% (w/v) sorghum slurry was completed in 1 h with B. *licheniformis* α-amylase (BLA) concentration of 0.08% (v/w) of flour in the absence of $CaCl_2$ supplementation. However, Aggarwal *et al*. [15] mentioned that the optimum α-amylase enzyme concentration was 0.15% (v/w) for 1 h of liquefaction time, which is higher than the concentration used in this study.
The saccharification time has slightly lower negative effect on DE production compared to the effect of saccharification temperature. As the saccharification time increases, the amount of DE produced decreases. Ejiofor *et al*. [17] saccharified cassava starch at 55 °C only for 2 h.

3.2 Optimisation of hydrolysis parameters for glucose production using central composite design

The significant hydrolysis parameters such as liquefaction and saccharification temperature, and glucoamylase enzyme as independent variables were optimised for the maximum glucose production from sorghum starch. Experiments were carried out as designed by using central composite design (CCD) (Table 5), and the average glucose production obtained was used as the response. The optimal values of glucose produced within the experimental constrains were predicted by fitting a second order polynomial model to the experimental results for the dextrose equivalent by the Design-Expert software (v 8.0). The regression model developed relating the variables are as follows:

$$Z = 1492.04 + 17.68X_1 + 27.94X_2 + 897.52X_3 - 0.09X_1^2 - 0.22X_2^2 - 1782.18X_3^2 - 0.06X_1X_2 + 2.54X_1X_3 - 5.68X_2X_3 \quad (4)$$

where the dextrose equivalent (Z) is a function of liquefaction temperature (X_1), saccharification temperature (X_2) and amount of glucoamylase (X_3).

Table 5: The central composite design for the optimization of hydrolysis parameters

Run	Factors			Response	
	X_1 (°C)	X_2 (°C)	X_3 (% (v/w))	Z (% (w/w))	
				Observed	Predicted
1	80	45	0.15	38.62	44.73
2	90	45	0.15	54.98	52.39
3	80	55	0.15	44.54	42.69
4	90	55	0.15	47.24	44.11
5	80	45	0.25	52.26	57.96
6	90	45	0.25	63.74	68.15
7	80	55	0.25	45.08	50.24
8	90	55	0.25	57.74	54.19
9	75	50	0.20	55.92	49.64
10	95	50	0.20	57.54	61.25
11	85	40	0.20	55.20	49.67
12	85	60	0.20	30.70	33.67
13	85	50	0.10	32.48	34.49
14	85	50	0.30	62.38	57.80
15	85	50	0.20	62.24	63.97
16	85	50	0.20	62.12	63.97
17	85	50	0.20	62.36	63.97
18	85	50	0.20	66.14	63.97
19	85	50	0.20	70.40	63.97
20	85	50	0.20	63.12	63.97

At the model level, the correlation measures for the estimation of the regression equation are the determination coefficient R^2. The correlation between the observed and predicted values is better when the value of R^2 is closer to 1. In this experiment, the value of R^2 was 0.8636. This value indicates a high degree of correlation between the observed and predicted values. The value of R^2 indicates that 86.36% of the variables: liquefaction temperature, saccharification temperature and amount of glucoamylase play an important role to the response. The value of R^2 is also a measure of fit of the model and it can be mentioned that only about 13.64% of the total variations were not explained by the dextrose equivalent [18].

Table 6: Analysis of variance (ANOVA) for optimisation

Source	Sum of Squares	*F*-value	*p*-value > *F*
Model	2038.28	7.04	0.0026
X_1	134.79	4.19	0.0679
X_2	256.00	7.95	0.0181
X_3	543.36	16.88	0.0021
X_1^2	114.12	3.55	0.0891
X_2^2	781.58	24.29	0.0006
X_3^2	499.11	15.51	0.0028
X_1X_2	19.47	0.60	0.4547
X_1X_3	3.23	0.10	0.7581
X_2X_3	16.13	0.50	0.4951

The optimization results were analysed using the analysis of variance (ANOVA) as appropriate to the experimental design used as shown in Table 6. The computed *F*-value (7.04) indicates that the model was significant at high confidence level. The probability p-value was also relatively low (p-value > F = 0.0026) indicates the significance of the model. It was observed that the linear and square terms of both saccharification temperature (X_2) and glucoamylase (X_3) were significant ($p < 0.05$). Meanwhile, the linear and square terms of liquefaction temperature (X_1), and also the interactive terms between liquefaction temperature and saccharification temperature (X_1X_2), liquefaction temperature and glucoamylase (X_1X_3) and saccharification temperature and glucoamylase (X_1X_3) shown in the ANOVA analysis were not significant ($p > 0.05$).

The 2D contour plots and 3D response surface are the graphical representation of the regression model used to determine the optimum values of the parameters within the considered ranges [19]. The 2D and 3D plots for the interaction between two variables among three the variables are shown in Figure 2 to Figure 4. The purpose of response surface is to determine the optimum values of the variables, which mean the response is at maximum value [19]. The contour plot represents an infinitive number of combinations of the two test variables while the other variable maintained at zero level (centre). The maximum predicted value is obtained from the surface confined in the smallest ellipse in the contour plot. Elliptical contours are obtained when there is a perfect interaction between the two independent variables [20]. Meanwhile, the 3D surface plot shows whether the ellipse in the contour plot is at maximum or minimum.

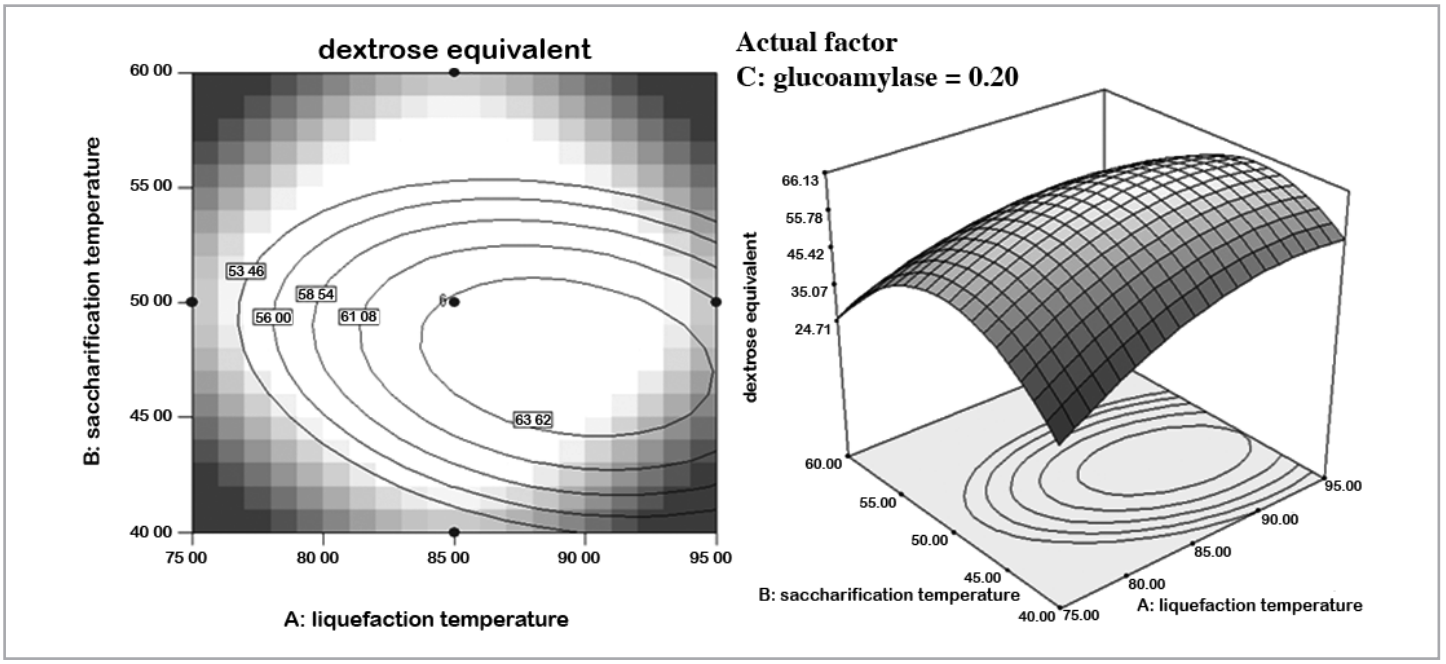

Figure 2: 2D contour plot and 3D response surface show the effect of liquefaction temperature (°C) and saccharification temperature (°C) on the dextrose equivalent [% (g/g)] [glucoamylase was 0.20 % (v/w)]

Figure 2 illustrates the elliptical response surface of dextrose equivalent from the interaction of liquefaction temperature and saccharification temperature. The predicted dextrose equivalent decreased at lower and higher values of ranges for both liquefaction and saccharification temperature. The maximum dextrose equivalent of about 66.13% (g/g) was predicted at liquefaction and saccharification temperature around 89 °C and 47 °C while glucoamylase concentration was 0.20% (v/w).

An elliptical response surface in Figure 3 shows the variation of dextrose equivalent as a function of liquefaction temperature and glucoamylase by making saccharification temperature a constant. About 67.14% (g/g) of maximum dextrose equivalent was obtained from the response surface at liquefaction temperature, glucoamylase concentration, and saccharification temperature was about 89 °C, 0.24% (v/w) and 50 °C, respectively.

Figure 4 is the response surface plot for the dextrose equivalent with the interaction of saccharification temperature and glucoamylase concentration. The maximum dextrose equivalent was predicted at given ranges of both saccharification temperature and glucoamylase concentration. Thus, the maximum dextrose equivalent of about 66.94% (g/g) was obtained when saccharification temperature around 47 °C, glucoamylase concentration was 0.24% (v/w), and liquefaction temperature was about 85 °C.

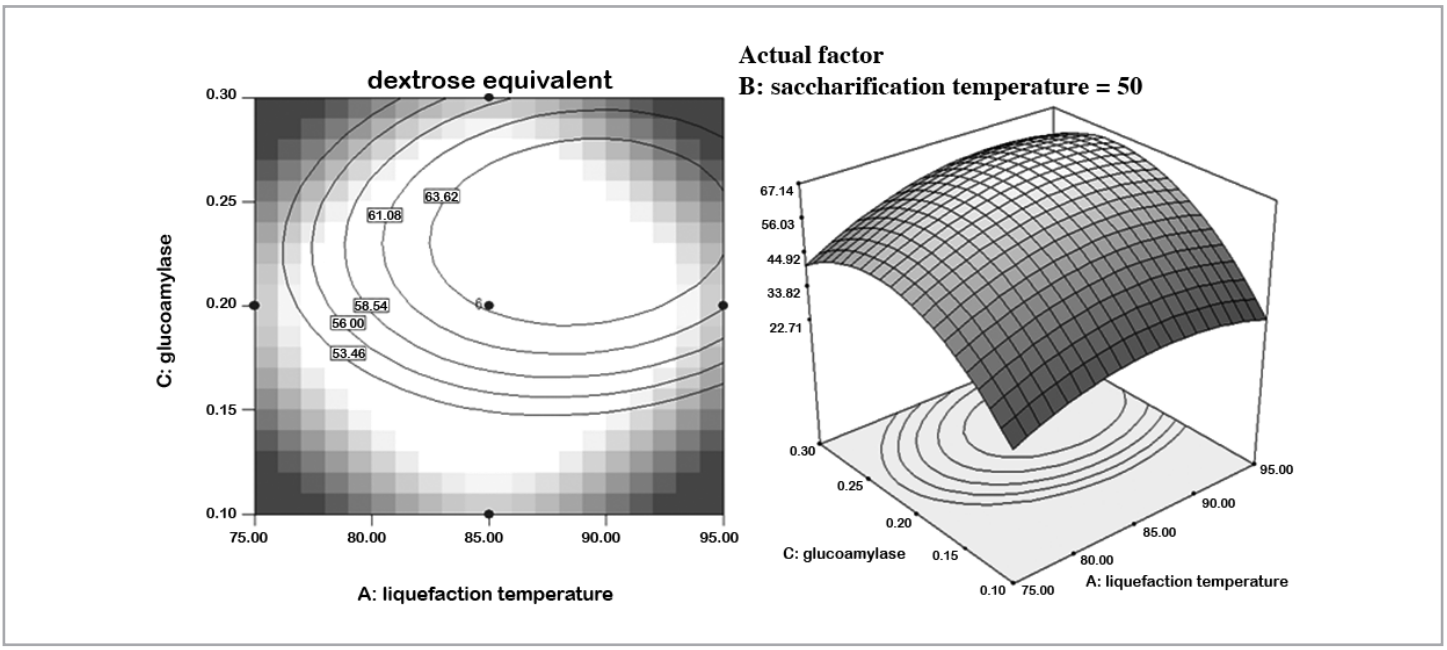

Figure 3: 2D contour plot and 3D response surface show the effect of liquefaction temperature (°C) and glucoamylase [% (v/w)] on the dextrose equivalent [% (g/g)] (saccharification temperature was 50 °C)

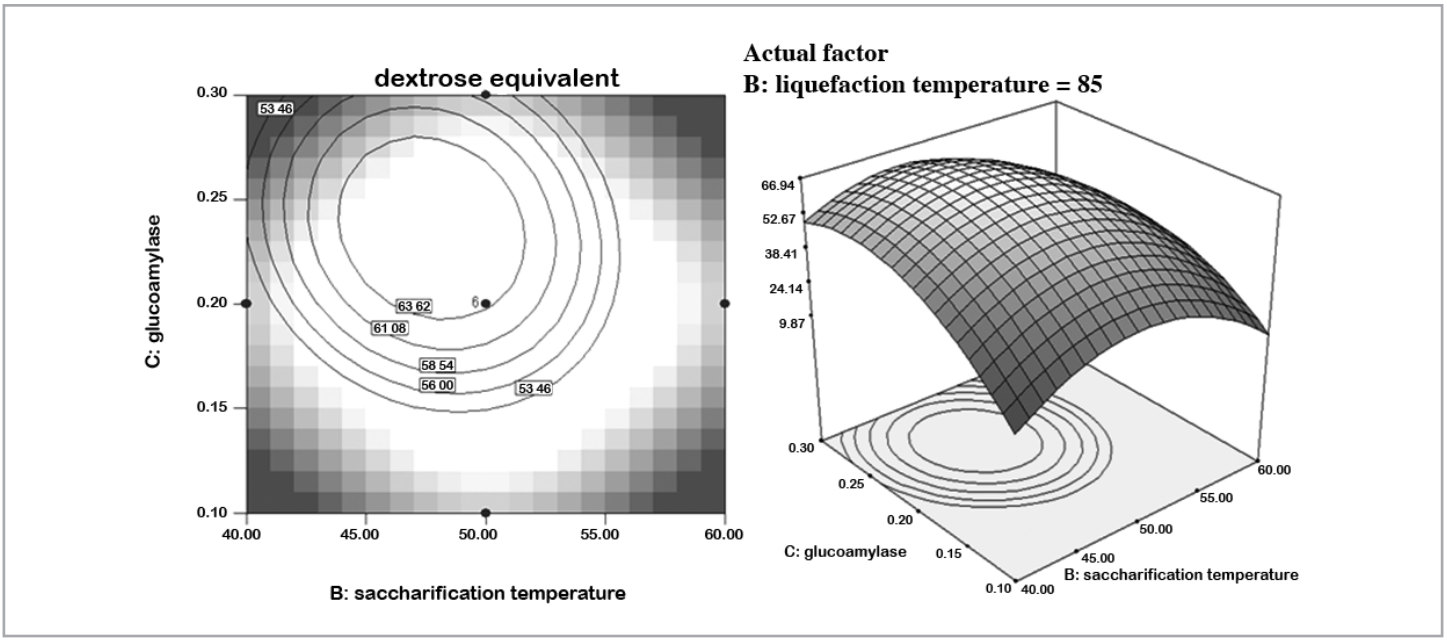

Figure 4: 2D contour plot and 3D response surface show the effect of saccharification temperature (°C) and glucoamylase [% (v/w)] on the dextrose equivalent [% (g/g)] (liquefaction temperature was 85 °C)

The optimum hydrolysis conditions for maximum dextrose equivalent of 69.07% (g/g) were predicted at 90 °C of liquefaction temperature, 47 °C of saccharification temperature, and 0.24% (v/w) of glucoamylase enzyme. Even though the liquefaction temperature is not significant, the interaction of all factors are significant since the probability *p*-value of the whole model was very low (*p*-value > *F* = 0.0026).

According to Shewale and Pandit [16], there are two effects occur simultaneously as the liquefaction temperature was increased from 75 to 95°C. The first one is when the gelatinisation rate of starch increases, and the second is when the dextrinisation rate of the starch molecules decreases due to enzyme deactivation at high temperatures. Therefore, there exists an optimum temperature for the liquefaction process. Moreover, for amylases to attack starch, the suspension should be brought to high temperatures (90-110 °C) for the breakdown of starch kernels [21]. The increase in hydrolysis of starch could also be connected to the effect of high temperature or heat on the weaker areas on the starch granule, allowing the enzyme to break the starch granules more extensively [10]. Aggarwal *et al*. [15] found that the maximum saccharification occurred at 45 °C as the rate of saccharification reduced substantially at higher temperature. Meanwhile, Shewale and Pandit [16] mentioned that 55 °C is the optimum temperature for saccharification to occur. Also, the glucoamylase enzyme activity increased progressively with an increase in temperature from 20 °C and reaching maximum at 60 °C [19].

4.0 CONCLUSION

In this study, three hydrolysis parameters, liquefaction and saccharification temperature, and amount of glucoamylase enzyme were selected by the two-level factorial design as the significant factors for dextrose equivalent. These factors were further optimized by using the central composite design. The dextrose equivalent of 61.62% (g/g) found during the screening process by two-level factorial design was increased to a predicted value of 69.07% (g/g) during optimisation using central composite design. The variables of saccharification temperature and glucoamylase concentration showed significant effects on the dextrose equivalent. ■

REFERENCES

[1] Zhan, X., Wang, D., Tuinstra, M.R., Bean, S., Seib, P.A., and Sun, X.S. (2003). "Ethanol and lactic acid production as affected by sorghum genotype and location." Ind. Crop. Prod., 18(3): pp245-255.

[2] Lin, Y., and Tanaka, S. (2006). "Ethanol fermentation from biomass resources: current state and prospects." Appl. Microbiol. Biotechnol., 69(6): pp 627-642.

[3] Lynd, L.R., Cushman, J.H., Nichols, R.J., and Wyman, C.E. (1991). "Fuel ethanol from cellulosic biomass." Science, 251(4999): pp1318-1323.

[4] Nigam, P., and Singh, D. (1995). "Enzyme and microbial system involved in starch processing." Enzyme Microb. Technol., 17(9): pp770-778.

[5] Bryan, W.L. (1990). "Solid-state fermentation of sugars in sweet sorghum." Enzyme Microb. Technol., 12(6): pp437-442.

[6] Jasberg, B.K., Montgomery, R.R., and Anderson, R.A. (1983). "Preservation of sweet sorghum biomass." presented at the 5th Symp. on Biotechnology for Fuels and Chemicals, 10-13th May 1983, Gatlinburg, Tennessee.

[7] Bvochora, J.M., Read, J.S., and Zvauya, R. (2000). "Application of very high gravity technology to the cofermentation of sweet stem sorghum juice and sorghum grain." Ind. Crop. Prod., 11(1): pp11-17.

[8] Kosaric N., and Vardar-Sukan, F. (2001). Potential source of energy and chemical products, in The biotechnology of ethanol: classical and future applications, Roehr, M. Ed. Wiley-VCH, ISBN 3527301992.

[9] Jackman, E.A. (1987). Industrial alcohol, in Basic biotechnology, Bu'lock, J., and Kristiansen, B. Eds. Academic Press, ISBN 9780121407520.

[10] Shariffa, Y.N., Karim, A.A., Fazilah, A., and Zaidul, I.S.M. (2009). "Enzymatic hydrolysis of granular native and mildly heat-treated tapioca and sweet potato starches at sub-gelatinization temperature." Food Hydrocolloids, 23(2): pp434-440.

[11] Buléon, A., Colonna, P., Planchot, V., and Ball, S. (1998). "Starch granules: structure and biosynthesis." Int. J. Biol. Macromol., 23(2): pp85-112.

[12] Mojović, L., Nikolić, S., Rakin, M., and Vukasinović, M. (2006). "Production of bioethanol from corn meal hydrolyzates." Fuel, 85(12-13): pp1750-1755.

[13] Verma, G., Nigam, P., Singh, D., and Chaudhary, K. (2000). "Bioconversion of starch to ethanol in a single-step process by coculture of amylolytic yeasts and *Saccharomyces cerevisiae* 21." Bioresour. Technol., 72(3): pp261-266.

[14] Imandi, S.B., Bandaru, V.V.R., Somalanka, S.R., Bandaru, S.R., and Garapati, H.R. (2008). "Application of statistical experimental designs for the optimization of medium constituents for the production of citric acid from pineapple waste." Bioresour. Technol., 99(10): pp4445-4450.

[15] Aggarwal, N.K., Nigam, P., Singh, D., and Yadav, B.S. (2001). "Process optimization for the production of sugar for the bioethanol industry from sorghum, a non-conventional source of starch." World J. Microbiol. Biotechnol., 17(4): pp411-415.

[16] Shewale, S.D., and Pandit, A.B. (2009). "Enzymatic production of glucose from different qualities of grain sorghum and application of ultrasound to enhance the yield." Carbohydr. Res., 344(1): pp52-60.

[17] Ejiofor, A.O., Chisti, Y., and Moo-Young, M. (1996). "Culture of *Saccharomyces cerevisiae* on hydrolyzed waste cassava starch for production of baking-quality yeast." Enzyme Microb. Technol., 18(7): pp519-525.

[18] Alam, M.Z., Jamal, P., and Nadzir, M.M. (2008). "Bioconversion of palm oil mill effluent for citric acid production: statistical optimization of fermentation media and time by central composite design." World J. Microbiol. Biotechnol., 24(7): pp1177-1185.

[19] Tanyildizi, M.S., Özer, D., and Elibol, M. (2005). "Optimization of α-amylase production by *Bacillus* sp. using response surface methodology." Process Biochem., 40(7): pp2291-2296.

[20] Muralidhar, R.V., Chirumamila, R.R., Marchant, R., and Nigam, P. (2001). "A response surface approach for the comparison of lipase production by *Candida cylindracea* using two different carbon sources." Biochem. Eng. J., 9(1): pp17-23.

[21] Sánchez, O.J., and Cardona, C.A. (2008). "Trends in biotechnological production of fuel ethanol from different feedstocks." Bioresour. Technol., 99(13): pp5270-5295.

PROFILES

NAJIAH NADIR

Najiah Nadir is a postgraduate student, currently doing her M.Sc (Biotechnology Engineering) at Faculty of Engineering of International Islamic University Malaysia. She has a B.Eng (Biochemical-Biotechnology Engineering) from IIUM. Her researches are related to biotechnology process engineering (extraction, fermentation, kinetics, and bioreactors scale-up).

DR MAIZIRWAN MEL

Dr Maizirwan Mel is an Associate Professor at the Department of Biotechnology Engineering, Faculty of Engineering, International Islamic University Malaysia (IIUM), Gombak 50728, Kuala Lumpur. He obtained his PhD in Bioprocess Engineering from Universiti Teknologi Malaysia in 2002. His research interest is in the area of Fermentation Kinetics and Design, Optimization and Modeling of Bioprocess, Biologics Separation and Purification, and Biopharmaceutical Manufacturing of Vaccine and Antibody, Bioenergy Technology and Engineering. He has over 8 years experience in teaching and research on Bioprocess Facility Design and Regulatory, and Biopharmaceutical manufacturing. Dr Maizirwan also serves as a regular referee for many international and national journals such as Bioresource Technology, World Journal of Microbiology and Biotechnology, Cytotechnology and IIUM Engineering Journal. He is currently a member of Institution Engineers of Indonesia (PII). He is also currently the Coordinator, Engineering Industrial Training Unit of IIUM.

PROF. DR MOHAMED ISMAIL ABDUL KARIM

Prof. Dr Mohamed Ismail Abdul Karim is presently a Professor at the Department of Biotechnology Engineering, Faculty of Engineering, International Islamic University Malaysia, Selangor. He obtained his PhD (Fermentation Technology) from University of Arkansas, U.S.A. His research interest is in the area of Fermentation and Microbial Biotechnology, bioremediation of industrial wastes, treatment and utilization of agricultural wastes and wastewater, bioconversion of agricultural wastes and raw material into value added products and fermentation of food. He is also currently the Director, Sustainable Development of Muslim World (Engineering and Technology), Research and Innovation, IIUM.

PROF. DR MOHD ROSLI YUNUS

Prof. Dr Mohd Rosli Yunus is presently a Professor at the Department of Chemical Engineering Faculty of Chemical and Natural Resources Engineering Universiti Malaysia Pahang (UMP), MEC City, 26300 Gambang, Kuantan. His research interest is in the area of Membrane Separation Processes, Ultrasonic Assisted Processes, Microwave Assisted Processes, and Waste to Wealth. His latest achievement was the patenting of his Acousto Cyclo Reactor Scheme for Production of Biodiesel. He is Registered Chemical Engineer, Board of Engineers, Malaysia (1997-present). His latest achievement is the patenting of his Acoustic Cyclo Reactor Scheme for Production of BiodieselHe is also currently the Deputy Vice Chancellor, UMP Kuantan.

HETEROGENEOUS ESTERIFICATION OF FREE FATTY ACID TO BIODIESEL

(Date received: 1.3.2010/ Date accepted: 19.8.2010)

Siti Eda Eliana Misi[1], Wan Nor Nadyaini Wan Omar[2] and NorAishah Saidina Amin[3]
[1,2,3] Chemical Reaction Engineering Group (CREG),
Faculty of Chemical and Natural Resources Engineering,
Universiti Teknologi Malaysia, 81310 UTM, Skudai, Johor
E-mail: [3] noraishah@fkkksa.utm.my

ABSTRACT

The potential of sulphated zirconia (SZ) as heterogeneous acid catalyst for esterification of free fatty acid (FFA) to biodiesel has been investigated. Experiments using oleic acid as a model compound preceded the esterification of palm oil free fatty acid (POFFA) mixtures. The relation of reaction time, SZ loading and methanol to oil molar ratio on biodiesel yield and conversion was investigated. Optimisation of esterification process via response surface methodology (RSM) for blended POFFA revealed maximum biodiesel yield (FAME) and conversion were 80.2% and 78.4%, respectively. The optimum conditions were operating reaction time = 87min, catalyst loading = 0.98wt% and molar ratio methanol to oil = 11.6:1. The fuel properties of biodiesel from POFFA and oleic acid blends were found to conform to the ASTM standard.

Keywords: *Biodiesel; Free Fatty Acid; Heterogeneous; Response Surface Methodology, Optimisation*

1.0 INTRODUCTION

Petrol and diesel contribute to environmental problems since the exhaust gas from these fuels emits green house gases (GHG) such as carbon monoxide (CO), nitrogen oxide (NOx) and particulate matter [1]. The GHG can be hazardous to human health besides it being a factor to global warning. According to Marchetti *et al*. [2], biodiesel can be defined as a fuel comprised of mono-alkyl esters of long chain fatty acids derived from vegetable oils or animal fats. Biodiesel is green fuel since it is biodegradable and non-toxic, and it significantly reduces toxic and other emissions when burned as fuel. Therefore, biodiesel might become a good alternative for sustainable environment development.

Vegetable oils such as palm, soybean, peanut and olive oil and animal fats such as beef tallow are attractive as raw material for biodiesel production. However, the prices of these oils and fats are relatively high and increase cost for biodiesel production. Therefore, alternative feedstock is being evaluated to identify less expensive materials that could serve as cheaper feedstock for biodiesel. Substantial efforts have been devoted to the development of non-edible oil and waste edible oil such as jatropha oil and waste cooking oil respectively as a biodiesel feedstock [3-8]. Meanwhile, the development of other feedstock such as POFFA is also of interest [9, 10]. POFFA is fatty acids residual based palm oil which is a by-product from distillation and recovery of desired fatty acids. The POFFA is attractive not only to further increase the economic viability of biodiesel, but it is also easier to obtain from the palm oil refineries.

Base-catalysed transesterification is the most common way to produce biodiesel since the reaction proceeds faster than the acid-catalysed reaction. In addition, the alkaline catalysts are less corrosive than acidic ones and therefore are more favourable in industrial processes [2]. The reaction directly converts the triglycerides to form their corresponding fatty acid methyl ester (FAME) in the presence methanol and catalyst. However, POFFA contains high amount of free fatty acid (FFA) (93 wt% or more) [10]. According to Marchetti *et al*. [2], if the amount of FFA in the feedstock exceeds 0.5%, direct esterification will inherently take place. Figure 1 illustrates the reaction path of esterification where **R** and **R'** denotes any hydrocarbon chain.

Esterification can be carried out in the presence of homogenous or heterogeneous catalyst. However, homogeneous catalyst is not recommended in the biodiesel production because of saponification and problems to separate the catalyst from the product[2, 11]. Heterogeneous catalyst seems to be better than homogeneous catalyst for obtaining high biodiesel yield.

Several researchers have studied the performance of zirconia based catalyst for biodiesel production. Jitputti *et al*. [12] studied ZrO_2, ZnO, SO_4^{2-}/SnO_2, SO_4^{2-}/ZrO_2 (SZ), KNO_3/KL zeolite and KNO_3/ZrO_2 for the transesterification of crude palm kernel oil (PKO) and crude coconut oil (CCO). They reported SZ solid

acid catalyst exhibited the highest activity for both crude palm kernel oil and CCO transesterification compared to the other catalysts. Meanwhile, Satoshi *et al*. [13] reported three types of solid superacid catalyst, sulphated tin oxide (STO), tungstated zirconia-alumina (TZA) and sulphated zirconia-alumina (SZA) were able to contribute in esterification of n-octanoic fatty acid and transestrification of soybean oil. TZA was quite effective and gave high performance in biodiesel production. Over 90% conversions in both transesterification and esterification were reported. However, STO only showed high activities in the esterification due to its strong acidity compared to the others with 100% conversion.

Kiss *et al*. [14] has investigated the manufacturing of biodiesel via dodecanoic acid esterification using various super acid catalysts such as SZ, SO_4^{2-}/TiO_2, SO_4^{2-}/SnO_4^{2-}, H-ZSM5 and ion exchange resin. These catalysts were environmentally superior such as low corrosion, easy separation, and produced no acid waste problems. From the results, SZ was found to be a good catalyst for the catalytic biodiesel production. The catalyst possessed strong acid sites, highly selective with high thermal stability under the process conditions.

Therefore, SZ was a potential catalyst for biodiesel production from POFFA since SZ was less expensive and has an economical advantage due to productivity improvement resulting from its good catalytic activity. In addition, SZ has large pores which allow the diffusion of fatty acid molecules. Thus, it can produce high alkyl esters yield [15] and can be easily separated from the product [16]. In this paper, the potential of SZ as heterogeneous acid catalyst for esterification of POFFA to biodiesel is investigated. The relationship of reaction time, SZ loading and methanol to oil molar ratio on biodiesel yield and conversion of oleic acid was investigated using central composite design (CCD). The esterification of oleic acid as model compound was initially optimized via response surface methodology (RSM). Next, the esterification of POFFA and oleic acid mixture at the suggested optimum condition was studied.

Figure 1: Esterification reaction

2.0 EXPERIMENTAL

2.1 Material

Pure oleic acid was purchased from Reidel De Haen Company (U.S.A) while POFFA was obtained from Natural Oleochemical Sdn Bhd, Pasir Gudang, Johor, Malaysia. POFFA was received as dark brown liquid with mild odour. The components of POFFA were identified by GC-MS and tabulated in Table 1. Zirconia was purchased from Merck (Germany). Meanwhile, 0.5 N H2SO4, analytical grade methanol (98%) and n-hexane were purchased from Q-Rëc (New Zealand).

2.2 Catalyst Preparation

SZ, SO_4^{2-}/ZrO_2 catalyst was prepared via wet impregnation method. The zirconia was immersed in 0.5N H_2SO_4 solution and heated to 110ºC to evaporate the water. After the solution turned slurry, it was oven dried at 120°C overnight and calcined at 600°C for 1h.

2.3 Esterification Process

The esterification of model compound, oleic acid and POFFA were conducted in a 250 ml round bottom flask equipped with a reflux condenser and thermometer. The oleic acid, SZ and methanol were mixed at a desired amount. Then, the mixture was stirred at 200rpm and heated at methanol reflux temperature (65ºC). Next, the solution was allowed to cool to room temperature. The catalyst was separated from the product mixture using vacuum filtration at 5mmHg. The product was then poured into a separating funnel and left to settle for 24h to separate the excess methanol.

2.4 Analysis

The compositions of methyl ester was determined by using an Agilent Technologies 6890N Gas Chromatograph- Mass Spectroscopy (GC-MS) with inert mass selective detector 5975. The capillary column was Agilent 19091S-433 HP-5MS (30mm x 250µm x 0.25µm) and helium (2 ml/min) was used as carrier gas. The oven temperature was held at initial temperature 80°C for 0.5 min, and then ramped to a final temperature of 250°C for 5min at a rate of 10°C/min, with the total run time of 42 min. The injector and detector temperatures were 325 oC and 250°C, respectively. The acid value of the oil was determined by titration method using 0.1N potassium hydroxide solution. The optimal conditions of oleic acid and POFFA esterification was analysed by using STATISTICA 6.0 software.

Table 1: FFA profiles and physical properties of residual palm oil

Properties	
Free Fatty Acid Profile (%)	
Lauric acid 12:0	3.39
Stearic acid 18:0	12.68
Oleic acid 18:1	81.44
Others	2.49
Density (g/ml)	67.5
Viscosity (mm^2/s)	0.927

3.0 RESULTS AND DISCUSSION

3.1 Design of Experiments on Esterification Process using CCD

The effect and interaction of reaction time (X_1), catalyst loading (X_2) and molar ratio methanol to oil (X_3) over two observed responses; conversion (Y_1) and ester yield (Y_2) was analysed using response surface methodology (RSM). Meanwhile, the reaction temperature was maintained at methanol boiling point(65°C) since the methanol would evaporate at higher temperature. A central composite design (CCD) with full 2^3 factorial designs (three factors each at two levels, six star points and two center points) was employed. Table 2 lists the range and level coded of independent variables while the complete design matrix of CCD and results of ester yield and conversion are given in Table 3.

Table 2: Experimental ranges and levels of independent variables

Factors	Symbol	Range and Levels				
		– α (–2)	-1	0	+1	+ α (+2)
Reaction Time, min	X_1	30	45	60	75	90
Catalyst loading, wt%	X_2	0.6	0.8	1.0	1.2	1.4
Molar ratio methanol: oil	X_3	4:1	5:1	6:1	7:1	8:1

Note: *+ α: high star point level; +1: high factorial point level; 0: central point level; -1: low factorial point level; -α: low star point level.*

Table 3: Experiment matrix and experimental results

Manipulated variables			Responses	
X_1	X_2	X_3	Y_1	Y_2
Reaction time (min)	*Catalyst loading (wt%)*	*Molar ratio (alcohol:oil)*	*Conversion (%)*	*Ester yield (%)*
45(-1)	0.8(-1)	5:1(-1)	46.78	35.13
45(-1)	0.8(-1)	7:1(1)	51.74	48.06
45(-1)	1.2(1)	5:1(-1)	50.80	49.80
45(-1)	1.2(1)	7:1(1)	67.94	51.35
75(1)	0.8(-1)	5:1(-1)	46.23	47.27
75(1)	0.8(-1)	7:1(1)	56.62	52.400
75(1)	1.2(1)	5:1(-1)	52.21	43.31
75(1)	1.2(1)	7:1(0)	61.39	59.72
60(0)	1(0)	6:1(0)	63.18	46.99
34(-α)	1(0)	6:1(0)	56.8	40.87
86(+α)	1(0)	6:1(0)	69.83	46.98
60(0)	0.65(-α)	6:1(0)	45.92	38.26
60(0)	1.35(+α)	6:1(0)	56.05	50.49
60(0)	1(0)	4.24:1(-α)	49.48	41.62
60(0)	1(0)	7.76:1(+α)	64.48	55.32
60(0)	1(0)	6:1(0)	57.92	55.8

3.2 FFA Conversion

The empirical mathematical model equation of the FFA conversion is presented in Equation 2:

$$Y_1 = -123.705 + 0.413\,X_1 + 178\,X_2 + 18.866\,X_3 - 0.002\,X_1^2 - 89.147\,X_2^2 - 1.639\,X_3^2 - 0.395\,X_1 X_2 - 0.021\,X_1 X_3 + 6.856\,X_2 X_3 \quad (2)$$

Where, Y_1 is the predicted percentage of FFA conversion. The parity plot in Figure 2 indicates the determination coefficient (R^2) for conversion of methyl ester is 0.8566. The empirical model is adequate to explain most of the variability in the assay reading which should be at least 0.75 [17].

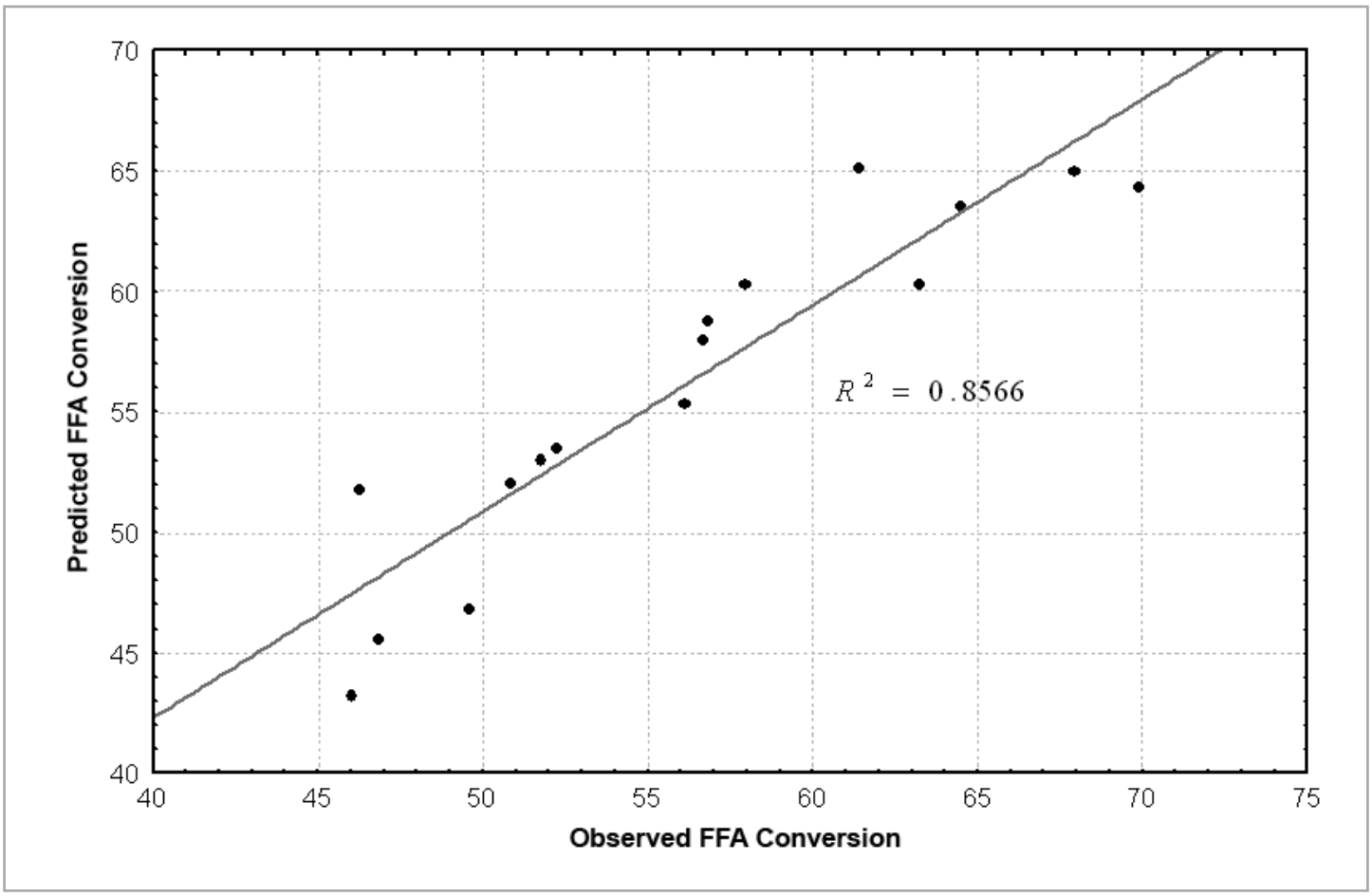

Figure 2: Parity plot for the observed and the predicted conversion

Table 4: Analysis of variance (ANOVA)

Sources	Sum of Squares (SS)	Degree of Freedom (d.f)	Mean Squares (MS)	F-value	Fα
FFA conversion Model					
Regression (SSR)	749.5847	9	83.2872	3.98	$F_{0.10} < 2.96$
Residual	125.4884	6	20.9147		
Total (SST)	875.0732	15			
ME yield model					
Regression (SSR)	535.6392	9	59.5154	2.71	$F_{0.25} < 1.77$
Error (SSE)	131.4633	6	21.9106		
Total (SST)	667.1025	15			

Meanwhile, in the analysis of variance (ANOVA), the ***F***-value of the model (***F***= 3.98) was greater than the tabulated ***F***-value (***F***0.10, 9, 6 = 2.96) (Table 4) indicating that the model was statistically significant at 90% confidence level. Figure 3 illustrates the Pareto chart and the corresponding ***p***-value of variable to check the significance of regression coefficients of the conversion model. As shown, the largest effect on conversion of methyl ester was linear term of methanol to oil molar ratio (X_3) which implied a higher ***t***-value (3.9501) and lowest ***p***-value (0.0075) at 99% significant level. Catalyst loading in linear(X_2) and quadratic (X_2^2) term could also be regarded as significant variables in FFA conversion at 97% and 95% significant level, respectively.

The three dimensional surface and contour plots of conversion over reaction time, catalyst loading and molar ratio are represented in Figure 4. These figures exhibit that the catalyst loading (SZ) and methanol to oil molar ratio have the most significant effect on the methyl ester conversion compared to reaction time. As illustrated in Figure 4a, the conversion of methyl ester started at 0.6wt% catalyst loading and reached maximum around 1.0wt% and became constant which may be due to catalyst deactivation. On the other hand, Figure 4b exhibits the conversion increased when excess methanol was applied in the reaction. Meanwhile, reaction time has a slight significant effect on the conversion (Figures 4a and 4b). The relationship between catalyst loading and molar ratio of methanol to oil is depicted in Figure 4c.

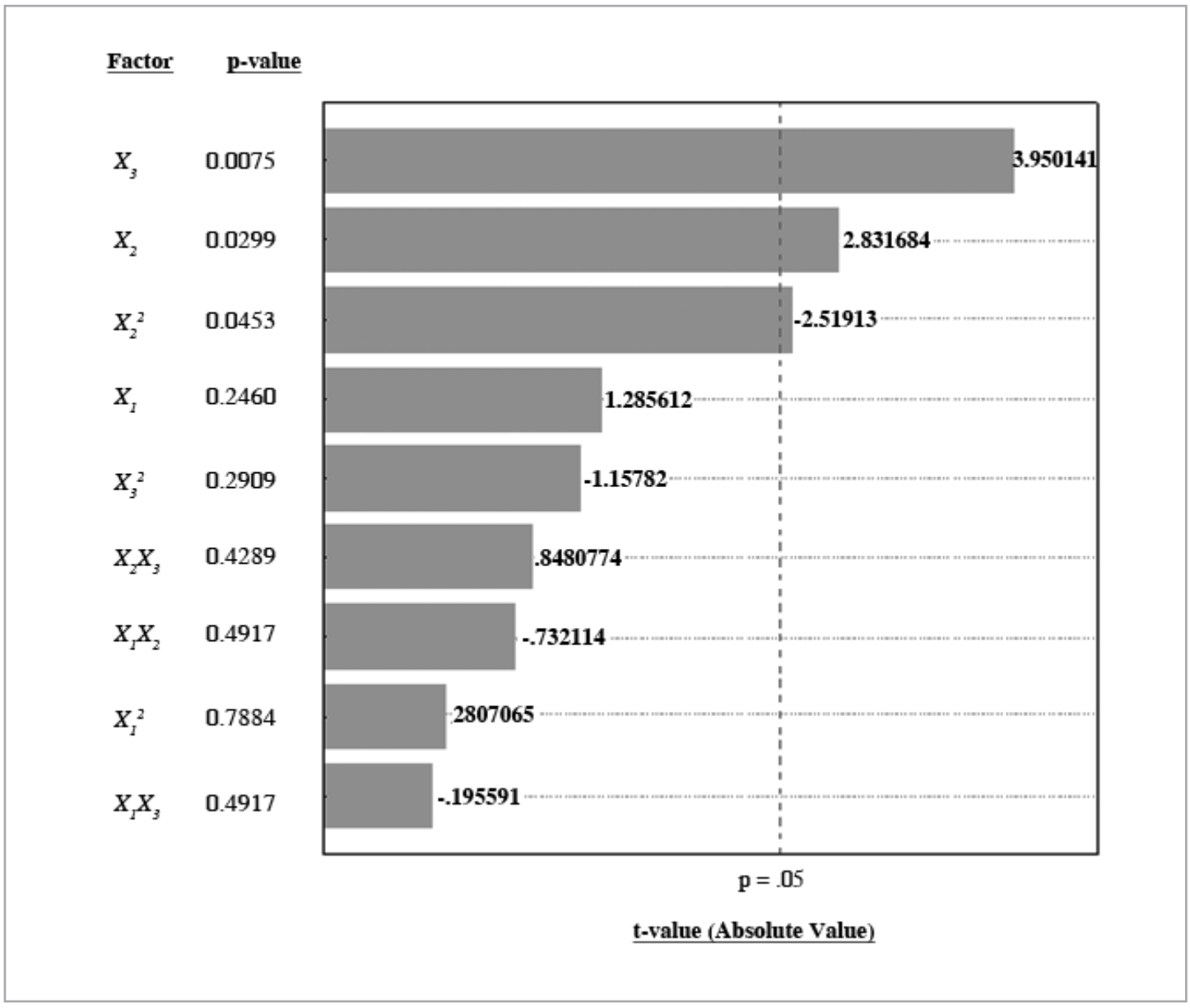

Figure 3 : Pareto chart and p-value of conversion

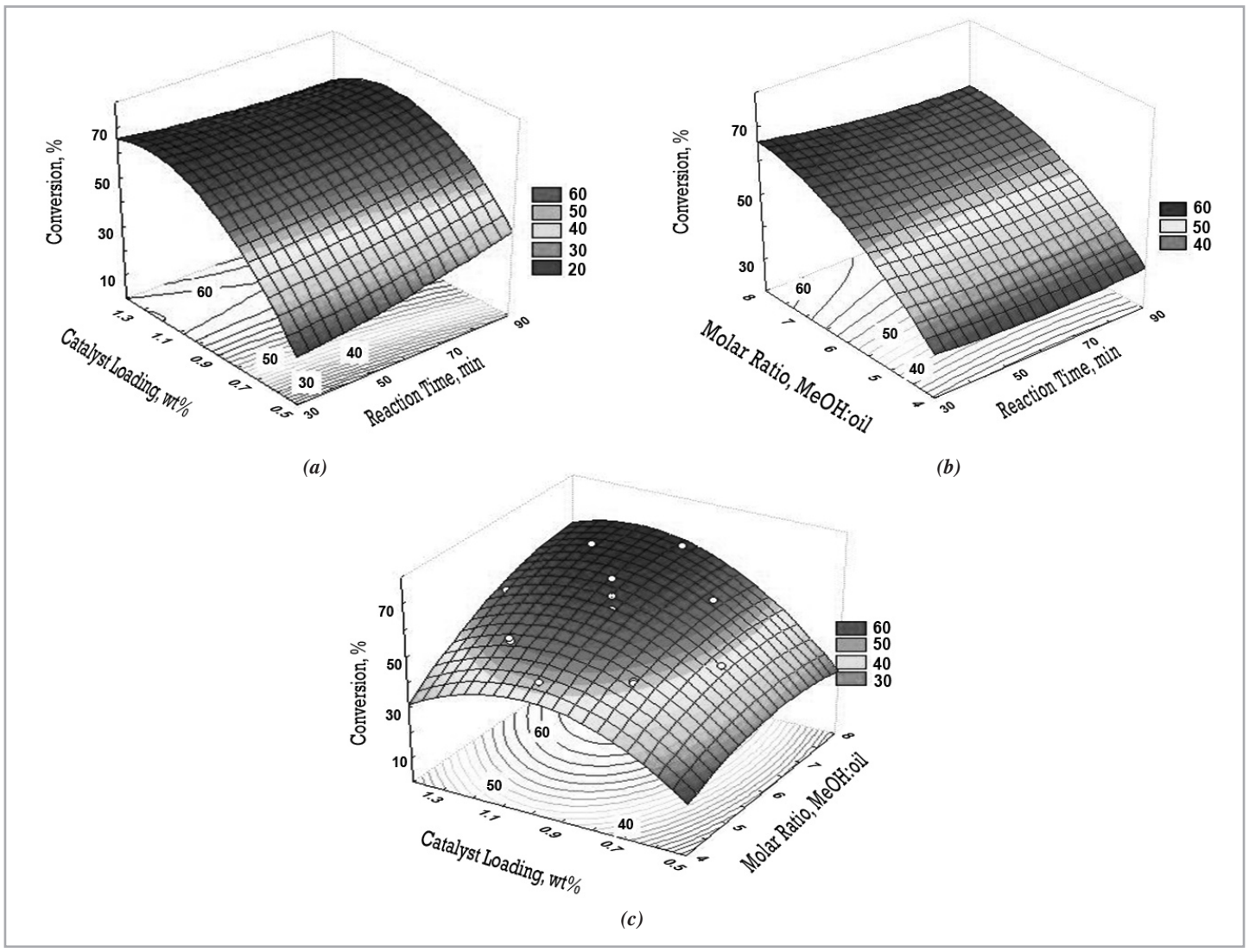

Figure 4: The response surface plot of conversion as a function of (a) catalyst loading and reaction time at methanol to oil molar ratio = 8:1 (b) methanol to oil molar ratio and reaction time at catalyst loading = 1.4wt% (c) methanol to oil molar ratio and catalyst loading at reaction time = 60min

3.3 Ester Yield

The model equation for ester yield with coefficients in coded units of factors is given in Equation (3).

$$Y_2 = -108.93 + 1.45\,X_1 + 143.65\,X_2 + 6.975\,X_3 - 0.009\,X_1^2 - 45.845\,X_2^2 - 0.518\,X_3^2 - 0.608\,X_1 X_2 + 0.059\,X_1 X_3 - 0.062\,X_2 X_3 \quad (3)$$

where, Y_2 is the predicted percentage of ester yield.

The determination coefficient, $\mathbf{R}^2$ obtained was 0.8493 as shown in the parity plot in Figure 5. Therefore, it can be implied that the 84.93% of variability in the data fitted to the model. In the analysis of variance (ANOVA) (Table 4), F-value for experimental (F =2.71) was lower compared to the tabulated F-value ($F_{0.25,\,9,\,6}$ = 1.77). This indicated that the fitted model exhibited no lack of fit at the 75 % confidence level. Meanwhile, the Pareto chart and corresponding p-value in Figure 6 display the linear term of molar ratio methanol to oil (X_3) in the model have the largest effect on ester yield as the factor variable have larger t-value (3.4093) and smaller p-value (0.0143). This indicated that coefficients of the factor variable affect over ester yield at 99% significant level while other variables could be considered less significant to affect ester yield. Meanwhile, linear term of catalyst loading (X_2) could also affect ester yield at 95% significant level.

The empirical model is plotted as a three-dimensional surface representing the response (ester yield) as a function of two factors for experimental range considered (Figure 7). The surface response of operating reaction time and catalyst loading on ester yield is confined in the smallest ellipse as illustrated in Figure 7a. The ester yield increased when the reaction time and catalyst loading increased and decreased slightly after the optimum value is achieved. Meanwhile, Figure 7b exhibits high molar ratio of methanol to oil produced high ester yield. The same trend for methanol to oil molar ratio can be observed in Figure 7c where the interaction with catalyst loading denoted the largest effect on ester yield.

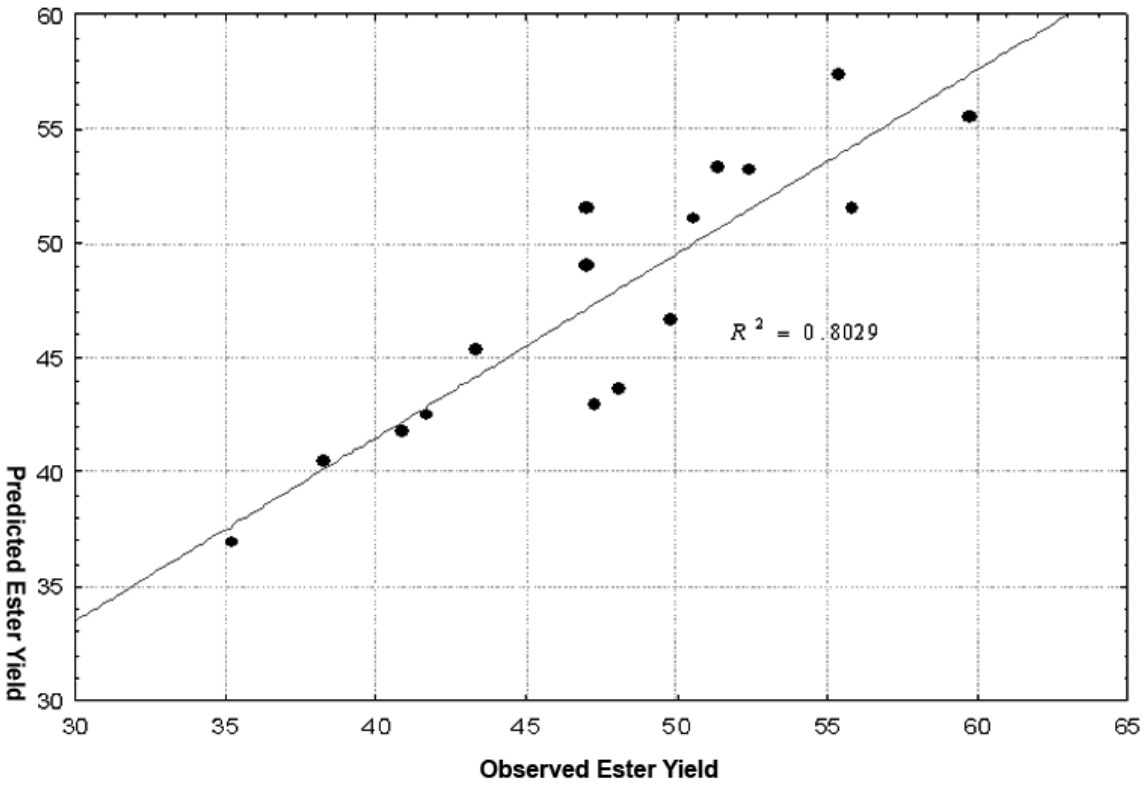

Figure 5: Parity plot for the observed and the predicted ester yield

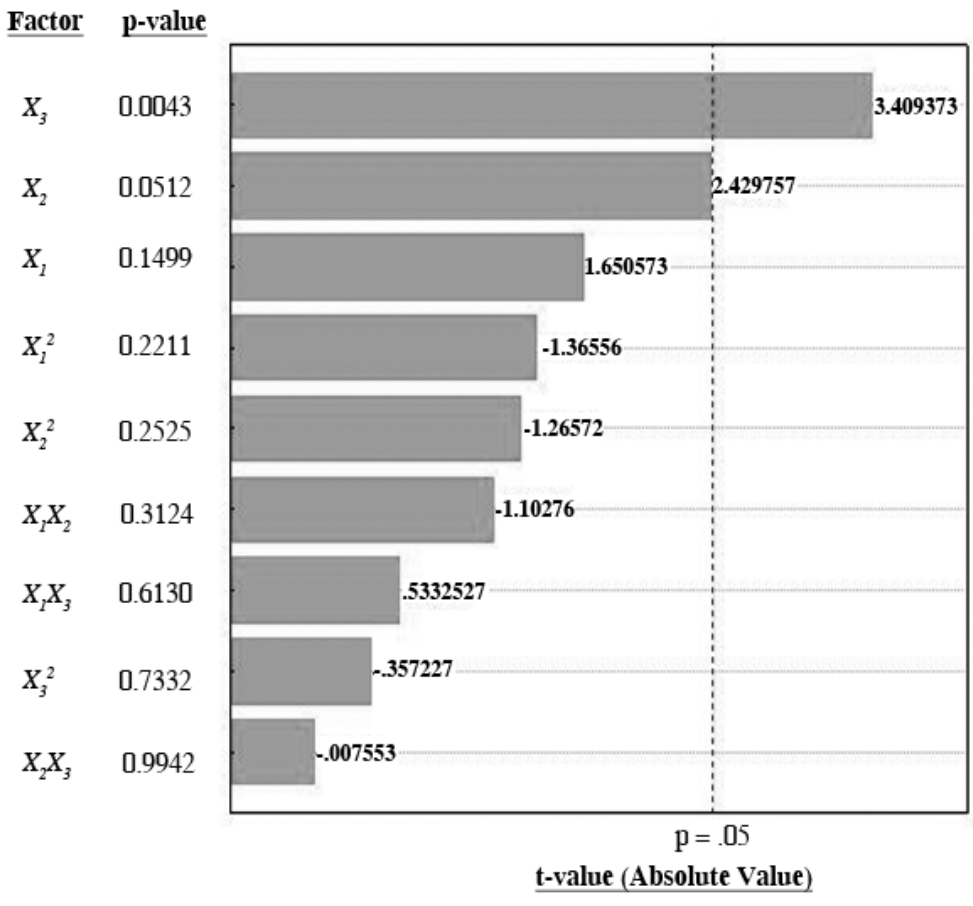

Figure 6: Pareto chart and p-value of ester yield

3.4 Optimisation Ester Yield of Esterification Oleic Acid

In this work, the model compound, oleic acid was optimized since the major component in POFFA is oleic acid. The response surface analysis using Statistica 6.0 software indicated that the predicted optimum ester yield of oleic acid esterification is 65.2% at operating reaction time = 87.3 minutes, 0.98wt% catalyst loading (SZ) and molar ratio methanol to oil = 11.6:1 as tabulated in Table 5. Although reaction time was found to have no statistically significant effect on either yields or conversion, in any of the terms (linear, interaction or quadratic) of the regression models at 95% confident level, the extended reaction time is considered since the ME yield model was accepted at 75% confident level for the ANOVA. Additional experiment was carried out to validate the optimisation result obtained by the response surface analysis. The experimental yield and differences between the predicted and observed values were reported as 64.60 % and 0.95%, (Table 5), respectively. The errors were considered small as the observed values are within the 5% level of significance. Therefore, the optimization condition of ester yield of oleic acid with RSM was at operating reaction time = 87.3 minutes, 0.98wt% catalyst loading (SZ) and molar ratio methanol to oil is 11.6:1.

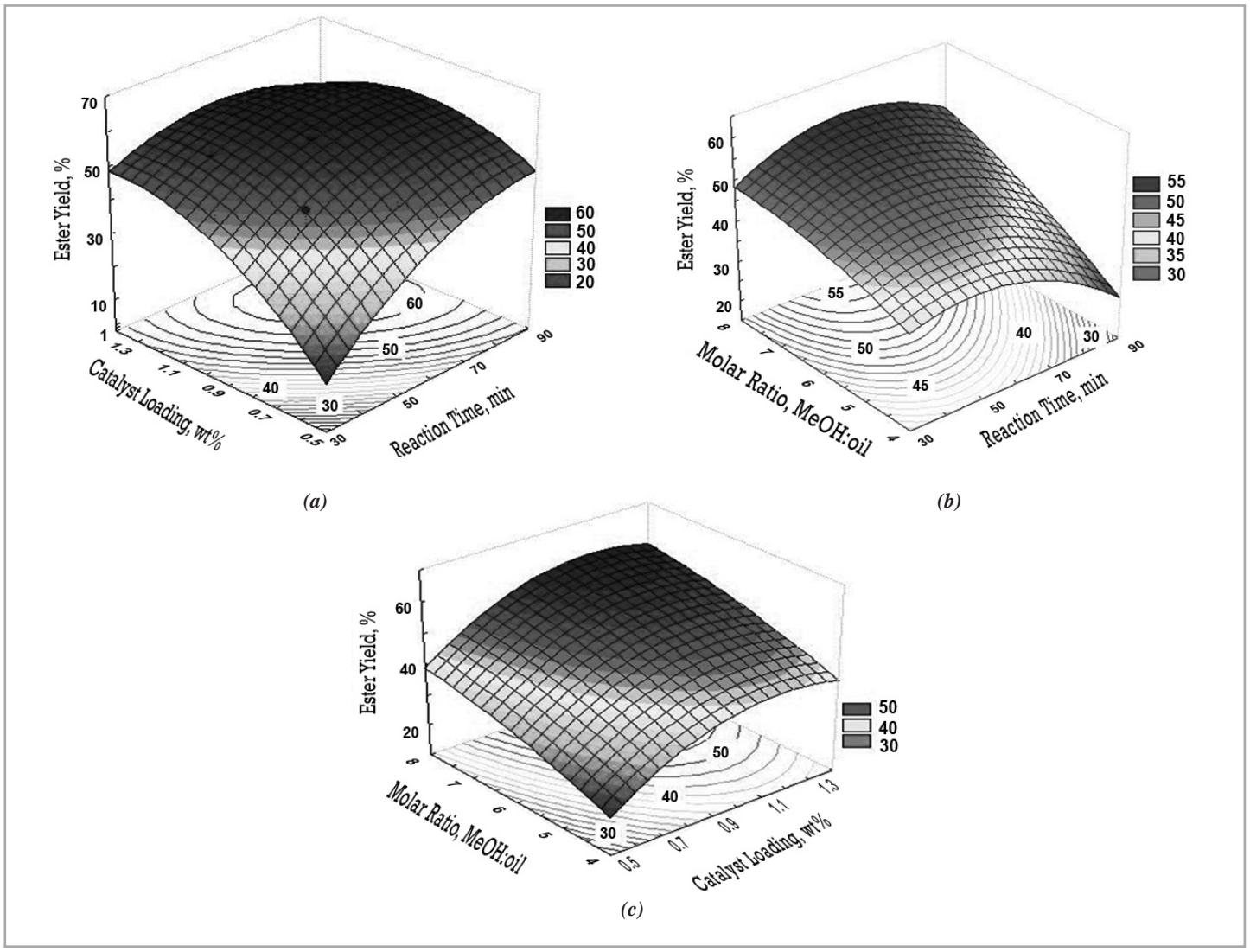

Figure 7: The response surface plot of ester yield as a function of (a)catalyst loading and reaction time at methanol to oil molar ratio =8:1(b) methanol to oil molar ratio and reaction time at catalyst loading = 1.4wt% (c) methanol to oil molar ratio and catalyst loading at reaction time = 60min

3.5 Heterogeneous Esterification of POFFA at Optimum Condition

Heterogeneous esterification of POFFA did not produce any FAME as the final product since the kinematic viscosity of POFFA was considerably high at 67.53 mm2s-1. As an alternative, the viscosity of POFFA has to be reduced to allow the reaction to occur at a lower temperature . Thus, POFFA was blended with 75% of free fatty oleic acid (kinematic viscosity = 21.1mm2s-1) in order to reduce the kinematic viscosity of POFFA. Table 6 presents the experimental results at optimum condition by using model compound (*i.e* oleic acid) and blend POFFA (25% POFFA + 75% oleic acid) as a sample.

The model compound gave a good yield as predicted in the response surface analysis indicating that the statistical approach

is valuable in the optimisation of process. Therefore, the blended POFFA which demonstrated an excellent ester yield and conversion of 80.2% and 78.4%, respectively can be accepted as an alternative source to produce biodiesel.

In addition, Fig. 8 depicts the methyl ester yields for catalytic SZ and non catalytic esterification of oleic acid and blended POFFA at optimum condition. Esterification of oleic acid and blended POFFA using SZ as heterogeneous catalyst produced a high yield of methyl ester compared to non catalytic esterification. At optimum condition, 64.6% and 80.2% of methyl ester yield was produced from oleic acid and blended POFFA, respectively while non-catalytic reaction gave methyl ester yield of only 4.37% and 3.80%, respectively. This demonstrates that the SZ significantly enhanced the rate of esterification as reported in previous studies [12, 14].

3.6 Properties of Methyl Ester

The kinematic viscosity and density of oleic acid and blend POFFA as well as biodiesel produced from oleic acid and blend POFFA are summarised in Table 7. As for the standard, the value is given by ASTM D6751[18]. Density for oleic methyl ester (0.858) is slightly lower than the ASTM D6751 limit. However, it is still in good agreement with the standard because the biodiesel produced is lighter than the water. Meanwhile, biodiesel from blend POFFA was comparable with the limit.

Table 5: Critical values results for ester yield

Factor	Observed Minimum	Critical Values	Observed Maximum
Reaction time (min)	33.5	87.4	86.5
Catalyst loading (wt %)	0.65	0.98	1.35
Molar ratio (methanol: oil)	4.24:1	11.6:1	7.76:1
Predicted ester yield (%)		65.22	
Experimental ester yield (%)	64.60		
Error (%)	0.95		

Table 6: Experimental results at optimum conditions

Sample	Ester Yield (%)	Conversion (%)	Observation (Colour)
Free fatty oleic acid	64.6	100	Light yellow
POFFA 25% + Oleic acid 75%	80.2	78.4	Light Brown

Kinematic viscosity is an important property for fuel as it is an indication of the ability of a material to flow. The higher viscosity value will increase the tendency of the fuel to cause problem in the combustion engine and oil line. For biodiesel, the kinematic viscosity at 40ºC should be between 1.9 and 6.0mm^2/s [19]. From the specification analysis, both methyl ester from oleic acid and blended POFFA met the requirements with values being 3.51mm^2/s and 3.53mm^2/s, respectively. Hence, no modifications are required for handling the biodiesel from oleic acid and blend POFFA in the existing engine.

Table 7: Properties of sample and FAME

Properties	Feedstocks		Biodiesel			
	Oleic acid	*Blend POFFA*	*B100 (Malaysia)*	*ASTM D6751 (USA)*	*Oleic acid*	*Blended POFFA*
Density (20ºC) (g/ml)	0.868	0.927	0.878	0.87-0.9	0.858	0.878
Kinematic viscosity, 40ºC (mm^2/s)	21.2	25.6	4.4	1.9 - 6.0	3.51	3.53

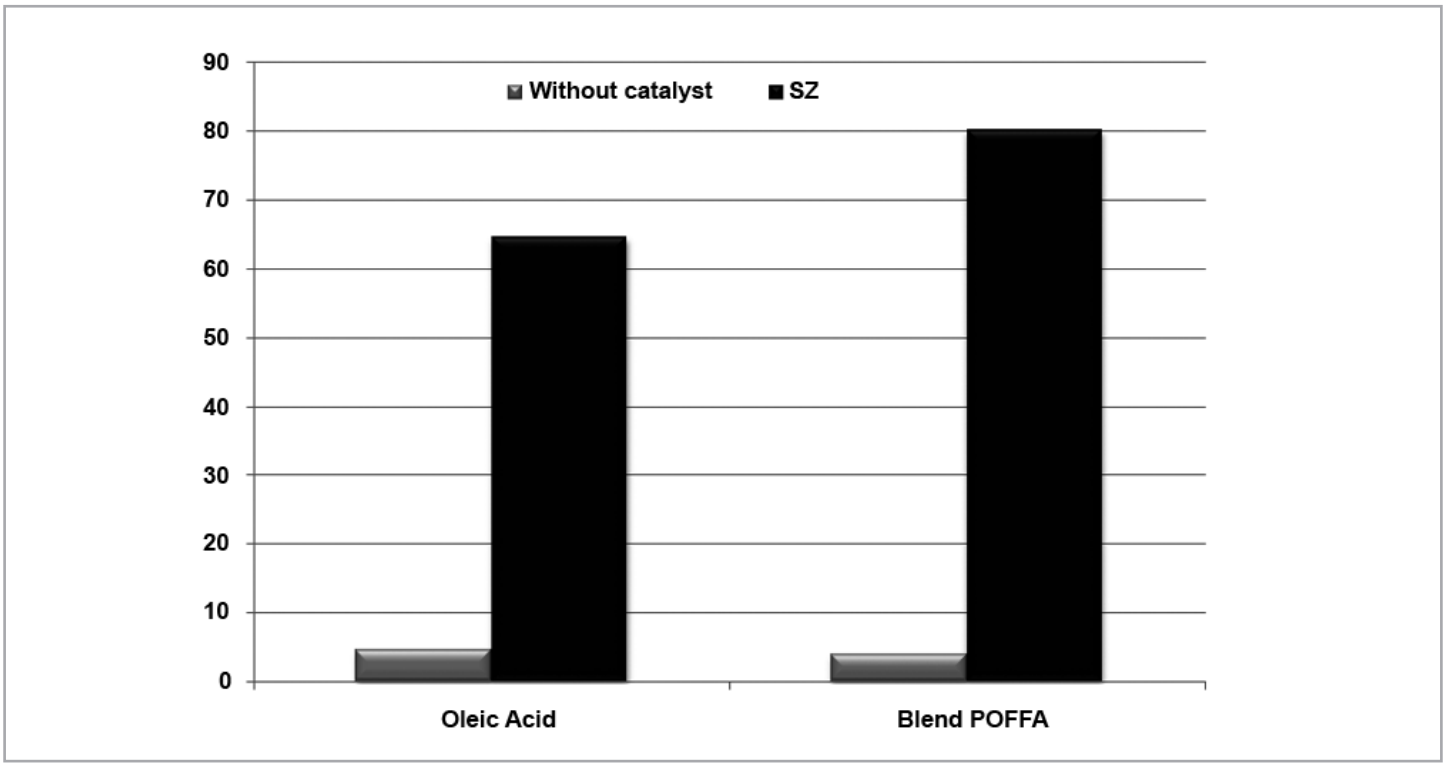

Figure 8: Methyl ester yields for catalytic and non catalytic esterification of oleic acid and blended POFFA at operating reaction time = 87.38 minutes, 0.98wt% catalyst loading (SZ) and methanol to oil molar ratio = 11.6:1

4.0 CONCLUSION

All the parameters such as reaction time, catalyst loading and methanol to oil molar ratio gave a significant effect on the heterogeneous esterification of oleic acid and blended POFFA. Longer reaction time increased the biodiesel production. Apart from that, excess alcohol led to complete reaction. The maximum biodiesel yield from blended residual palm oil was 80.2% at optimum conditions 87 min of reaction time, 0.98wt% of SZ catalyst and methanol to oil molar ratio = 11.6:1. The results indicated that blended POFFA has the potential to be used as a source for biodiesel production. From the cost perspective, biodiesel from blended POFFA is able to compete with the conventional petroleum diesel since POFFA is a by-product of palm oil refinery. In addition, the fuel properties of biodiesel from blended POFFA were within the standard requirement of ASTM D6751 for density and kinematic viscosity.

5.0 ACKNOWLEDGEMENT

The authors would like to express their sincere gratitude to Ministry of Science, Technology and Innovation (**MOSTI**) for the National Science Fellowship to one of the authors (Wan-Omar WNN). They are also grateful to the Ministry of Higher Education (MOHE) for supporting the project under the Fundamental Research Grant Scheme (FRGS) Vote 78402. ■

REFERENCES

[1] Canakci, M. and Gerpen, V. J. (2001). "Biodiesel Production from Oils and Fats with High Free Fatty Acids." American Society of Agriculture Engineers. 44(6): pp1429-1436.

[2] Marchetti, J.M., Miguel V. U. and Errazu, A.F. (2007). "Possible Methods for Biodiesel Production." Renewable and Sustainable Energy Reviews 11: pp1300-1311.

[3] Sree, R., Seshu Babu, N., Sai Prasad, P.S. and Lingaiah, N. (2009). "Transesterification Of Edible and Non-Edible Oils Over Basic Solid Mg/Zr Catalysts." Fuel Processing Technology 90:pp152-157.

[4] Patil, P.D. and Deng, S. (2009)."Optimization of Biodiesel Production from Edible and Non-edible Oils". Fuel 88:pp1302-1306.

[5] Pahn, A.N. and Pahn, T.M. (2008). "Biodiesel Production from Waste Cooking Oils." Fuel 87: pp3490-3496.

[6] Canakci, M., (2007). "The Potential of Restaurant Waste Lipids as Biodiesel Feedstocks". Bioresource Technology 98: pp183-190.

[7] Wang, Y., Ou, S., Liu, P., Xue, F. and Tang, S. (2006). "Comparison Of Two Different Processes To Synthesis Biodiesel By Waste Cooking Oil". Journal of Molecular Catalysis A: Chemical. 252: pp107-112.

[8] Haas, M.J. and Foglia, T.A. (2005). Alternate Feedstocks and Technologies for Biodiesel Production. In Knothe, G., J.V. Gerpen, and J. Krahl. The Biodiesel Handbook (pg 42-61).Urbana, Illinois. AOCS Press.

[9] Ooi, Y. S., Zakaria, R., Mohamed, A. R. and Bhatia, S. (2004). "Catalytic Conversion Of Palm Oil-Based Fatty Acid Mixture To Liquid Fuel". Biomass and Bioenergy. 27: pp477-484.

[10] Chongkhong, S., Tongurai, C., Chettpattananondh, P., and Bunyakan. C. (2007). "Biodiesel Production by Esterification of Palm Fatty Acid Distillate." Biomass and Bioenergy 31: pp563-568.

[11] Marchetti, J. M., Miguel, V. U. and Errazu, A. F. (2007). "Heterogeneous Esterification of Oil With High Amount Of Free Fatty Acids." Fuel. 86: pp906-910.

[12] Jitputti, J., Kitiyanan, B., Rangsunvigit, P., Bunyakiat, K., Attanatho L. and Jenvanitpanjakul, P. (2006). "Transesterification of Crude Palm Kernel Oil And Crude Coconut Oil By Different Solid Catalysts". Chemical Engineering Journal. 116: pp61-66.

[13] Satoshi, F., Hiromi, M. and Kazushi, A. (2004). "Biodiesel Fuel Production with Solid Superacid Catalyst In Fixed Bed Reactor Under Atmospheric Pressure". Catalyst Communications. 5: pp721-723.

[14] Kiss, A. A., Omota, F., Dimian, A. C. and Rothenberg, G. (2006). "The Heterogeneous Advantage: Biodiesel by Catalytic Reactive Distillation". J. of Catalysis. 40: pp141-150.

[15] Furuta, S., Matsuhashi, H. and Arata, K. (2004). "Biodiesel Fuel Production with Solid Superacid Catalysis in Fixed Bed Reactor Under Atmospheric Pressure." Catalysis Communications. 5:pp721-723.

[16] Liu, X., He, H., Wang, Y. and Zhu, S. (2007). "Transesterification Of Soybean Oil To Biodiesel Using SrO As A Solid Base Catalyst". Catalysis Communications. 8: pp1107-1111.

[17] Haaland, P. D. (1989). "Experimental Design in Biotechnology", Marcel Dekker Inc., New York.

[18] Masjuki, H.H., Kalam, M.A. and Shioji, M. (2008. "Feasibility of Bio-Fuels in Internal Combustion Engines". Proceeding of Natural Resources & Energy Environment, 24-25 November 2008, Kyoto, Japan.

[19] Fernando, S., Karra, P., Hernandez, R. and Jha, S. K. (2007). "Effect Of Incompletely Converted Soybean Oil On Biodiesel Quality". Energy. 32: pp844-951.

PROFILES

WAN NOR NADYAINI WAN OMAR
Wan Nor Nadyaini Wan Omar is currently doing her master in chemical engineering at UTM. Her research areas are catalytic engineering and chemical reaction, specializing in biodiesel production and reactor design. She graduated with B.Eng (Chemical) from UTM in 2008.

SITI EDA ELIANA MISI
Siti Eda Eliana Misi is currently doing her master in chemical engineering at Universiti Teknologi Petronas (UTP). Her research areas are in catalysis and chemical reaction. She graduated with B.Eng (Chemical) from UTM in 2008.

PROFESSOR DR NORAISHAH SAIDINA AMIN
Professor Dr NorAishah Saidina Amin (Prof NASA) is the head of Chemical Reaction Engineering Group (CREG) at the Faculty of Chemical Engineering, Universiti Teknologi Malaysia. Her fields of expertise are catalytic reaction engineering and modeling of chemical reaction systems. She is involved with research, development and consultancy (RD&C) related to applied catalysis and conversions of methane, palmoil, glycerol and biomass to important chemicals such as hydrogen, syngas, C_2^+ and liquid fuels (GTL,BTL). Her current passion is in development of green technology for sustainable development.

PROCESS ROUTE SELECTION FOR INHERENTLY SAFER DESIGN BASED ON CONSEQUENCES ANALYSIS

(Date received: 28.2.2010/ Date accepted: 16.8.2010)

Mardhati Zainal Abidin[1] and Mohd Sobri Takriff [2]
[1,2] Department of Chemical and Process Engineering,
Faculty of Engineering and Built Environment
Universiti Kebangsaan Malaysia, 43600 UKM Bangi, Selangor
E-mail: [2]sobri@eng.ukm.my

ABSTRACT

Increased public awareness of safety and stringent requirements by the authority has led to the consideration of inherent safety in the design of processing plants. Inherent safety approach ensures the safety of a process by eliminating or minimizing the hazard from a process rather than implementing engineering control to manage the hazard. The opportunity for such an approach is the highest at the early stages of the design. In addition, the effectiveness of the hazard reduction measures by employing the inherent safety principles must also be assessed at the early stages of the process design so that the design engineers can make an informed decision on the process design. This paper describes the methodology for integrating the assessment of fire hazards with process simulation at the early stage of process design. The methodology was illustrated by comparing process routes for dimethyl ether (DME) production plant using substitution principle. The process design simulation was carried out in iCON® process simulator, while assessment of the fire hazards was carry out in Excel® using a seamless two-way data transfer facility that is available in iCON®. The results from the case study showed that the potential consequences of a fire can be reduced by employing the substitution principle of inherent safety. The methodology that has been developed in this work enables simultaneous technical and safety assessments at the early stages of the process design.

Keywords: *Consequence Analysis, Inherent Safety, Process Design, Simulation, Synthesis Gas*

1.0 INTRODUCTION

Optimisation of process design according to economics, operational, environmental and safety requirement is the origin to an economical, safer and environmentally benign process throughout the whole lifetime of the plant. In addition, due to general society expectation, company image and economic reasons, safety of a processing plant should achieve a common acceptable level [1]. For instance in Malaysia, the Occupational Safety and Health act 1994 [2] states that, it is the responsibility of the company to ensure safety and well being of its workers and the general public. The rapid growth in the use of hazardous chemicals in the industry has brought significant risk to both workers and general public, whose well being could be endangered at any time by accident involving these chemicals. For the above reasons, the inherent safety principles since its introduction by Trevor Kletz in has gained popularity as an approach for safety improvement in the design of processing plants[3]. Inherent safety strives to enhance process safety by introducing fundamentally safer characteristics into process design as well as selecting and designing the process to eliminate or minimise hazards rather than accepting the hazards and implementing add-on systems to control it [4]. One of the principles of inherent safety is substitution. This can be accomplish by using alternative chemistry that allows the use of less hazardous materials or less severe processing conditions [5,6].

The opportunity for incorporating inherent safety features decreases exponentially from conceptual design stage to operational stage as illustrated in Figure 1 [5]. Thus, it is best to apply inherent safety principles and to assess their effectiveness in improving process safety at early stages of process design. In order to apply inherent safety principles successfully at the early stages of process design, a systematic assessment methods and tools must be available to assist the implementation. One possible option is to integrate safety assessment with the process simulation. Numerous process simulation software are used by process design engineers such as Aspen Plus® [7], HYSYS® [8] and the locally developed iCON® [9]. Each software has its own strength and unique features. However, to integrate safety assessment with process simulation, the latter should have features that allow for interfacing with other readily available and accessible softwares.

Most existing safety assessment methods focus on existing plants or later phases of process design, where most of the process engineering details are known [1]. For example, the conventional risk assessment is typically done at the detailed engineering stage. Hence, the effects of changes in process synthesis route and operating conditions on the potential consequence and risk level cannot be studied in a timely manner during the design stages [10]. At the process simulation stage, adequate data are available for safety assessment using the *consequence analysis technique*. However, a methodology that automatically extracts data from process simulation and carries out the consequence analysis is currently not available. Without an automated methodology, the consequence analysis will be a tedious process, requires manual extraction of data and is very time consuming. Such a situation makes the effort to assess the effectiveness of inherently safer design at process simulation stage an unattractive option when the designs engineers are under pressure to meet the scheduled target. This paper discusses the integration of consequence analysis with process simulation at preliminary design stage. The method enables process design decision making takes into account the potential consequence of the process accidents by considering the selection of process synthesis route and process conditions.

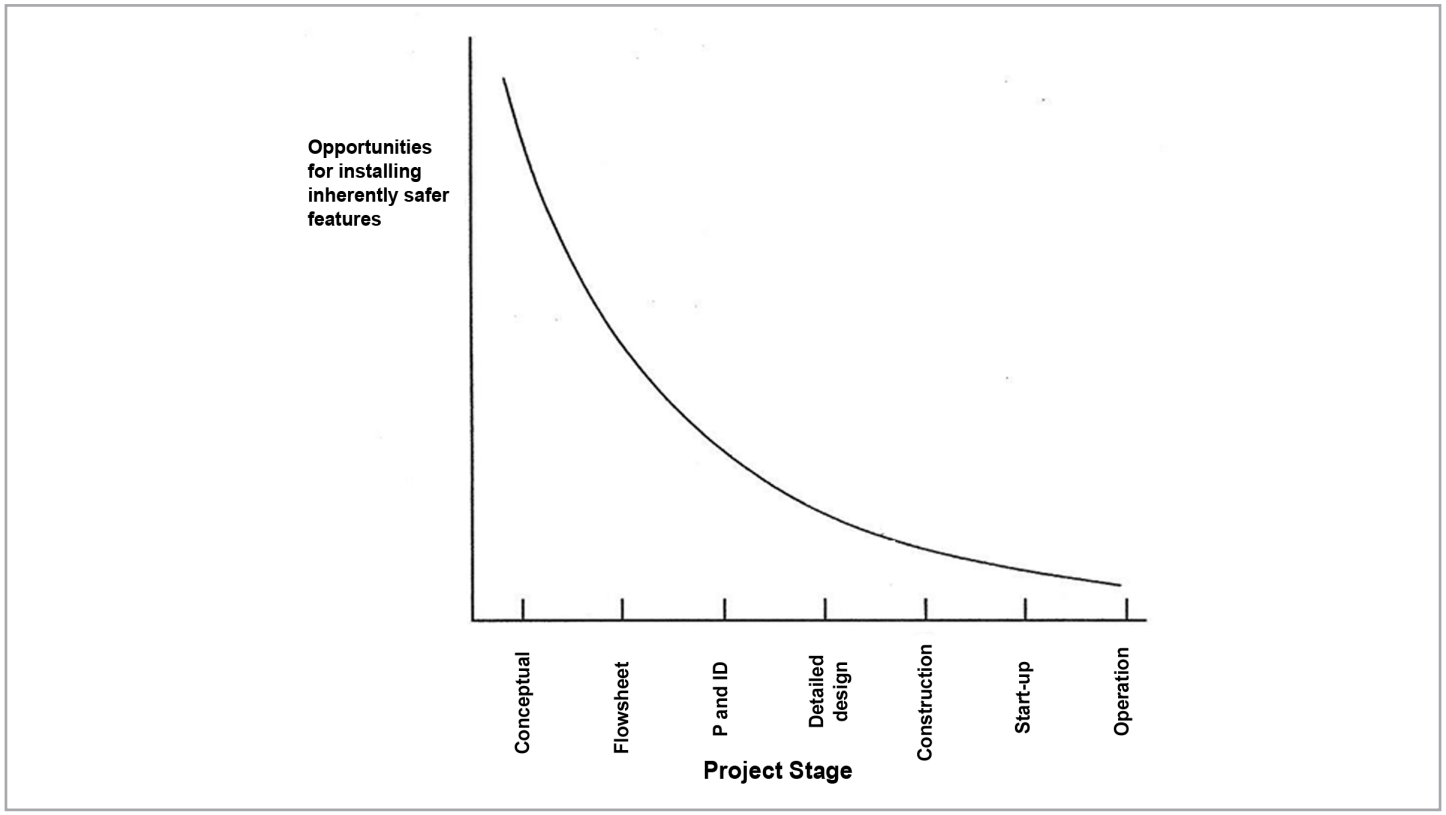

Figure 1: Opportunity for implementing inherent safety features [5]

2.0 INTEGRATING CONSEQUENCE ANALYSIS WITH PROCESS SIMULATION

Figure 2 shows the framework for integrating consequence analysis with process simulation in iCON®. The first step is to simulate a base design case using iCON® process simulator that was later used as a basis for comparison. A unit operation was then selected for assessment based on consequence analysis. The Excel® worksheet is then call upon using the worksheet option that is provided in iCON®. The required input variables from process simulation were identified and the necessary equations for consequence analysis for fire effects were then set-up in the worksheet. All major equipment in the plant should be considered and consequence analysis was done for all process routes that were considered before selecting the best process route for detailed design.

iCON® provides a seamless two way data transfer with Excel® allowing a user to link Excel® spreadsheets directly to iCON®. Any changes that is made either on iCON® or through Excel® is immediately captured and new set of process simulation and consequence analysis calculations are triggered automatically in the other software. Such features allows a user to manipulate any process parameter from either iCON® or Excel® to meet the required safety criteria. The available process data from simulation at early stage of process design are adequate for consequence analysis purposes. Data needed for consequence analysis such as process conditions, physical properties, flammability data and others were transferred from the process simulator to the Excel® worksheet using the import/export features available on iCON®. These data are used as input in modeling the potential consequence of various unwanted events such as fires, and in generating useful data such as thermal

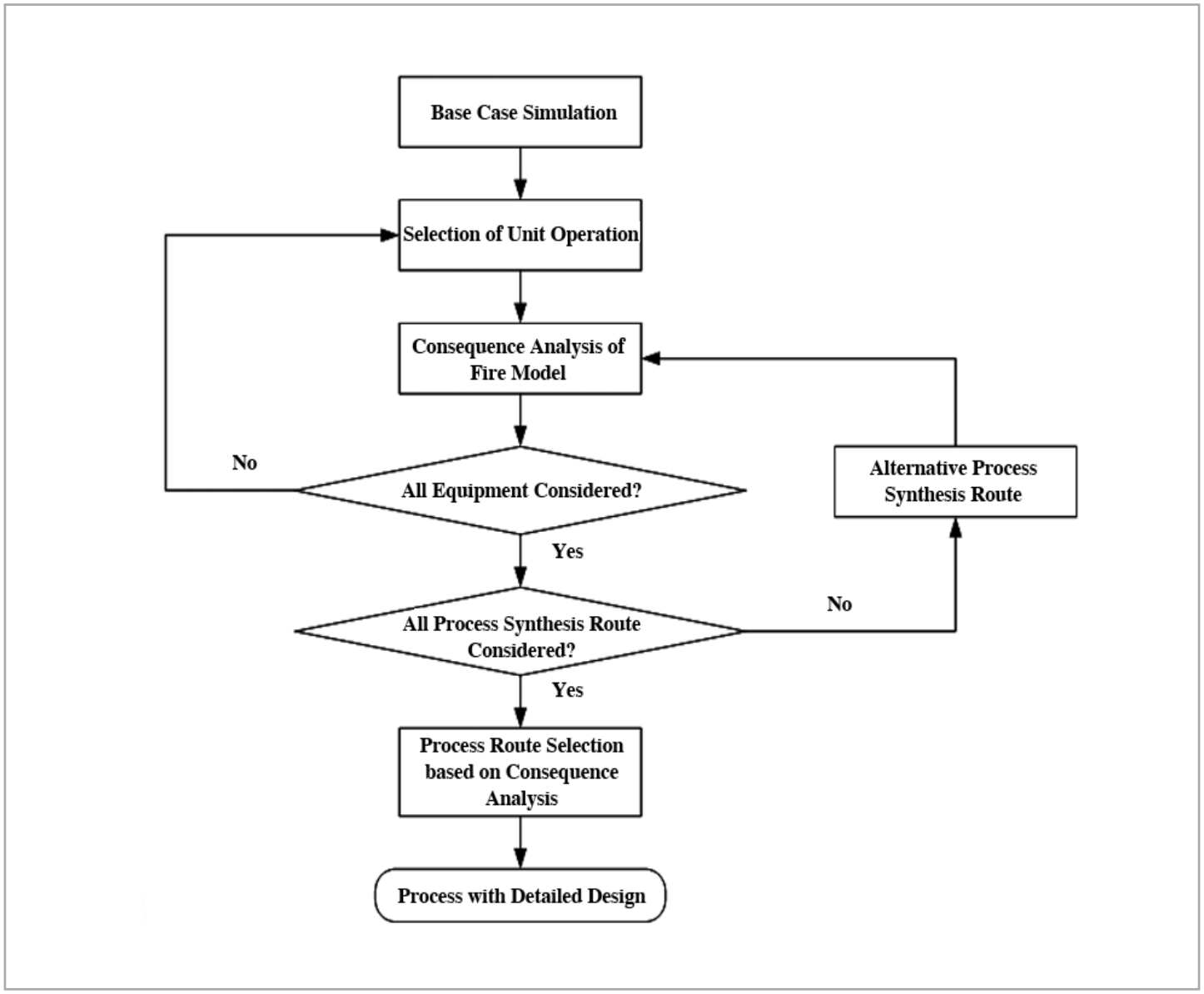

Figure 2: Consequence analysis approach for fire analysis in inherently safer design

radiation intensity versus distance. The consequences onto various receptors such as human is then determined using the vulnerability model [11]. The results of assessment can then be used as indicators on the potential consequence of accidents in the plant, which provides a basis for selecting process synthesis route or the operating conditions that will meet the safety requirements.

3.0 CASE STUDY: FIRE MODEL IN A DIMETHYL ETHER PLANT

The assessment of two alternative process synthesis routes for dimethyl ether (DME) production was selected as a case study. In this case study, the substitution approach can be accomplished by using alternative process chemistry with different catalyst that allows process to be carried out at less severe processing conditions and less severe potential consequence of accidents at the plant. In the first route, DME was synthesis from syngas using Cu-based catalyst and γ-Al2O3 catalyst and the stoichiometric equations are presented in equations (1) through (3) [12].

$$CO + 2H_2 \rightarrow CH_3OH \quad (1)$$

$$2CH_3OH \rightarrow CH_3COH_3 + H_2O \quad (2)$$

$$CO + H_2O \rightarrow CO_2 + H_2 \quad (3)$$

In the second route, DME was produced from the dehydration of methanol over acid-zeolite catalyst [13] as shown in equation (4).

$$2CH_3OH \rightarrow (CH_3)_2\ O + H_2O \quad (4)$$

The simulation flowsheet for the two DME plants are presented in Figures 3 and 4, respectively. The occurrence of a major jet fire at the reactor and absorber as well as pool fire at

the distillation columns were selected as illustrations in using consequence analysis as a basis for process route selection. The DME plant employing the syngas reaction was used as a base case design. The simulation flowsheet for the base case design with excel® worksheet interface is shown in Figure 5.

A jet fire occurs when there is a loss of containment of pressurized flammable gas that is immediately ignited. Detailed description on modeling the consequence of a jet fire may be obtained from the AIChE Guideline [11]. The main equations and brief description in modelling a jet fire are presented in Table 1. For estimation of potential consequences due to a jet fire, several input data are needed, *e.g.* release diameter for calculation of mass flow rate of flammable gas, combustion reaction for flammable gas leak, height above ground and receptor distance from the flame. The release diameter used in this work was 100 mm, as recommended by the AIChE Guideline [11].

A pool fire occurs when there is a loss of containment of liquid phase of flammable substance that is immediately ignited [10]. A pool fire model for the estimation of incident thermal radiation is shown in Table 2. Detailed description on the modeling of the consequence of a pool fire may be obtained from the AIChE Guideline [11]. The main equations with a brief description for the modeling of a jet fire are presented in Table 2. For estimation of potential consequences due to a pool fire, several input data are needed, *e.g.* release diameter for the calculation of mass flow rate of flammable substance, heat of combustion, heat of vaporisation, *etc*.

The damaging effect of fire model is from its thermal radiation and the consequence that is experienced by a receptor, depending upon the intensity of thermal radiation and the exposure duration. Longer exposure durations, even at a lower thermal radiation level, can produce serious physiological effects. The consequence of thermal radiation onto a human receptor was estimated using the probit analysis [11,14]. The probit variable, *Y*, for heat radiation lethality is given by Equation (20) and the conversion from probit value to percentage of fatalities is given by Equation (21), respectively.

$$Y = 1.49 + 2.56\, in\left(\frac{t1^{4/3}}{10^4}\right) \tag{20}$$

$$P = 50\left[1 + \frac{Y-5}{|Y-5|}\, erf\left(\frac{|Y-5|}{\sqrt{2}}\right)\right] \tag{21}$$

where Y is the probit variable (unitless), t is the duration of exposure (s), I is the thermal radiation intensity (W/m2), P is fatalities percentage (%) and "*erf*" is the error function.

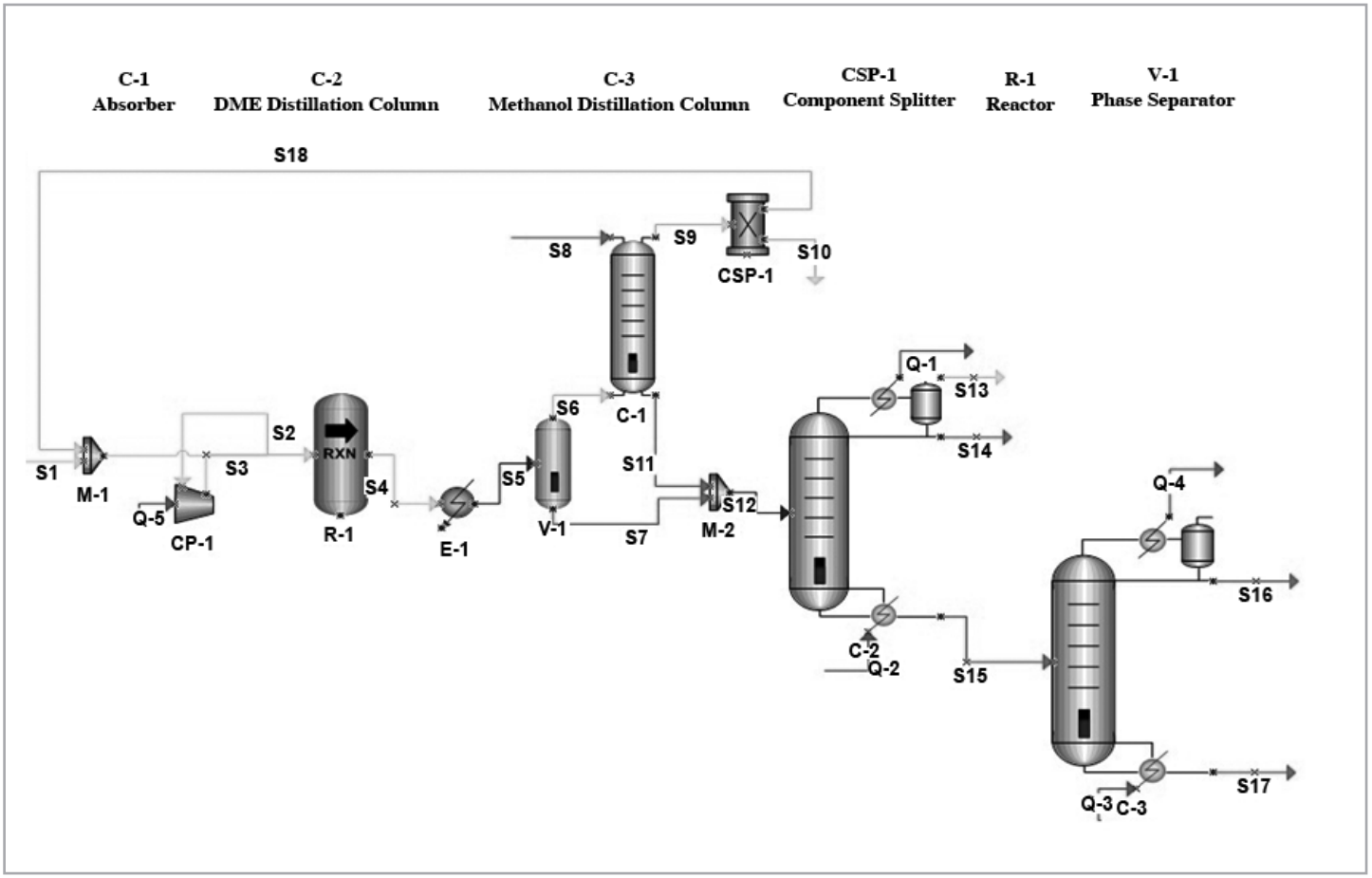

Figure 3: Preliminary simulation flowsheet for the production of DME from syngas

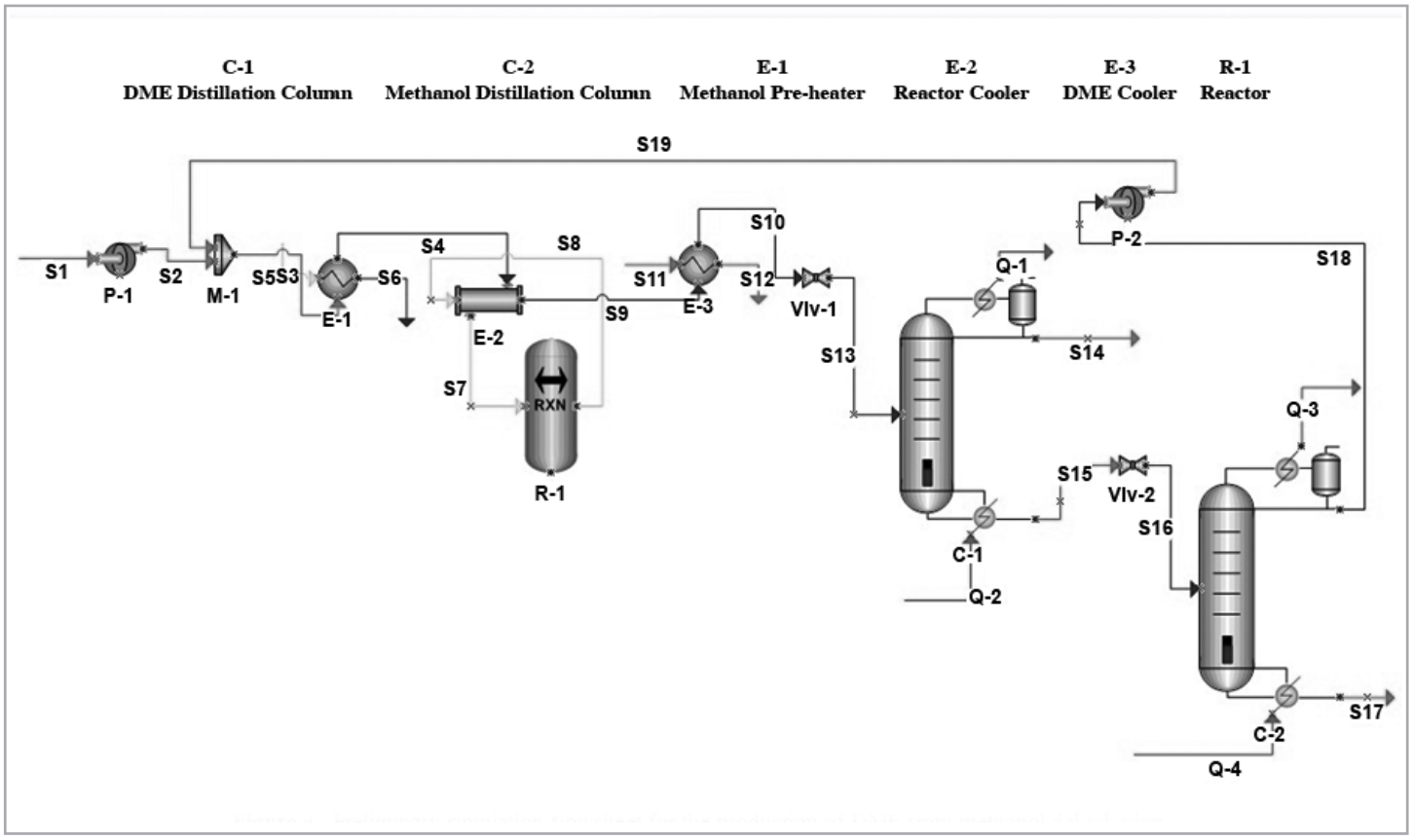

Figure 4: Preliminary simulation flowsheet for the production of DME from methanol dehydration

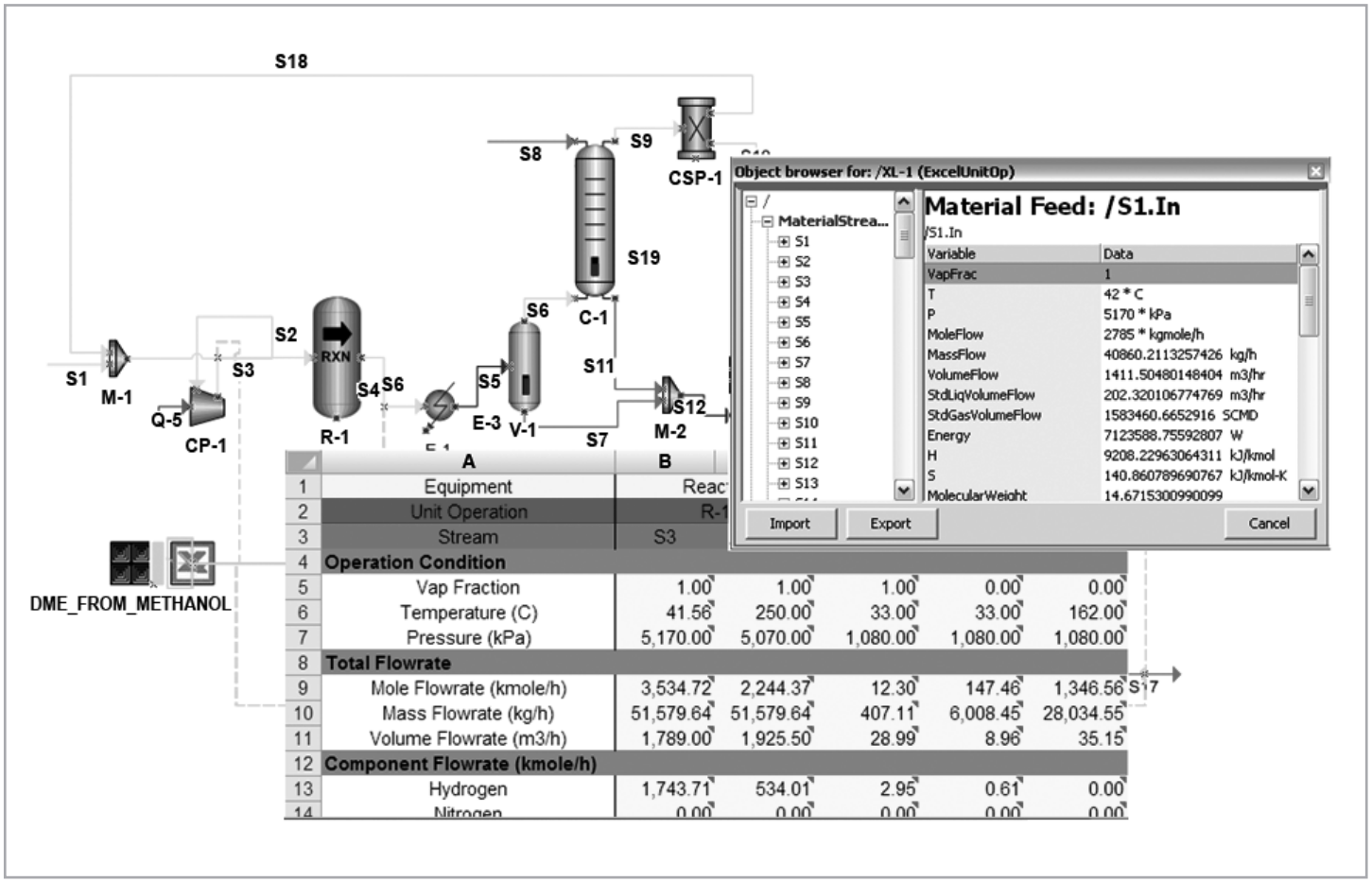

	A	B				
1	Equipment	Reac				
2	Unit Operation	R-1				
3	Stream	S3				
4	**Operation Condition**					
5	Vap Fraction	1.00	1.00	1.00	0.00	0.00
6	Temperature (C)	41.56	250.00	33.00	33.00	162.00
7	Pressure (kPa)	5,170.00	5,070.00	1,080.00	1,080.00	1,080.00
8	**Total Flowrate**					
9	Mole Flowrate (kmole/h)	3,534.72	2,244.37	12.30	147.46	1,346.56
10	Mass Flowrate (kg/h)	51,579.64	51,579.64	407.11	6,008.45	28,034.55
11	Volume Flowrate (m3/h)	1,789.00	1,925.50	28.99	8.96	35.15
12	**Component Flowrate (kmole/h)**					
13	Hydrogen	1,743.71	534.01	2.95	0.61	0.00
14	Nitrogen	0.00	0.00	0.00	0.00	0.00

Figure 5: Simulation flowsheet for base case design with Excel® interface

Table 1: Consequence model for jet fire [10]

Item	Description
Source Model	$$\boldsymbol{m}_{choked} = C_D A P_1 \sqrt{\frac{k g_c M}{R_g T_1}\left(\frac{2}{K+1}\right)^{(k+1)(k-1)}} \quad (5)$$ ***m*** is mass flow rate of gas through the hole (kg/s), A is area of the hole (m^2), C_D is discharge coefficient (unitless), g_c is the gravitational constant (kg m/s^2), P_1 is pressure upstream of the hole (*Pa*), k is heat capacity ratio, C_p/C_v (unitless), M is molecular weight of the gas (kg/kgmole), R_g is ideal gas constant (Pam^3/kgmole.K) and T_1 is initial upstream temperature of the gas (K).The equation representing mass flow rate for sonic, or choked case. The pressure ratio required to achieve choking is given by; $$\frac{P_{choked}}{P_1}\left(\frac{2}{K+1}\right)^{k/(k-1)} \quad (6)$$ Equation (2) demonstrates that choking conditions are readily produced – an upstream pressure of greater than 13.1 psig for an ideal gas is adequate to produce choked flow for a gas escaping to atmospheric. For real gases, pressure of 20psig is typically used.
Jet Fire Model	$$\frac{L}{d_j} = \frac{15}{C_T}\sqrt{\frac{M_a}{M_f}} \quad (7)$$ ***L*** is the length of the visible turbulent flame measured from the break point (m), *dj* is the diameter of the jet, that is, the physical diameter of the nozzle (m), C_T is fuel mole fraction concentration in a stoichiometric fuel-air mixture (unitless), M_a and M_f are molecular weight of air and fuel (kg/kgmole). $$F_p = \frac{1}{4\pi\pi^2} \quad (8)$$ F_p is the point source of view factor (m^{-2}), x is the distance from the point source to the target (m) which can be obtained using the hypoteneous of a right triangle and π is a mathematical constant = 3.142 (unitless). $$E_r = \tau_a \eta \boldsymbol{m} \Delta H_c F_p \quad (9)$$ where *Er* is the radiant flux at the receiver (kW/m^2), τ_a is the atmospheric transmissivity (unitless), η is the fraction of total energy convert ed to radiation (unitless), *m* mass is flow rate of the gas through the hole (kg/s), ΔH_c is energy of combustion of the fuel (kJ/kg) and F_p is the point source of view factor (m^{-2}).

Table 2: Consequence model for pool fire [10]

Item	Description
Source Model	$$\frac{g_c (P_2 - P_1)}{\rho} + g(z_2 - z_1) + \frac{1}{2} v_2^2 + g_c \sum e_f = 0 \quad (10)$$ where ρ is the density of the fluid (kg/m^3), g_c is the gravitational constant (kg m/s^2), P_1 is the pressure upstream of the hole (Pa), P_2 is the pressure downstream of the hole (Pa), g is the acceleration of gravity (9.81 m/s^2), z_1 and z_2 is initial and final reference point (m), v_2 is fluid velocity (m/s) and $\sum e_f$ is the frictional loss term given by equation (11); $$\sum e_f = \sum K_f \frac{v_2^2}{2g_c} \quad (11)$$ where $\sum e_f$ is the frictional loss term(m/kg), $\sum K_f$ is the excess head loss due to the pipe or pipe fitting (unitless), v_2 is fluid velocity (m/s) and gc is the gravitational constant (kg m/s^2). $$\boldsymbol{m} = \rho v_2 A \quad (12)$$ where ***m*** is the liquid discharge rate (kg/s), ***A*** is the area of the hole (m^2), v^2 is fluid velocity (m/s) and ρ is the density of the fluid (kg/m^3).

Pool Fire Model

$$y_{max} = 1.27 \times 10^{-6} \frac{\Delta H_c}{\Delta H^*} \quad (13)$$

where y_{max} is the vertical rate of liquid decrease (m/s), ΔH_c is the net heat of combustion (kJ/kg) and ΔH^* is the modified heat of vaporization (kJ/kg) at the boiling point of the liquid given by equation (12)

$$\Delta H^* = \Delta H_v + \int_{T_a}^{T_{BP}} C_p dT \quad (14)$$

where T_{BP} is the boiling point temperature of the liquid (K), T_a is the ambient temperature (K) and C_p is the heat capacity of the liquid (kJ/kg.K).

$$m_B = y_{max} \times \rho \quad (15)$$

where m_B is the mass burning rate (kg/m^2 s) and ρ is the liquid density (kg/m^3)

$$\frac{H}{D} = 42 \left(\frac{m_B}{\rho_a \sqrt{gD}} \right)^{0.61} \quad (16)$$

where H is the visible flame height (m), D is the equivalent pool diameter (m), m_B is the mass burning rate (kg/m^{2}s), ρ_a is the air density (1.2 kg/m^3), g is the acceleration of gravity (9.81 m/s^2).

$$D_{max} = 2 \sqrt{\frac{V_L}{\pi y}} \quad (17)$$

where D_{max} is the equilibrium diameter of the pool (m), V_L is the volumetric liquid spill rate (m^3/s), and y is the liquid burning rate (m/s) and π is a mathematical constant = 3.142 (unitless).

$$F_p = \frac{1}{4\pi\pi^2} \quad (18)$$

F_p is the point source of view factor (m^{-2}), x is the distance from the point source to the target (m) which can be obtained using the hypoteneous of a right triangle and π is a mathematical constant = 3.142 (unitless).

$$E_r = \tau_a \eta m_B \Delta H_c A F_p \quad (19)$$

where E_r is the radiant flux at the receiver (kW/m^2), τ_a is the atmospheric transmissivity (unitless), η is the fraction of total energy converted to radiation (unitless), m_B is the mass burning rate (kg/m2s), ΔH_c is energy of combustion of the fuel (kJ/kg), A is the total pool area and F_p is the point source of view factor (m^{-2}).

For simplification purpose, from this point forward, production of dimethyl ether from syngas referred as process route 1 and production of dimethyl ether from methanol referred as process route 2. The results of the consequence analysis are presented in Tables 3 and 4, whilst Table 5 [14] presents various levels of damages as a result of exposure to thermal radiation. The results of the consequences analysis of a jet fire that has the potential to occur at the two alternative process routes along with the potential fatal consequences onto human receptors are presented in Table 3. Based on Table 3, the impact zone as well as the potential for fatal consequence as a result of the occurrence of jet fire at reactor was higher for process route 1. As shown, zero fatality is expected at a distance more than 50 m for process route 1. On the other hand, zero fatality is expected at a distance more than 25 m for process route 2. In addition, the distance of radiation limit that can cause pain to workers who are unable to reach for a cover in 20 seconds are more than 65 m and 35 m for process routes 1 and 2, respectively. The results of consequence analysis of a jet fire that has the potential to occur at the absorber at the plant using process route 1 shows that zero fatality is expected at a distance almost more than 37 m. Based on Table 5, the distance of radiation limit effects from potential jet fire at absorber that can cause pain to worker who are unable to reach for a cover in 20 seconds is more than 55 m.

The potential effects of thermal radiation from pool fire at distillation columns at the two alternatives routes are presented in Table 4a and b. Based on the results, thermal radiation effect from pool fire at DME distillation in both routes will cause zero fatality at more than 25m distance. However, longer exposure durations can produce serious physiological effects to the receiver. The impact zones for the methanol distillation columns in both routes are much smaller compare to the DME distillation column. Based on the assessment results for main components as presented in Tables 3 and 4, process route 2 is safer compared to process 1, thus process route 2 should be selected for the subsequent stages of the design of the DME production plant.

Table 3: Consequence of a jet fire at several distances for both process routes

Process Route	Process Route 1				Process Route 2	
Equipment	*Reactor*		*Absorber*		*Reactor*	
Distance (m)	*Flux (kW/m²)*	*Fatalities Percentage (%)*	*Flux (kW/m²)*	*Fatalities Percentage (%)*	*Flux (kW/m²)*	*Fatalities Percentage (%)*
25	32.78	76.39	29.25	62.95	8.66	0.01
27	28.95	61.60	21.95	25.76	7.64	0.00
30	24.26	37.88	16.90	6.14	6.41	0.00
33	20.55	19.08	13.32	0.93	5.43	0.00
35	18.50	10.88	10.73	0.10	4.89	0.00
37	16.73	5.74	8.79	0.01	4.42	0.00
40	14.49	1.94	7.32	0.00	3.83	0.00
45	11.61	0.24	6.18	0.00	3.07	0.00
50	9.48	0.02	5.28	0.00	2.50	0.00
55	7.88	0.00	4.56	0.00	2.08	0.00
60	6.63	0.00	3.97	0.00	1.75	0.00
65	5.66	0.00	3.49	0.00	1.49	0.00

Table 4a: Consequence of a pool fire at several distances for both process routes

Process Route	Process Route 1		Process Route 2	
Equipment	*DME Distillation Column*			
Distance (m)	*Flux (kW/m²)*	*Fatalities Percentage (kW/m²)*	*Flux (kW/m²)*	*Fatalities Percentage*
5	15.56	3.41	15.70	3.64
10	13.55	1.08	13.64	1.15
15	11.89	0.31	11.95	0.32
20	10.51	0.08	10.55	0.08
25	9.35	0.02	9.37	0.02
30	8.36	0.00	8.37	0.00
35	7.52	0.00	7.52	0.00
40	6.80	0.00	6.79	0.00
45	6.17	0.00	6.16	0.00
50	5.63	0.00	5.61	0.00
55	5.15	0.00	5.13	0.00

Table 4b: Consequence of a pool fire at several distances for both process routes

Process Route	Process Route 1		Process Route 2	
Equipment	*Methanol Distillation Column*			
Distance (m)	*Flux (kW/m²)*	*Fatalities Percentage (kW/m²)*	*Flux (kW/m²)*	*Fatalities Percentage*
5	13.65	1.16	13.61	1.13
10	11.76	0.27	11.72	0.26
15	10.21	0.06	10.18	0.05
20	7.02	0.00	6.99	0.00
25	7.90	0.00	7.87	0.00
30	7.02	0.00	6.99	0.00
35	6.27	0.00	6.25	0.00
40	5.64	0.00	5.61	0.00
45	5.09	0.00	5.07	0.00
50	4.62	0.00	4.60	0.00
55	4.21	0.00	4.19	0.00

Table 5: Thermal radiation limit [14]

Thermal Intensity (kW/m²)	Exposure Limit
37.5	Intensity at which damage is caused to process equipment
15.6	Intensity on structures where operators are unlikely to be performing and where shelter is available.
9.5	Intensity at design flare release at locations to which people have access and where exposure would be limited to a few seconds for escape
6.3	Intensity in areas where emergency actions lasting up to one minutes may be required without shielding but with protective clothing
4.5	Intensity sufficient to cause pain to personnel unable to reach for covers in 20 seconds, though blistering of skin (first degree burn) unlikely
1.6	Intensity insufficient to cause discomfort for long term exposure

4.0 DISCUSSION

The methodology that has been developed in this work links and automates the consequence analysis of fire hazards at process simulation stage using a standard process simulator and readily available Microsoft Excel® software. It enables the assessment on the selection of process synthesis route based on the potential impact of process accidents in addition to technical and economical criteria. The framework that has been presented in Figure 2 can be extended further to include other possible incident outcomes such as explosion and dispersion of toxic gas for a more comprehensive assessment on the selected process route.

The above case study illustrated the implementation of the methodology that has been developed in this work.

It allows for assessment of the effectiveness of the implementation of the inherent safety at the process simulation stage. The results of the consequence modeling of fire can be a useful input in the management decision making process. By knowing the thermal radiation vs. distance, the plant layout of a new plant can be designed such that the spacing between unit operations satisfy the exposure limit and adequate safe distance is provided for evacuation purpose. For modification or expansion of an existing plant, the information on thermal radiation vs. distance is very useful to determine the location of the new unit operations so that the necessary spacing distances are fulfilled.

5.0 CONCLUSION

A tool that integrates the consequence analysis of fire hazards with process simulation was successfully developed and demonstrated. It automatically extracts the required data from the process simulator to carry out the consequence analysis and generate useful data such as thermal radiation versus distance as well as consequences onto various receptors. The tool can be used to carry out safety assessment on process route selection based on inherent safety principles. With simultaneous technical and safety assessments are done at early stage of the process design, the process designers are provided with better information to make an informed decision on the process design.

ACKNOWLEDGEMENT

The authors wish to thanks Universiti Kebangsaan Malaysia for funding this project under grant number UKM-GUP-BTT-07-25-167. ■

REFERENCES

[1] Hurme, M., and Rahman, M., 2005, Implementing Inherent Safety Throughout Process Lifecycle, *Journal of Loss Prevention in the Process Industries*, **18**: 238-244.

[2] Malaysian Government, 2006, Guidelines on Occupational Safety and Health Act 1994, Department of Occupational Safety and Health, Kuala Lumpur.

[3] Kletz, T, 1978, What you don't have can't leak, Chemical Industry, May 6th, 287-292

[4] Rahman, M., Hekkilä, A-M., and Hurme, M., 2005, Comparison of Inherent Safety Indices in Process Concept Evaluation, *Journal of Loss Prevention in the Process Industries*, **18**: 327-334.

[5] Kletz, T. 1998, Process Plants: A Handbook for Inherently Safer Design, Taylor & Francis, London.

[6] Crowl, D. A and Louvar, J.F, 2002, Chemical Process Safety, Prentice Hall Inc., New Jersey.

[7] Aspen Plus, Version 11.1, 2001,User Manual, Aspen Technology. Inc.

[8] Hysys, Release 3.2, 2003, Hysys User Guide, Hyprotech

[9] iCON, 2007, iCON User Manual, Petronas.

[10] Mohd Shariff, A., Rusli, R., Leong, C.T., Radhakrishna V. R. and Buang, A., 2006, Inherent Safety Tool for Explosion Consequences Study, *Journal of Loss Prevention in the Process Industries*, **19**: 409-418.

[11] AIChE, 1999, Guidelines for Consequence Analysis of Chemical Releases, CCPS, New York.

[12] Dong-sheng, W., Yi-sheng, T., Yi-zhuo, H., Noritatsu, T., 2008 Study on Deactivation of Hybrid Catalyst for Dimethyl Ether Synthesis in Slurry Reactor, *Journal Of Fuel Chemistry And Technology*, **36**(2): 171-175.

[13] Turton, R, Bailie, R.C, Wallace, W.B, and Shaeiwitzet, J.A, 1998, Analysis, Synthesis and Design of Chemical Processes, Prentice Hall Inc., New Jersey.

[14] Lees, F.P, 1996, Loss Prevention in the Process Industries, Butterworth-Heinemann, London.

PROFILES

MARDHATI ZAINAL ABIDIN
Mardhati Zainal Abidin received her Bachelor of Engineering in Chemical Engineering from University Kebangsaan Malaysiain 2008. She is currently a Master student in area of process safety at the Department of Chemical and Process Engineering, Faculty of Engineering and Built Environment, UKM.

DR MOHD SOBRI TAKRIFF
Dr Mohd Sobri Takriff is a Professor and a Deputy Dean at the Faculty of Engineering and Built Environment, Universiti Kebangsaan Malaysia. He received his PhD from the University of Arkansas in 1996. His research interest include fluid mechanics, multiphase flow, process safety and bioprocesses

INHERENT OCCUPATIONAL HEALTH CONCEPT FOR CHEMICAL PROCESSES: A NEW PERSPECTIVE

(Date received: 29.1.2010/ Date accepted: 26.8.2010)

Mimi H. Hassim[1,2], Markku Hurme[3]
[1, 3] Plant Design, School of Science and Technology,
Aalto University, FIN-02015, Finland
[2] Department of Chemical Engineering,
Universiti Teknologi Malaysia, 81310 UTM Skudai, Johor
E-mail: [1,2]mharyani@gmail.com

ABSTRACT

The concept of inherent safety was known since the last few decades. The idea was quickly spread from the origin UK to the USA and later, to the other parts of the world. The idea was then extended to environment and subsequently health aspects. Various works have been done related to inherent safety and environmental friendliness in chemical process industries. Such works on occupational health however, are lacking. Unlike the other aspects, the term inherent occupational health has never been defined in literatures. This paper proposes a definition of the inherent occupational health concept as well as the background of inherent health studies, which was designed for chemical processes. The definition, which was carefully developed based on deep understanding and extensive works in this research area will have a huge impact on the chemical process industry (CPI) especially related to their efforts in considering occupational health aspect early in process development and design.

Keywords: *Definition; Inherent Occupational Health; Inherent Safety; Chemical Process Industry; Terminology*

1.0 INTRODUCTION

Inherent safety initiatives in the chemical process industry (CPI) are known since 30 years ago. The idea has been thought up after enormous efforts to improve chemical process safety have failed to stop or reduce catastrophic plant disasters from occurring. History has witnessed hundreds and thousands of deaths and higher number of injuries due to major accidents even though the most updated add-on protective equipment were installed and the best safety managements were practiced. Among the accidents and the reported number of deaths are: Flixborough in 1974 (28), Bhopal in 1984 (2 000 to 8 000), Piper Alpha in 1987 (167), Mexico City in 1984 (650), and Pasadena in 1989 (23). These aftermaths show the need for CPI to shift from conventional safety approaches to inherent safety.

The concept of inherent safety was first introduced to enhance process safety in chemical industries and oil and gas refineries. It is widely accepted as it put forward ideas and principles that are making sense and back-to-basic. Trevor Kletz [1], the father of inherent safety, proposed that the concept applies also to the prevention of pollution (environment) and the avoidance of small continuous leaks into the atmosphere of the workplace (industrial hygiene/health), but he did not evolve it further. The concept has later been extended to environmental and subsequently health aspects. This agrees with the idea of sustainability which incorporates safety, health, and environmental besides economic and technical criteria when developing a new process.

Various researches have been conducted in the area of inherent safety, inherent environmental friendliness as well as integrated inherent safety, health, and environmental friendliness (ISHE) in chemical process design. However inherent occupational health aspect has not been widely researched in the design of chemical plants, but active work has been done dominantly from medical point of view. Being the earliest and the most researched subject, the concept of inherent safety is well defined and discussed. Even though research studies on inherent environmental friendliness and ISHE are also active, not much attention has been put on defining the terms. The definitions however, are still available. As for inherent occupational health, no definition has been found; even the use of the terminology in CPI-related studies is rare. In this paper, inherent occupational health is defined from the perspective of CPI. This is very important since there is an increasing demand to evaluate the health impacts of substances used in the process industries. For example an European Community Regulation on chemicals and

their safe use called the Registration, Evaluation, Authorization and Restriction of Chemicals (REACH) which has been enforced on 1 June 2007 requires anyone manufacturing or importing a chemical substance to be placed on the market in the European Union countries, in quantities above 1 tonne per year, to register that substances for the uses to which it will be put. The hazardous effects of these chemicals also need to be reported.

In order to conduct a comprehensive health hazard and risk assessment of chemical process design, definitions of the related terms itself are important. A properly designed definition of inherent occupational health could bring a huge impact to the CPI because it somehow describes the objective and scope of inherent occupational health assessment of a chemical process, besides indirectly provides means for preventing health hazards and making process changes as early as in the development and design phases. For better appreciation of the subject matter, brief discussions on the background of inherent safety, inherent environmental friendliness, and ISHE as well as their definition are also given.

2.0 INHERENT SAFETY

Inherent safety ideology started to develop in 1970's. Professor Trevor Kletz was the first to propose the concept in 1971 [2]. The idea was thought up when he was a member of the organizing committee for the symposium on 'Loss Prevention in the Process Industries' held in Newcastle, UK, in 1971. A paper presented on the manufacture of nitroglycerin [3] and temperature control of methanol vaporizer [4] had led to a remark made by T. A. Kantyka, who is the chairman of the committee, that it was far better to avoid the need for complex safety or control systems than to install them. Kantyka's remark had the effect on Kletz on his earliest idea of inherent safety.

The idea however, remained latent until the explosion at Flixborough four years later. At the 1975 loss prevention symposium, Kletz [5] delivered the idea on the inventory reduction to avoid Flixborough type of explosions, but the words 'inherently safer' was not used. The inherent safety principles were then formalised [6]. In 1977, Kletz gave an annual Jubilee lecture 'What you don't have, can't leak' to the Society of Chemical Industry in London, which devoted entirely to inherently safer design.

2.1 Definition

Before discussing the definition of inherent safety, it is important to first, understanding the related terms. *Safety* is the prevention of accidents [7] through hazards identification and their elimination. *Accident* is defined as any unplanned event that results in injury or ill health of people or loss to property, plant, materials, or the environment or a loss of a business opportunity [8]. *Occupational safety* is the protection of people from physical injury from accidents at work [9]. An *occupational injury* is any personal injury, disease, or death resulting from an occupational accident [10] *e.g.* instantenous exposure in the working environment [11]. *Process safety* is the prevention of accidents through the use of appropriate technologies to identify and eliminate the hazards of a chemical plant [7]. Figure 1 summarises the concept of safety. When introducing the inherent safety concept, Kletz's focus was on process and not occupational safety. Therefore inherent safety discussion in this paper will be revolved around process safety subject. However for better understanding, the difference between occupational health, process safety, and occupational safety will be discussed in Section 5.1.

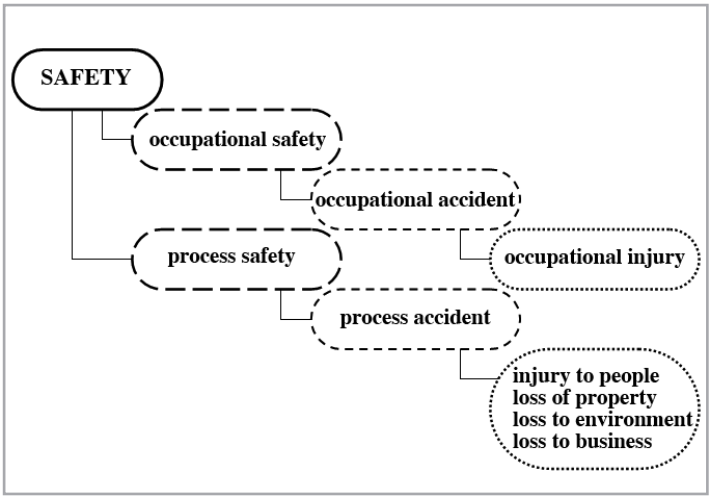

Figure 1: Safety concepts

The topic of safety is closely related to hazard and risk; therefore definition of these terms worth the attention. The definition of hazard is widely available in various publications [*e.g.* 7-8; 12-15]. Basically, hazard is a chemical or physical condition that has a potential to cause damage. A safety hazard alone is something that has the potential to cause an injury. Specific definitions of environmental and health hazards will be given in subsequent sections.

Like hazard, the definition of risk can be easily found not only for CPI, but also for other fields [*e.g.* 7-8; 12-13; 15-16]. In general, risk is a measure concerning both the likelihood and magnitude of loss. Inherent safety was introduced as a new measure of risk reduction through hazards elimination or minimisation.

Inherent means that which is intrinsic to something. American College Dictionary [17] defines inherent as existing in something as a permanent and inseparable element, quality, or attribute. Compared to extrinsic safety that relies on add-on engineered safety systems and procedural controls [18-19], inherent safety associates with the intrinsic properties of the process itself. If add-on safety relates to prevention of risk of accidents (prevention of likelihood and magnitude), inherent safety concerns with prevention of hazards (prevention of hazard potential in a system) through the use of more benign chemicals and technologies. The idea of inherent safety is to avoid problems by solving them at their roots rather than to manage the consequences [20].

The terminology of inherent safety varies somewhat throughout the process safety community [2]. Based on the

discussions of the term by several researches in this area inherent safety is commonly defined as a proactive approach to loss prevention that tries to avoid or eliminate hazards, or reduce their magnitude, severity, or likelihood of occurrence by careful attention to the fundamental design and layout [1; 2; 12; 18-19; 21-28].

2.2 Related Research Efforts

Since the introduction of the concept in 1970s, researches on inherent safety have been very dynamic and continuously growing. The researches cover wide range of areas, but major efforts have been put on inherent safety assessment during process design, which involve the development of various tools and methodologies. Among research groups that actively work in this field and some of their members are; Loughborough University (D. W. Edwards, T. A. Kletz, F. P. Lees), Aalto University School of Science and Technology (M. Hurme, A.-M. Heikkilä, M. Rahman), Indian Institute of Technology, Kanpur (J. P. Gupta), Swiss Federal Institute of Technology (ETH) (K. Hungerbühler, G. Koller, S. Shah, U. Fischer), Memorial University of Newfoundland (F. I. Khan), Dalhousie University (P. R. Amyotte, C. B. Etowa), Pondicherry University (S. A. Abbasi), The Mary Kay O'Connor Process Safety Centre at Texas A&M University (M. S. Mannan, M. Gentile, W. J. Rogers), National University of Singapore (C. Palaniappan, R. Srinivasan. R. Tan), Universiti Teknologi Petronas (Azmi M. Shariff), The Dow Chemical Company (T. Overton), Rohm and Haas Company (D. C. Hendershot, K. Study), and National Research Council of Canada (R. Sadiq). The list is endless as process safety awareness among industries, academia, and regulators around the world is everyday improving and the concept of inherent safety is rapidly propagating.

3.0 INHERENT SAFETY, HEALTH AND ENVIRONMENTAL FRIENDLINESS (SHE)

A review of the status of inherently safer process design in UK conducted by Health and Safety Executive (HSE) stressed the need for methodologies that address safety, health, and environmental issues in an integrated manner [29]. Among the established publications on the SHE evaluation during process design are as follows [28; 30-35]. However, no definition of inherent SHE terminology was given. Srinivasan and Nhan [35] used the term inherent benign to describe a process which is inherently less hazardous in all the SHE aspects, but no proper definition was provided. In the early 1990s the European Union started the INSIDE Project to promote inherent safety, health, and environmental protection within the European industries. A toolkit was developed to enhance to enhance the use of inherent SHE approaches to process plant development and design [30]; however no definition of inherent SHE was given.

The definition of the terminology was finally found in a pharmaceutical book [16]. Inherent SHE is defined as the elimination of hazards by suitable process design so that processes are, by their very nature, safe, healthy, environmentally friendly, unaffected by change and stable [36]. Upon our knowledge, this is the only inherent SHE definition formally published up till now.

4.0 INHERENT ENVIRONMENTAL FRIENDLINESS

Despite the advantages of integrating all the SHE aspects, aggregating disparate indexes into one meaningful integrated index is difficult and fraught with the danger of being unrepresentative, subjective, and user-dependent [25; 37]. Some of these drawbacks can be overcome by considering the SHE aspects separately. A survey [26] conducted to cross-section of chemical engineering professionals from 11 countries found that some of the respondents suggested different indices for each of the safety, health and environment elements rather than a composite one to help in decision-making. Most of the methods that assess all the SHE criteria do not fairly addressing the aspects in balance. Usually they focus more on the inherent safety, waste minimization, and green chemistry concepts; with health aspect is often assessed very minimum. Some examples of such methods are given in Section 5.2.

Various studies have been conducted on environmentally conscious chemical process design, which include the assessment of environmental hazards of a design concept and substances [*e.g.* 27; 38-44]. An environmental hazard is a potential to cause harm to the environment [45]. However, none used the term inherent environmental friendliness or related terms in their publications, moreover defined it. A group in Loughborough University was the first to introduce the terminology formally and also defined it [45-47]. They suggested that an inherently environmentally friendly chemical plant would have small levels of actual and potential environmental impacts - the impacts encompass those due to a catastrophic failure, its emissions due to normal operational activities and also the small-scale accidental emissions during the life of the plant.

5.0 INHERENT OCCUPATIONAL HEALTH

Before inherent occupational health is defined, the associated terms are first discussed. *Health* in general is defined as a state of physical and mental well-being (as an opposite to illness) [48]. *Occupational health* is the protection of the bodies and minds of people from illness resulting from materials, processes, or procedures used in the workplace [9] and its aim is the promotion and maintenance of the highest degree of physical, mental, and social well-being of workers in all occupations by preventing departures from health, controlling risks, and the adaptation of work to people and people to their jobs [49]. OSHA [50] defines an *occupational disease* or *illness* as any abnormal condition or disorder, other than one resulting from an occupational injury, caused by exposure to factors associated with employment. *Occupational diseases* concern with a disease contracted as a result of an exposure over a period of time to risk factors arising from work activity. Figure 2 summarizes the concept of health.

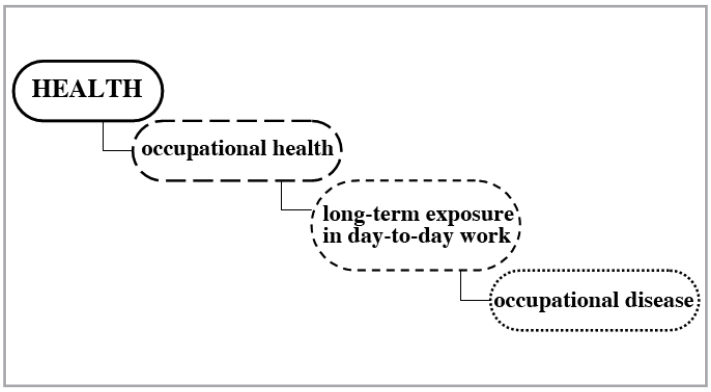

Figure 2: Health concept

Based on the earlier discussions on occupational safety (Section 2.1) and health (in this section), *occupational safety and health* is the discipline dealing with the prevention of injuries and diseases of workers resulting from the materials, processes, or procedures used in the workplace [9; 51]. The two words are normally used together and the borderline between health and safety is ill defined [20]. This is further discussed in the next section.

5.1 Related Research Efforts

Occupational health differs from occupational safety and process safety in terms of several criteria; the exposure pattern, duration of event, exposure scenario, and process state. The details about the differences are summarised in Table 1.

From Table 1, occupational health is related to normal everyday work activities and long-term exposure to chemicals. Occupational safety also is concerned with normal activity, but short-term accident due to physical hazards. Meanwhile process safety refers to major accidents, loss prevention, and acute short-term exposure in abnormal situations. The occupational health and safety hazards directly affect human's life only compared to process safety hazards, which also have interest on the plant, property, and cost. The nature of risk is also different; since airborne toxic substances are harmful at much lower concentrations than merely corrosive and flammable ones, their effects extend to much greater distances. These imply that although the occurrence of occupational health effect is long-term and less dramatic, the impact could be more serious in the long run than the occurrence of safety-related events. The insidious nature of occupational disease is the reason for it rarely reaches the news and is not well publicised as the industrial accident cases.

Health effects can be divided into acute and chronic effects due to short-term and prolonged exposures, respectively. Occupational health mainly deals with chronic exposure as a result of regular operations and day-to-day (routine) working activities. In large-scale process industry, chronic exposure is mainly contributed by fugitive emissions. Acute exposure may also occur in large-scale process industry primarily due to periodic emissions, which are mainly from occasional but acceptable working practices *e.g.* manual operations. Occupational health assessment should cover both chronic and acute occupational exposures as presented in Figure 3.

Table 1: Occupational health vs. occupational/process safety criteria

Criteria	Occupational health	Occupational safety	Process safety
Exposure pattern	Chronic (repeated)	Acute (single)	Acute (single)
Event duration	Long-term	Short-term	Short-term
Exposure scenario	Routine activity	Accident, routine activity	Accident,loss of containment
Process state	Normal	Normal	Abnormal

5.2 Occupational Health Studies in Chemical Process Industries

Unlike safety and environment, studies on occupational health aspect in CPI are very limited, but often being evaluated alongside the other two aspects, with health always being the least analyzed criteria. There are several methods available for health hazard assessment in chemical process. The methods however, are more diversified due to the complicated underlying principle of the aspect itself. Even though they have been developed for the purpose of health assessment; the scope, approach, and considered aspects vary. The review of 51 chemical ranking and scoring systems demonstrates that there was no consensus regarding an appropriate framework for evaluating adverse impacts to human health from exposure to chemicals [52].

The two basic types of health studies are the substance and process-type indices. Majority of the methods developed earlier are chemical substance-based and they are widely known as hazard indices. Hazard indices aim to rank substances in a process by their hazard potential. They take into account the volatility and the toxicity of a substance. As for process-based assessment, the methods are more disparate. Basically, the methods can be classified into those which:

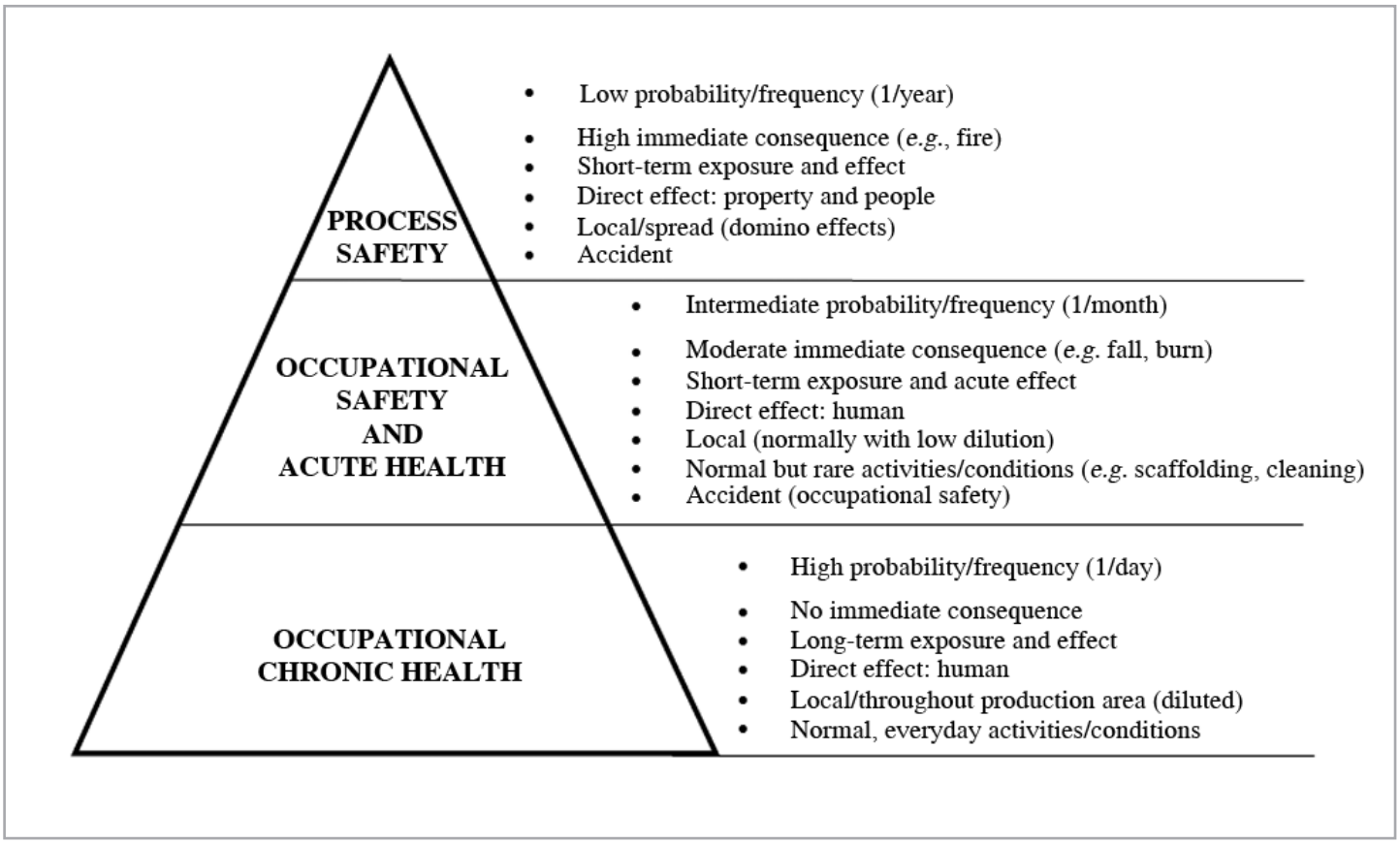

Figure 3: Occupational health vs. occupational/process safety [20]

Category 1 – health aspect is addressed only as minor part of the safety and/or environmental assessments [*e.g*. 28; 31-32; 35; 53].

Category 2 – health is not being evaluated from the occupational context. For example, some of them focus only on the acute hazards due to accidental chemical release, some concern with the effects on public community, and some address the environmental health impacts [*e.g*. 54-55].

Category 3 – occupational health assessment is not suitable for process screening during the early design stage, but is intended for process operation [*e.g*. 56]. Inherent occupational health studies have the largest benefits on process design stage.

Category 4 – health impacts are adapted in an existing Life-Cycle Assessment (LCA) method [*e.g*. 55].

Category 5 – inherent occupational health assessment is feasible during the design stage of chemical processes [*e.g*. 57-64].

The methods in Category 1 intend to cover all the SHE aspects, however health is often not as well assessed as the other two. In the INSET Toolkit [53], health hazards are assessed simply based on R-phrases and brief scoring system called Leak Factor to estimate the fugitive release rate in the process. In the EHS [32] and Inherent Benign-ness Indicator (IBI) [35] methods, only chemical health effects are assessed (based on *e.g*. exposure limit values and National Fire Protection Association (NFPA) ranking) without considering the chemical exposure aspect. However a proper risk assessment requires both the chemical exposure and the effect to be evaluated [65].

5.3 Concept and Definition

Health hazard refers to damaging potential of substance, activity, or process, which is described by the inherent health properties [20]. Hazards that might affect workers' health can be divided into five major categories of physical, chemical, biological, ergonomic/mechanical, and psychosocial [66-67]. During chemical process design, the major focus is the chemical and some physical hazards. The other categories cannot be evaluated due to the limited data available in the early stages of design. At the early design stage *e.g*. R&D, chemical health hazards can be evaluated from toxicity properties of materials whereas physical health hazards are based on process conditions *e.g*. operating temperature that may cause burn.

Health risk can be defined as the probability that an individual exposed to a chemical substance may experience an adverse health effect subsequent to the exposure [68]. The effect can be either acute or chronic depending on the duration of exposure; short-term or long-term, respectively. The level of health risk in chemical plant is determined by: a) the potential for harm and b) the potential for exposure. The potential for harm is a function of the toxicity characteristics of chemicals present in

the workplace. In principle chemicals will only be a risk to health once human are exposed to them. The exposure is determined by materials' physical properties (*e.g.* volatility), operating and workplace conditions, leaking tendency of equipment, working activities (duration and frequency), and human behavior.

In order to design the definition of inherent occupational health, it is vital to first understand the levels of inherent health studies in chemical process design. The study of inherent health can be made in three levels (see Figure 4):

i) Inherent health hazard potential

Inherent health hazard potential includes hazards of materials in a process that are potentially harmful to health. However, leak or exposure aspect is not yet considered. Therefore the focus of the very early assessment is typically on material's toxicity.

ii) Inherent leak hazard potential

In petrochemical plants, process materials may escape from the system through flanges, valves etc. through fugitive emissions. In this case the materials (hazard) are no longer contained but they are released into air. The inherent release rate depends on the complexity of process, the types of equipment involved, and physical properties of fluids. No specific protection layers are considered; therefore the evaluation of material release sources (leak potential) is still a hazard and not a risk-level study.

iii) Inherent exposure potential and risk

Chemical exposure assessment requires information on chemical concentration (a function of leak rate and dilution), exposure (a function of frequency and duration of exposure), protective equipment, and type of work procedure (*e.g.* manual operation close to the emission source). From inherent stand point, protective equipment should not be considered in order to give the worst-case scenario. Only at this level, some protective layers and human aspect start to get involved, thus allowing health risk to be quantified.

Inherent occupational health is a prevention of occupational health hazards (*i.e.* chemical or physical condition) that have the potential to cause health damage to workers by trying to eliminate the use of hazardous chemicals, process conditions, and operating procedures that may cause occupational hazards to the employees. Here inherent occupational health hazards can be defined as a condition, inherent to the operation or use of material in a particular occupation or environment, that can cause death, injury, acute or chronic illness, disability, or reduced job performance of personnel by an acute or chronic exposure.

There are twofold aims of inherent occupational health: Firstly to reduce the hazards from inherent properties of chemicals (such as toxicity and high vapor pressure) by using friendlier chemicals or the chemicals in safer physical condition (such as lower temperature) to eliminate the exposure. Secondly to reduce such process steps or procedures which involve inherent danger of exposure to the chemicals. Examples of such operations are some manual operations where the worker is in close contact with the material, such as the manual handling and dosing of chemical, emptying, and cleaning of the equipment etc. For reducing the occupational hazards, evaluation methods are of prime importance. With the establishment of the inherent occupational health definition, the associated assessment methods can be developed more easily and systematically.

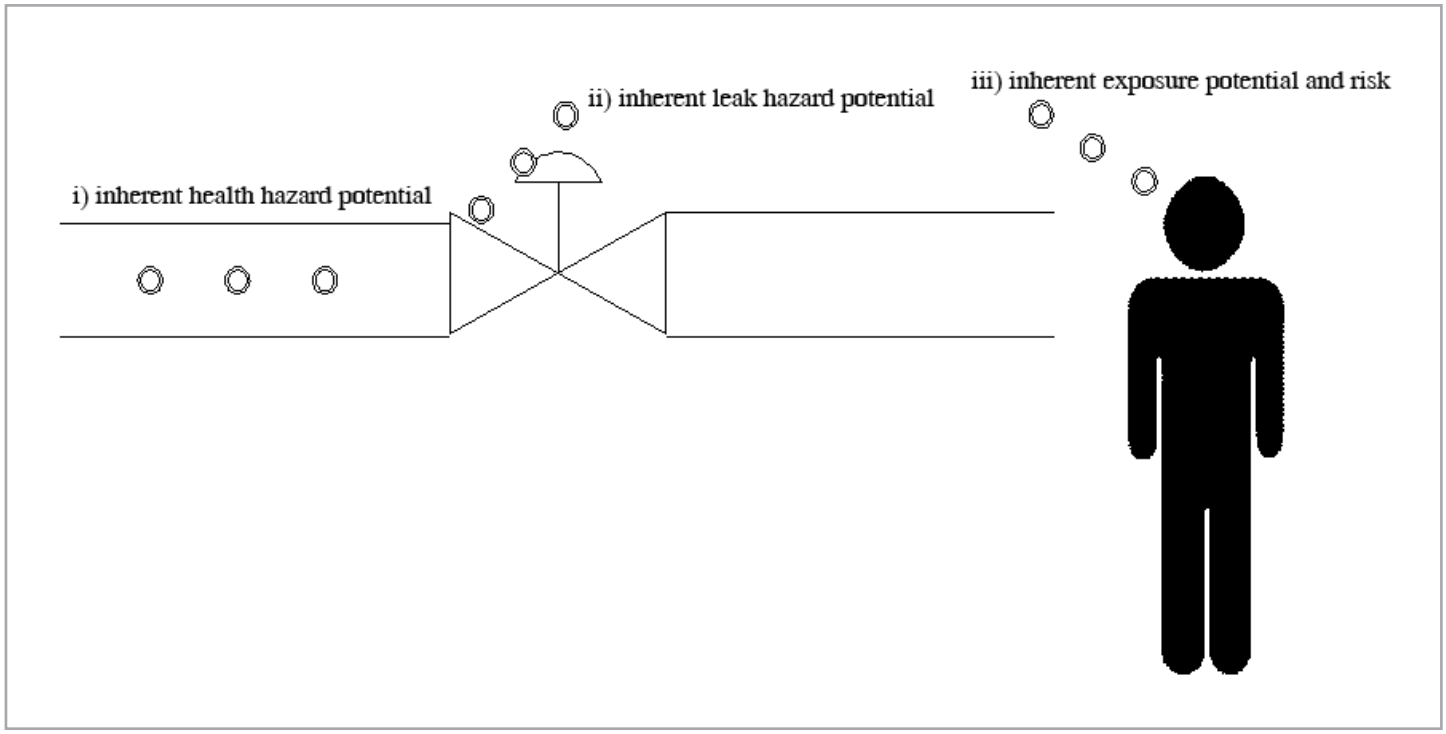

Figure 4: Levels of inherent health study

6.0 CONCLUSION

Occupational health is an important part of sustainability together with process safety and environmental issues. Each year, more people die from work-related diseases than are killed in industrial accidents. Every year new chemicals and technologies are being introduced which present new and often unknown hazards to workers. Therefore occupational health issue has been gradually gaining attentions especially from chemical process industries (CPI).

This paper introduces a new concept of inherent occupational health. Inherent occupational health is a prevention of occupational health hazards that have the potential to cause health damage to workers by trying to eliminate the use of hazardous chemicals, process conditions, and operating procedures that may cause occupational hazards to the employees. The paper also discusses the existing methods for assessing occupational health of chemical processes. Majority of the methods are not appropriate because they either evaluate health minorly as part of safety and environmental assessments, they focus on acute toxicity (process safety related) or environmental health impacts but not occupational health, and they are intended for process operation which receives less benefits from inherent level-related studies.

The introduction of the inherent occupational health concept as well as the establishment of its definition will have a significant impact on the appreciation and understanding of this subject matter especially in the CPI. Based on the definition, the objective and scope of occupational health assessment in CPI especially in the design stage become more certain. It also gives initial ideas on how health hazards can be eliminated early and process can be designed towards becoming inherently healthier. ■

REFERENCES

[1] Kletz T.A. (1984). Cheaper, Safer Plants, or Wealth and Safety at Work, Rugby: Institution of Chemical Engineers.

[2] Khan F.I. and Amyotte P.R. (2003). "How to Make Inherent Safety Practice a Reality." The Canadian Journal of Chemical Engineering, 81: pp2-16.

[3] Bell N.A.R. (1971). "Loss Prevention in the Manufacture of Nitroglycerine." In Loss Prevention in the Process Industries, Symposium Series No. 34, Rugby: Institution of Chemical Engineers, pp50-53.

[4] Pickles R.G. (1971) "Hazard Reduction in the Formaldehyde Process." In Loss Prevention in the Process Industries, Symposium Series No. 34, Rugby: Institution of Chemical Engineers.

[5] Kletz T.A. (1976). "Preventing Catastrophic Accidents." Chemical Engineering, 83(8): pp124-128.

[6] Kletz T.A. (1985). "Inherently Safer Plants." Plant/ Operations Progress, 4: pp164-167.

[7] Crowl D.A. and Louvar J.F. (2002). Chemical Process Safety: Fundamentals with Applications, 2nd Edition, New Jersey: Prentice Hall.

[8] Hughes P. and Ferrett E. (2005). Introduction to Health and Safety at Work, 2nd Edition, Oxford: Elsevier Butterworth-Heinemann.

[9] Hughes P. and Ferrett, E. (2008). Introduction to Health and Safety in Construction: The Handbook for Construction Professionals and Students of NEBOSH and Other Construction Courses, 3rd Edition, Amsterdam: Elsevier/ Butterworth-Heinemann.

[10] ILO (1998). "Resolutions Concerning Statistics of Occupational Injuries (Resulting from Occupational Accidents)." Adopted by the Sixteenth International Conference of Labour Statisticians.

[11] National Safety Council (1999). Injury Facts, Chicago.

[12] Kletz T.A. (1998). Process Plants: A Handbook for Inherently Safer Design, Philadelphia: Taylor & Francis.

[13] Jones D.A. (1992). Nomenclature for Hazard and Risk Assessment in the Process Industries, 2nd Edition, Rugby: Institution of Chemical Engineers.

[14] Herber R.F.M., Duffus J.H., Christensen J.M., Olsen E., and Park M.V. (2001). "Risk Assessment for Occupational Exposure to Chemicals: A Review of Current Methodology." International Union of Pure and Applied Chemistry, 73(6): pp993-1031.

[15] Crowl D.A. and Louvar J.F. (2002). Chemical Process Safety: Fundamentals with Applications, 2nd Edition, New Jersey: Prentice Hall.

[16] Bennett B. and Cole G. (2002). Pharmaceutical Production: An Engineering Guide, Great Britain: Institution of Chemical Engineers.

[17] American College Dictionary. (1967). New York: Random House.

[18] Etowa C.B., Amyotte P.R., Pegg M.J., and Khan F.I. (2002). "Quantification of Inherent Safety Aspects of the Dow Indices." Journal of Loss Prevention in the Process Industries, 15: pp477-487.

[19] Khan F.I. and Amyotte P.R. (2005). "I2SI: A Comprehensive Quantitative Tool for Inherent Safety and Cost Evaluation." Journal of Loss Prevention in the Process Industries, 18: pp310-326.

[20] Hassim M.H. (2010). Inherent Occupational Health Assessment in Chemical Process Development and Design, Doctoral Thesis, Espoo: Aalto University.

[21] Kletz T.A. (1991). Plant Design for Safety, Bristol, PA: Taylor & Francis.

[22] Kletz T.A. (1991). Plant Design for Safety: A User-friendly Approach, New York: Hemisphere Publishing Corporation.

[23] Kletz T.A. (1978). "What You Don't Have, Can't Leak." Chemistry and Industry, May 6: pp287-292.

[24] Edwards D.W. and Lawrence D. (1993). "Assessing the Inherent Safety of Chemical Process Routes: Is There a Relation Between Plant Costs and Inherent Safety?" Process Safety and Environmental Protection, 71(B4): pp252-258.

[25] Hendershot D.C. (1997). "Measuring Inherent Safety, Health and Environmental Characteristics Early in Process Development." Process Safety Progress, 16(2): pp78-79.

[26] Gupta J.P. and Edwards D.W. (2002). "Inherently Safer Design-Present and Future." Process Safety and Environmental Protection, 80: pp115-125.

[27] Palaniappan C., Srinivasan R., and Halim I. (2002). "A Material-centric Methodology for Developing Inherently Safer Environmentally Benign Processes." Computers and Chemical Engineering, 26: pp757-774.

[28] Shah S., Fischer U., and Hungerbühler K. (2003). "A Hierarchical Approach for the Evaluation of Chemical Process Aspects from the Perspective of Inherent Safety." Process Safety and Environmental Protection, 81: pp430-443.

[29] Mansfield D., Turney R., Rogers R., Verwoerd M., and Bots P. (1995). "How to Integrate Inherent SHE in Process Development and Plant Design." IChemE Symposium Series, 139: pp467-484.

[30] Rogers R.L. (1997). "An Overview of the INSET Toolkit." IBC UK Conference on Inherent SHE-The Cost Effective to Improved Safety, Health and Environment Performance, London.

[31] Khan F.I. and Abbasi S.A. (1998). "Multivariate Hazard Identification and Ranking System." Process Safety Progress, 17(3): pp157-170.

[32] Koller G., Fischer U., and Hungerbühler K. (2000). "Assessing Safety, Health, and Environmental Impact Early During Process Development." Industrial & Engineering Chemistry Research, 39: pp960-972.

[33] Mulholland K.L., Sylvester R.W., and Dyer J.A. (2001). "Sustainability: Waste Minimization, Green Chemistry and Inherently Safer Processing." Environmental Progress, 19(4): pp260-268.

[34] Crawley F.K. and Ashton D. (2002). "Safety, Health of the Environment – Which Comes First?" Journal of Hazardous Materials, 93: pp17-32.

[35] Srinivasan R. and Nhan N.T. (2008). "A Statistical Approach for Evaluating Inherent Benign-ness of Chemical Process Routes in Early Design Stages." Process Safety and Environmental Protection, 86: pp163-174.

[36] Gillett J. (2002). Safety, Health and Environment (SHE). In B. Bennett and G. Cole, Pharmaceutical Production: An Engineering Guide, Great Britain: Institution of Chemical Engineers.

[37] Rushton A.G., Edwards D.W., and Lawrence D. (1994). "Inherent Safety and Computer Aided Process Design." Transactions of the IChemE, 72(B): pp83-87.

[38] Kraft R.L. (1992). "Incorporate Environmental Reviews into Facility Design." Chemical Engineering Progress, 88: pp46.

[39] Spriggs H.D. (1995). "Design for Pollution Prevention." AIChE Symposium Series, 90: pp1.

[40] Mallick S.K., Cabezas H., Bare J.C., and Sikdar S.K. (1996). "A Pollution Reduction Methodology for Chemical Process Simulators." Industrial & Engineering Chemistry Research, 35(11): pp4128-4138.

[41] Cano-Ruiz J.A. and McRae G.J. (1998). "Environmentally Conscious Chemical Process Design." Annual Review of Energy and the Environment, 23: pp499.

[42] Sharratt P. (1999). "Environmental Criteria in Design." Computers & Chemical Engineering, 23: pp1469.

[43] Chen H. and Shonnard D.R. (2004). "Systematic Framework for Environmentally Conscious Chemical Process Design: Early and Detailed Design Stages." Industrial & Engineering Chemistry Research, 43: pp535-552.

[44] Li C., Zhang X., Zhanga S., and Kenzi S. (2009). "Environmentally Conscious Design of Chemical Processes and Products: Multi-optimization Method." Chemical Engineering Research and Design, 87: pp233-243.

[45] Cave S.R. and Edwards D.W. (1997). "Chemical Process Route Selection Based on Assessment of Inherent Environmental Hazard." Computers and Chemical Engineering, 21: ppS965-S970.

[46] Gunasekera M.Y. and Edwards D.W. (2003). "Estimating the Environmental Impact of Catastrophical Chemical Releases to the Atmosphere: An Index Method for Ranking Alternative Chemical Process Route." Process Safety and Environmental Protection, 81: pp463-474.

[47] Gunasekera M.Y. and Edwards D.W. (2006). "Chemical Process Route Selection based upon the Potential Toxic Impact on the Aquatic, Terrestrial and Atmospheric Environments." Journal of Loss Prevention in the Process Industries, 19(1): pp60-69.

[48] Princeton Encyclopedia (2010). *wordnetweb.princeton.edu/perl/webwn*.

[49] ILO (1950). Joint ILO/WHO Committee on Industrial Hygiene: Report of the First Meeting, Geneva: ILO.

[50] OECD (2008). Glossary of Statistical Terms, *http://stats.oecd.org/glossary/detail.asp?ID=3565*.

[51] ILO (1997). Technical and Ethical Guidelines for Workers' Health Surveillance Report, *http://www.ilo.org/public/english/protection/safe-work/health/whsguide.htm*.

[52] Davis G.A., Swanson M., and Jones S. (1994). Comparative Evaluation of Chemical Ranking and Scoring Methodologies, EPA Order No. 3N-3545-NAEX, U.S: University of Tennessee, *http://eerc.ra.utk.edu/clean/pdfs/CECRSM.pdf*.

[53] INSIDE Project (2001). The INSET Toolkit, *http://www.aeat-safety-and-risk.com/html/inside.html*.

[54] Hertwich E.G., Pease W.S., and McKone T.E. (1998). "Evaluating Toxic Impact Assessment Methods: What Works Best?" Environmental Science & Technology, 32(5): pp138A-144A.

[55] Hertwich E.G., Mateles S.F., Pease W.S., and McKone T.E. (2001). "Human Toxicity Potentials for Life-cycle Assessment and Toxics Release Inventory Risk Screening." Environmental Toxicology and Chemistry, 20(4): pp928-939.

[56] Maidment S.C. (1998). "Occupational Hygiene Considerations in the Development of a Structured Approach to Select Chemical Control Strategies." Annals of Occupational Hygiene, 42(6): pp391-400.

[57] Hassim M. and Edwards D.W. (2006). "Development of a Methodology for Assessing Inherent Occupational Health Hazards." Process Safety and Environmental Protection, 84(B5): pp378-390.

[58] Hassim M., Edwards D.W., and Hurme M. (2006). "Assessing Inherent Occupational Health Hazards During the Conceptual Design Phase." Chemical Engineering Transactions, 9: pp119-124.

[59] Hassim M.H. and Hurme M. (2008). "Computer Aided Design of Occupationally Healthier Processes." Computer Aided Chemical Engineering, 25: pp1119-1124.

[60] Hassim M.H. and Hurme M. (2008). "Quantification of Fugitive Emissions for Proposed Chemical Plants." Proceeding of AIChE 100th Annual Meeting, Philadelphia.

[61] Hassim M.H. and Hurme M. (2008). "Estimation of Exposure Concentration During the Design Stage of Chemical Processes." Proceeding of United Kingdom-Malaysia Engineering Conference 2008, London, 124-126.

[62] Hassim M.H. and Hurme M. (2010). "Inherent Occupational Health Assessment During Process Research and Development Stage." Journal of Loss Prevention in the Process Industries, 23(1): pp127-138.

[63] Hassim M.H. and Hurme M. (2010). "Inherent Occupational Health Assessment During Preliminary Design Stage." Journal of Loss Prevention in the Process Industries, doi:10.1016/j.jlp.2009.12.004). 23(3): pp476-482.

[64] Hassim M.H. and Hurme M. (2010). "Inherent Occupational Health Assessment During Basic Engineering Stage." Journal of Loss Prevention in the Process Industries, 23(2): pp260-268.

[65] Tielemans E., Marquart H., de Cock J., Groenewold M., and van Hemmen J. (2002). "A Proposal for Evaluation of Exposure Data." Annals of Occupational Hygiene, 46(3): pp287-297.

[66] Hartley C. (1999). Occupational Hygiene. In: Ridley J., Channing J. (eds.) Occupational Health and Hygiene-Safety at Work Series, 3rd Edition, Great Britain: Butterworth-Heinemann.

[67] Negash D. (2002). "Work-Related Diseases." African Newsletter on Occupational Health and Safety, 12: pp51-54.

[68] Kumar A., Madasu R., and Manocha A. (1994). "An Evaluation of Smart Risk and ACE 2588 Health Risk Assessment Software." Environmental Progress, 13(4): ppN14-N19.

PROFILES

MIMI HASSIM

Mimi Hassim is a chemical engineering lecturer at the Universiti Teknologi Malaysia, Skudai. She received her BEng degree from Universiti Teknologi Malaysia, MSc degree from Loughborough University, UK and doctoral degree from Aalto University, Finland. Since 2001, she has been working in the area of inherent safety, but focusing on occupational health aspect. Her research studies also include process development and design based on inherently safer design (ISD) concept, multi-criteria decision making, industrial hygiene, process safety and loss prevention.

DR MARKKU HURME

Dr Markku Hurme is the Professor and incharge of Plant Design research group. His research interests are related to process development, evaluation and feasibility studies in the process industry. He has published articles on process design, safety and computer applications in process design. Before joining TKK he worked at Neste Engineering, the engineering office of a major Finnish oil refining company. He has been involved in the design or development of over 300 chemical, petrochemical, biochemical, food, and pulp and paper processes

INFORMATION FOR AUTHORS

SUBMISSION OF A CONTRIBUTION IS TAKEN TO MANIFEST THE FACT THAT THE SUBMISSION HAS NOT BEEN SUBMITTED, ACCEPTED, PUBLISHED OR COPYRIGHTED ELSEWHERE.

TO AVOID PUBLICATION DELAYS, PLEASE SEND ALL MANUSCRIPTS TO THE EDITOR AND OBSERVE THE FOLLOWING GUIDELINES.

A) SUBMISSION OF PAPER

Author(s) are required to send four (*4*) copies of the manuscript and also a short biodata / profile of all the author(s) attached with a photo together with the softcopy (*excluding via e-mail*) upon submission. Each copy should be completed with keywords, illustrations (*if any*) and an abstract. Submissions should be made to the address below:

Chief Editor
The Institution of Engineers, Malaysia
Bangunan Ingenieur, Lots 60 & 62, Jalan 52/4
P.O.Box 223 (Jalan Sultan)
46720 Petaling Jaya, Selangor Darul Ehsan
Tel: 03 – 7968 4001 / 7968 4002
Fax: 03 – 7957 7678
E-mail: pub@iem.org.my

Three types of papers are solicited for the IEM Journal:

(1) Regular Paper – Presentation of significant research, developments or applications in any field of engineering or within the scope of the journal. Tutorials and surveys are also considered. For submissions, the length should be about 30 pages; double-spacing, single column with font size 12 (*Times New Roman*).

(2) Brief Paper – A concise description of new technical concepts or applications within the scope of the journal. Submission should be about 20 pages; double-spacing, single column with font size 12 (*Times New Roman*).

(3) Technical Correspondence – Letter to the Editor, comments on established engineering topics and discussion of published papers. Submission should be about 10 pages; double-spacing, single column with font size 12 (*Times New Roman*).

NOTE:

Format for the manuscript: First Submission for review process: PDF format in double spacing, single column, 12pt (*Times New Roman*) Pre-production (*after review*): DOC format in double column, single spacing, 10pt (*Times New Roman*)

Manuscripts submitted as papers should state the significance of the problem in the introduction.

Paper size should be of A4 size (*210 cm × 297 cm*) with 2cm margin on the left, right and bottom, and 3cm from the top.

Enclose a signed letter giving your preferred address, telephone, fax number and e-mail address (*if available*) for correspondence and return of proofs.

If the manuscript has been presented, published or submitted for publication elsewhere, please inform the Editor. Our primary objective is to publish technical materials not available elsewhere, but on occasion, we publish papers of unusual merit that have appear or will appear before other audiences.

The language of the Journal is English. However, a paper in Bahasa Malaysia is also accepted and an abstract in English must be included.

Note that upon acceptance of an article for publication, the author is requested to submit a camera-ready format of the manuscript with single-spacing, double-column and font size 10 (*Times New Roman*). Illustrations and keywords of the paper should be included in the text. An electronic copy of the manuscript should also be submitted. The author is also requested to submit a passport-sized photograph and a short biography. This information will be sent to the author by the Editor.

B) STYLE FOR DRAFT OF MANUSCRIPT FOR REVIEW PROCESS

The draft of manuscript for a review process shall in PDF format.
The manuscript should be typewritten using double-spacing, font size 12 (*Times New Roman*); on one side of the sheet only and in a single column format. The format for IEM Journal follows that of the IEEE Transactions (*US*).

As we practice blind review, please do not put your name and address in the manuscript.

Provide an informative 100- to 250-word abstract at the head of the manuscript.

All sections should be numbered in Roman numeral such as I, II, *etc*. with the title in capital.

Subsections should be numbered in alphabets such as A, B, C, *etc*.

Sub-subsections (*if any*) should be numbered as A.1, A.2, *etc*.

Number all equations in round brackets ( ) flushed to the right. The equation should be in the centre.

References in the text should be cited each by a reference number in square brackets, *e.g.* [12] or [4-6], *etc*.

In the reference section, the references should be written as follows:

Style for papers:
Reference Number, Author, first initials followed by last name, title (*italics*), location and publisher, year, chapter or page number, month, and year.

Style for books:
Reference Number, Author, first initial followed by last name, title (*italics*), location and publisher, year, chapter or page number (*if desired*).

Sample format for references is as follows:

(for paper)
[3] M. Khalid, S. Omatu, and R. Yusof, "Temperature Regulations with Neural Networks and Alternative Control Schemes"' IEEE Trans on Neural Networks, Vol. 6, No. 3, pp. 572-582, May, 1995.

(for book)
[4] S. Omatu, M. Khalid, and R. Yusof, Neural-Control and Its Applications, London: Springer-Verlag, 1995.

If your paper is in Bahasa Melayu, please provide an ***abstract*** in English.

C) STYLE FOR CAMERA READY MANUSCRIPT (PRE-PUBLICATION)

In the event that the paper is accepted, we will require that the camera-ready manuscript be submitted in a double column format, single-spacing and font size 10 (*Times New Roman*). Include all illustrations in between the text (*if possible*). An electronic copy should be submitted. We strictly prefer a document format camera-ready manuscript for pre-publication.

D) STYLE FOR ILLUSTRATIONS

Try to include the illustrations in between the text.

Originals for illustrations should be sharp, noise-free and of good contrast.

Each illustration must be numbered such as "Figure 1, Figures 2-3, etc". and have a meaningful caption at the bottom. For tables, the caption must be at the top.

On graphs, show only the coordinate axes, or at most the major grid lines, to avoid a dense hard-thread result.

All lettering should be large enough to permit legible reduction of the figure to column width, perhaps as much as 4:1. Typing on figures is not acceptable.

Photographs should be glossy prints, of good contrast and gradation, and any reasonable size.

Number each original on the back, or at the bottom in the front, and also indicate the author's name.

Upon acceptance of your paper submit a set of the figures and a list of the captions. An electronic softcopy must be submitted in a document format. ■

SUBSCRIPTIONS

To subscribe Journal of IEM please contact

DIMENSION PUBLISHING SDN BHD (449732-T)
Suite 29, 3A Floor, IOI Business Park,
1 Persiaran Puchong Jaya Selatan,
Bandar Puchong Jaya, 47170 Puchong,
Selangor Darul Ehsan, Malaysia.
Tel: (603) 8070 9949
Fax: (603) 8070 0047
Email: info@dimensionpublishing.com
Website: www.dimensionpublishing.com